

AD \_\_\_\_\_

Award Number: DAMD17-00-1-0386

TITLE: Molecular Biology of Breast Neoplasia

PRINCIPAL INVESTIGATOR: Virgil C. Jordan, Ph.D.  
Robin Leikin, Ph.D.

CONTRACTING ORGANIZATION: Northwestern University  
Evanston, Illinois 60208-1110

REPORT DATE: September 2002

TYPE OF REPORT: Annual Summary

PREPARED FOR: U.S. Army Medical Research and Materiel Command  
Fort Detrick, Maryland 21702-5012

DISTRIBUTION STATEMENT: Approved for Public Release;  
Distribution Unlimited

The views, opinions and/or findings contained in this report are those of the author(s) and should not be construed as an official Department of the Army position, policy or decision unless so designated by other documentation.

REPORT DOCUMENTATION PAGE			Form Approved OMB No. 074-0188	
<small>Public reporting burden for this collection of information is estimated to average 1 hour per response, including the time for reviewing instructions, searching existing data sources, gathering and maintaining the data needed, and completing and reviewing this collection of information. Send comments regarding this burden estimate or any other aspect of this collection of information, including suggestions for reducing this burden to Washington Headquarters Services, Directorate for Information Operations and Reports, 1215 Jefferson Davis Highway, Suite 1204, Arlington, VA 22202-4302, and to the Office of Management and Budget, Paperwork Reduction Project (0704-0188), Washington, DC 20503</small>				
1. AGENCY USE ONLY (Leave blank)	2. REPORT DATE September 2002	3. REPORT TYPE AND DATES COVERED Annual Summary (1 Sep 01 -31 Aug 02)		
4. TITLE AND SUBTITLE Molecular Biology of Breast Neoplasia		5. FUNDING NUMBERS DAMD17-00-1-0386		
6. AUTHOR(S): Virgil C. Jordan, Ph.D. Robin Leikin, Ph.D.				
7. PERFORMING ORGANIZATION NAME(S) AND ADDRESS(ES)  Northwestern University Evanston, Illinois  E-Mail: vcjordan@northwestern.edu		8. PERFORMING ORGANIZATION REPORT NUMBER		
9. SPONSORING / MONITORING AGENCY NAME(S) AND ADDRESS(ES)  U.S. Army Medical Research and Materiel Command Fort Detrick, Maryland 21702-5012		10. SPONSORING / MONITORING AGENCY REPORT NUMBER		
11. SUPPLEMENTARY NOTES Original contains color photos. All DTIC reproductions will be in black and white.		20030226 023		
12a. DISTRIBUTION / AVAILABILITY STATEMENT Approved for Public Release; Distribution Unlimited				
		12b. DISTRIBUTION CODE		
13. Abstract (Maximum 200 Words) (abstract should contain no proprietary or confidential information)				
<p>The Robert H. Lurie Comprehensive Cancer Center at Northwestern University is an NCI-funded comprehensive cancer center. One of the major accomplishments for the Cancer Center has been to establish a nationally recognized program in breast cancer in both laboratory research and clinical activity. The Cancer Center has received \$4.2 million from the Avon Foundation and successfully competed for a SPORC in Breast Cancer from the National Cancer Institute. In September 2000 the Cancer Center received a four year award from the US Army for comprehensive training of graduate students and postdoctoral fellows conducting breast cancer relevant research entitled, "The Molecular Biology of Breast Neoplasia" (DAMD17-00-1-0386). In Year 02 the Selection Committee reviewed applications and assisted in the selection of 4 graduate students and two postdoctoral fellows for appointment to the Training Program. Trainees and mentors actively participated in the weekly meetings of the Breast Cancer Journal Club, as well as training program's course entitled, Advanced Topics in Breast Cancer. Year 03 appointments have just been completed.</p>				
14. SUBJECT TERMS training program, molecular biology, hormones, signal transduction			15. NUMBER OF PAGES 156	
			16. PRICE CODE	
17. SECURITY CLASSIFICATION OF REPORT Unclassified	18. SECURITY CLASSIFICATION OF THIS PAGE Unclassified	19. SECURITY CLASSIFICATION OF ABSTRACT Unclassified	20. LIMITATION OF ABSTRACT Unlimited	

## Table of Contents

Cover.....	1
SF 298.....	2
Table of Contents.....	3
Introduction.....	4
Body.....	4
Key Research Accomplishments.....	7
Reportable Outcomes.....	7
Conclusions.....	8
References.....	
Appendices.....	9
Appendix I	Trainee Abstracts
Appendix II	Journal Club
Appendix III	Advanced Topics in Breast Cancer
Appendix IV	Trainee Publications

## **INTRODUCTION**

The Robert H. Lurie Comprehensive Cancer Center has established a premier breast cancer program at Northwestern University, integrating basic laboratory research, clinical research and a program in cancer prevention and control. V. Craig Jordan, OBE, Ph.D., D.Sc. directs the breast cancer laboratory research program and Monica Morrow, M.D., directs the clinical breast cancer research program and the Lynn Sage Comprehensive Breast Center at Northwestern. Dr. Jordan is internationally recognized for his contributions to breast cancer research in development of the antiestrogen tamoxifen, an important drug used in the treatment and prevention of breast cancer. The Cancer Center has successfully competed for a grant from the NCI to establish a breast cancer program (NCI P20 CA65764), and a center grant from the US Army (DAMD17-96-2-6013) entitled "Increasing Access to Modern Multidisciplinary Breast Cancer Care". The Cancer Center also received a 4.2 million dollar award from the Avon Foundation in March 2000 for laboratory research and clinical treatment. The principal investigator is Monica Morrow, M.D. and co-principal investigator is V. Craig Jordan, Ph.D., D.Sc. The award expands the breast cancer research programs to medically underserved minority women. The Avon Foundation enhanced their commitment to breast cancer research at the Robert H. Lurie Comprehensive Cancer Center with an additional gift of \$10 million to build an Avon Breast Cancer Research Laboratory. In September 2000 the Cancer Center was selected by the National Cancer Institute to receive a SPORE in Breast Cancer (P50 CA89018). The Program Director of the SPORE is V. Craig Jordan, Ph.D., D.Sc. and the co-directors are Monica Morrow, M.D. and Ann Thor, M.D. The five-year award provides 13 million dollars in funding for six translational research projects investigating hormones and breast cancer, four core facilities, and career development and developmental research opportunities in breast cancer. In September 2000 the Cancer Center also received a four year award from the US Army for training of graduate students and postdoctoral fellows, "The Molecular Biology of Breast Neoplasia".

## **BODY**

The Department of Defense funded training program, The Molecular Biology of Breast Neoplasia, enables the Cancer Center to provide state of the art laboratory and didactic training to 4 predoctoral students and two postdoctoral fellows per year. The program enables trainees to be exposed to senior basic science faculty with research relevant to breast cancer and to clinical investigators who provide a translational link. Preceptors are nationally funded faculty with a history of excellence in research with a focus on the cellular and molecular aspects of breast cancer. Predoctoral trainees enroll in the core curriculum of biochemistry, cell biology, molecular biology and biostatistics. Postdoctoral trainees have already completed coursework in these areas. All trainees attend the Breast Cancer Journal Club that brings together the members of the Breast Cancer Program on a weekly basis to discuss journal articles relevant to the molecular biology of breast cancer. The journal club regularly attracts 15-25 graduate, postdoctoral and faculty participants in addition to the four predoctoral students and two postdoctoral fellows who are required to participate. Trainees are required to present one time per year at this meeting (see Appendix). In January 2002 we implemented a course in breast cancer biology and treatment, "Advanced Topics in Breast Cancer" (see Appendix). The monthly lectures present an integrated overview of clinical breast cancer for laboratory scientists. At the final meeting trainees present their research projects for the Advisory Committee responsible for monitoring trainee progress. Dr. Jordan provides further educational opportunities for the trainees in his role as Program Director for the NCI funded SPORE in Breast Cancer. The Selection Committee is responsible for selecting applicants and recommending admission to the Program. Ultimately, the goal of the Training Program is to prepare scientists to function as independent investigators in the field of breast cancer research and to integrate their research with therapeutic advances made by clinicians.

Dr. Gary Borisy and Dr. Vincent Cryns have been added to the list of preceptors on The Molecular Biology of Breast Neoplasia Training Grant. Dr. Cryns replaces Dr. Debra Tonetti who has left Northwestern University and Dr. Borisy replaces Dr. Ann Thor who left Northwestern University to become Chairman of Pathology at Oklahoma University. Dr. Cryns studies molecular regulation of apoptosis while Dr. Borisy is a nationally recognized leader in the field of metastases and tumor cell invasion.

Each year the Cancer Center solicits applications from faculty in the Breast Cancer Program nominating students. The Training Grant Selection Committee is responsible for the admission of students and fellows. Committee members include: V. Craig Jordan, Ph.D., D.Sc., Program Director, Steven Rosen, M.D., Director, Cancer Center, Robin Leikin, Ph.D., Scientific Program Director; Kathleen Rundell, Ph.D., Professor, Microbiology-Immunology and Jonathan Jones, Ph.D., Professor, Cell and Molecular Biology. Students are selected based upon their academic credentials, the relevance of their research projects to breast cancer and their potential as future academicians in breast cancer research. The Training Grant Executive Committee provides final approval for the trainee selections.

The following predoctoral and postdoctoral students have been allocated funds in Year 02 of the Grant:

**Year 2:**

<u>Name</u>	<u>Preceptor</u>	<u>Department</u>
<b>Predocs:</b>		
Danijela Vignjevic	Gary Borisy	Cell and Molecular Biology
Hao Wang	Gerald Soff	Medicine
Michael Werner	Vince Cryns	Medicine
Yi Wu	Sharon Stack	Cell and Molecular Biology
<b>Postdocs:</b>		
Sudhakar Baluchamy	Bayar Thimmapaya	Microbiology-Immunology
Suresh Pillai	Larry Jameson	Medicine

**Danijela Vignjevic**

The acquisition of a motile and invasive phenotype is an important step in the development of tumors and tumor metastasis. Electron microscopy analysis indicates that transformed breast cells differ from control cells by development of long filopodia, spike-like extensions of the cell. Actin bundling protein, fascin has a role in filopodia formation that leads to increased cell motility and malignancy. Increased levels of fascin are associated with overexpression of c-erbB2 in breast cancer cells, which correlates with poor prognosis in breast cancer patients. The Borisy lab has developed an in vitro system to study filopodia formation. Time lapse microscopy shows that formation of actin bundles into parallel bundles by fascin within filopodia may promote the linear extension and stiffness of filopodia. This may enable filopodia to extend and retract over long distances. Ultimately, we hope to understand the molecular mechanisms of filopodia formation and actin stars and their role in cancer metastasis and to use this knowledge in the development of novel targets for treatment of cancer.

**Selected by the DOD to receive a travel award to present at the Era of Hope Meeting in Orlando, 2002.**

**Yi Wu**

Yi Wu is studying the function of membrane type 1 matrix metalloproteinase (MT1-MMP) and its regulation in breast cancer cell invasion. The Stack laboratory are interested in membrane type 1-MMP (MT1-MMP)

because of studies that correlate enhanced expression with breast cancer disease progression as well as with invasiveness of cultured breast cancer cell lines. This is further supported by in vitro studies showing MT1-MMPs are the only subfamily of MMPs that mediates cellular invasion and knock-out studies revealing MT1-MMP is an in vivo collagenase. The overall hypothesis of this research is that proteolytic processing of MT1-MMP regulates its activity on the cell surface and thereby, controls cellular invasion through type I collagen. In our studies, we demonstrated that MDA-MB-231 cells invade type I collagen matrix, the most important matrix barrier for tumor, in an MT1-MMP-dependent manner. The invasiveness can be potentiated by overexpression of MT1-MMP but not the catalytic-inactive mutant E240A. Interestingly, we detected an inhibitory effect in invasion by overexpressing a truncation 44 kDa mutant, which is a naturally occurring cell surface autolytic product, suggesting MT1-MMP proteinase activity is tightly controlled in vivo. Currently we are vigorously investigating the dominant-negative function of the truncation mutant and its potential as a therapeutic target.

### **Hao Wang**

Hao Wang is studying the in vivo generation of angiostatin 4.5 (AS4.5) as an inhibitor of angiogenesis in breast cancer patients. In prior studies of conditioned media from human prostate cancer cells, plasminogen is converted to Angiostatin4.5 in a two step reaction. First, plasminogen is activated to plasmin by a plasminogen activator, which is followed by plasmin autoproteolysis in the presence of a free sulfhydryl donor. This human angiostatin isoform is designated angiostatin4.5, as it contains kringles 1-4, plus 85% of kringle 5 (amino acids Lys<sup>78</sup> to Arg<sup>529</sup>). We now demonstrate that plasminogen may also be converted to angiostatin4.5 in a plasma membrane-dependent reaction, involving uPA as the plasminogen activator, and a plasmin receptor, without the requirement of a small molecule free sulfhydryl donor. This reaction is dependent on kringle binding to the receptor, based on inhibition by the lysine analogue  $\epsilon$ -aminocaproic acid (EACA). While an angiostatin-related protein, A61, may be generated by cancer cells utilizing annexin II as a plasmin(ogen) receptor, our data indicate that annexin is not necessary for angiostatin4.5 generation. Instead, cell surface actin or an actin-related protein sharing the carboxyl terminus of actin could work as the plasmin receptor for angiostatin4.5 generation on cancer cells. The result will help us to understand how breast cancer cells generate angiostatin 4.5 and this can influence the future direction of breast cancer therapy.

### **Michael Werner**

Caspases are a conserved family of cysteine proteases that are universal effectors of programmed cell death. However, the molecular mechanisms by which caspases induce cell death are poorly understood. The Cryns laboratory has developed a novel expression cloning strategy to identify cDNAs encoding caspase substrates. They identified integrin  $\beta 4$  as a new caspase-3 substrate that is cleaved in breast cancer cells undergoing chemotherapy-induced apoptosis. Cleavage of integrin  $\beta 4$  removes a large portion of its cytoplasmic tail. Caspase cleavage of integrin  $\beta 4$  probably promotes apoptosis by specifically disrupting integrin  $\beta 4$ 's ability to activate the PI3K/Akt cell survival pathway. Once the exact cleavage site is identified, we will generate breast cancer cells that stably express wild-type integrin  $\beta 4$ , caspase-truncated integrin  $\beta 4$  (which lacks the tail portion removed by caspases), and caspase-cleavage resistant integrin  $\beta 4$  (which lacks the caspase cleavage site and cannot be cleaved by caspases). We will then compare the sensitivity of these breast cancer cells to chemotherapy-induced apoptosis and examine their ability to activate the PI3K/Akt cell survival pathway. We predict that the breast cancer cells expressing truncated integrin  $\beta 4$  will be most sensitive to apoptosis induction (because they will be unable to activate the PI3K/Akt cell survival pathway), while those expressing caspase cleavage-resistant integrin  $\beta 4$  will be the most resistant to chemotherapy-induced apoptosis (even more resistant than breast cancer cells expressing wild-type integrin  $\beta 4$ ). These experiments provide insight into the mechanisms of breast cancer apoptosis, and may lead to new breast cancer therapies specifically targeting integrin  $\beta 4$ .

**Suresh Pillai, Ph.D.**

Estrogen Receptors (ERs) initiate gene transcription via numerous pathways. In the "classical" pathway, ERs bind to discrete response elements on DNA to activate transcription. In the "tethered" pathway, ERs do not interact directly with response elements but alter transcriptional initiation by tethered interaction with other activators. To examine the effects of selective estrogen receptor modulator (SERM) activation of transcription via the tethered pathway, we used a mutated ER $\alpha$  and microarray profiling to identify target genes of this pathway. Amino acids within the DNA binding region of ER $\alpha$  were mutated to eliminate classical ER signaling, and an ER-negative breast cancer cell line (MDA-MB-231) was infected with adenoviral vectors containing these mutants. Cells were then treated with diluent alone, estradiol, ICI 182 780 (a pure anti-estrogen), or tamoxifen and raloxifen (partial ER $\alpha$  agonists). This experiment was conducted twice to assess the precision and accuracy of the data. RNA from these cells was then extracted, purified, and hybridized to Affymetrix U95A human gene arrays to compare gene expression profiles among the treatment groups. The data between the experiments correlated significantly, and an examination of genes regulated (stimulated or suppressed) at least 2.3-fold yielded a consensus gene set of 276 SERM targets. While few genes were regulated by estradiol, SERMS activated a much larger number of genes. This suggests that SERMS act, at least in part, through the tethered pathway. The consensus gene set will be used in the generation of custom spotted microarrays. We hope to use these custom arrays to screen in vitro (cancer cell lines) and in vivo (breast cancer biopsies) models of how the tethered pathway contributes to ER-mediated genes transcription in cancer.

**Sudhakar Baluchamy, Ph.D.**

Jun B is a member of Jun- protooncogene family of transcription factors. The functions of c-Jun are well understood, while cellular functions of Jun B are poorly understood. Jun B functions are clearly different from those of c-Jun. My goal is to study the role of Jun B in branching duct morphogenesis and mammary gland development. Northern blot analysis indicates that Jun B expression is induced about 3.5 fold during branching morphogenesis. To examine whether Jun B is essential for invitro morphogenesis we constructed a recombinant adenovirus vector which express antisense Jun B sequences (As-Jun B). Growing MCF 10A cells were infected with Ad-Jun B or a vector express b-gal (control vector) and morphogenesis was recorded using light microscopy. This experiment shows that cells expressing antisense Jun B form duct like structure poorly when compared to cells infected with B-gal control vector. These results suggest that elevated levels of Jun B may play an important role on duct morphogenesis. Now we are attempting to identify downstream targets of Jun B while cells undergoing branching duct morphogenesis using antisense Jun B vector by DNA microarray. We are also interested in studying overexpression of Jun B in duct morphogenesis in vivo.

**KEY RESEARCH ACCOMPLISHMENTS**

- Four predoctoral students and two postdoctoral fellows selected from a pool of candidates by Selection Committee
- Journal Club held on Tuesdays at 11 am throughout the academic year
- Students exposed to Advanced Topics in Breast Cancer course implemented in 2002
- Students exposed to translational relevance of their research through Breast SPORE meetings
- Advisory committee reviewed progress of 6 trainees and selected 3 for renewal of their funding in Year 03

**REPORTABLE OUTCOMES**

The success of the Robert H. Lurie Comprehensive Cancer Center's Training Program is exemplified by the publications by the trainees as a direct result of their funding through the Molecular Biology of Breast Neoplasia Training Grant. Publications include:

Ellerbroek, S. M., **Wu, Y. I.**, Overall, C. M., and Stack, M. S. (2001). Functional interplay between type I collagen and cell surface matrix metalloproteinase activity, *J Biol Chem* 276, 24833-42.

Ellerbroek, S. M., **Wu, Y. I.**, and Stack, M. S. (2001). Type I collagen stabilization of matrix metalloproteinase-2, *Arch Biochem Biophys* 390, 51-6.

Ghosh, S., **Wu, Y. I.**, and Stack, M. S. (2000) Proteolysis in ovarian carcinoma. In *Cancer Treatment and Research: Ovarian Cancer*. Stack, M. S. and Fishman, D. A., Eds. Rosen, S. Series Editor. Kluwer Academic Publishers, Boston. (in press)

Soff GA, **Wang H**, Schultz R, Kunz P, Cundiff D, French E, Hoppin EC, Rossbach HC. Therapeutic application of an angiostatic cocktail for patients with Refractory Cancer. *Nature Medicine* (Submitted for publication)

Munshi, H. G., **Wu, Y. I.**, Ariztia, E. V., and Stack, M. S. (2002) Calcium Regulation of Matrix Metalloproteinase-Mediated Migration in Oral Squamous Cell Carcinoma Cells. *J Biol Chem* (in press).

Tam, E. M., **Wu, Y. I.**, Butler, G. S., Stack, M. S., and Overall, C. M. (2002) Collagen binding properties of the MT1-MMP hemopexin C domain: The ectodomain of the 44-kDa autocatalytic fragment of MT1-MMP inhibits cell invasion by disrupting native type I collagen cleavage. *J Biol Chem* (in press).

Munshi, H. G., Ghosh, S., Mukhopadhyay, S., **Wu, Y. I.**, Sen, R., Green, K. J., and Stack, M. S. (2002) Proteinase suppression by E-cadherin mediated cell-cell attachment in premalignant oral keratinocytes. *J Biol Chem* (in press).

Cameron LA, Svitkina TM, **Vignjevic D**, Theriot JA, Borisys GG. Dendritic organization of actin comet tails. *Curr Biol*. 2001 Jan 23;11(2):130-5.

**Vignjevic D**, Yazar D, Welch M, Peloquin J, Svitkina T, Borisys GG. (2002) Formation of filopodial-like bundles in vitro from a dendritic network. *Journal of Cell Biology*, submitted

A complete list of trainee abstracts can be found in the Appendix.

## CONCLUSIONS:

The Molecular Biology of Breast Neoplasia has enabled the Cancer Center to provide state of the art laboratory and didactic training to 4 predoctoral students and two postdoctoral fellows in Year 02. Dr. Jordan has established the Breast Cancer Journal Club to bring together the members of the Training Program on a weekly basis to discuss relevant journal articles and areas of research. Predoctoral trainees on the Molecular Biology of Breast Neoplasia also participate in the Tumor Cell Biology and Carcinogenesis courses offered through the Integrated Graduate Program of Northwestern University Medical School as well as departmental seminars and journal clubs that have direct relevance to breast cancer. The Cancer Center's NCI funded SPORC in Breast Cancer Program provides further educational opportunities. In Winter Quarter 2002 we implemented an integrated course in breast cancer biology and treatment. The monthly lectures present an integrated overview of clinical breast cancer for laboratory scientists. The goal is to enhance the trainees' understanding of clinical breast cancer so that the relevance of their laboratory research can be stimulated.



APPENDIX I  
TRAINEE ABSTRACTS

**Abstracts:**

In vitro system for filopodia formation. **Vignjevic D**, Svitkina T, Borisy GG. 41st American Society for Cell Biology Meeting, Washington DC; 2001

Are Espins Mediators of Actin Polymerization in Parallel Actin Bundles? Changyaleket B, **Vignjevic D**, Eytan R, Zheng L, Borisy GG, Bartles JR. 41st American Society for Cell Biology Meeting, Washington DC; 2001

The role of alpha-actinin in actin based motility of Listeria. **Vignjevic D**, Peloquin J, Svitkina T, Borisy GG. 40<sup>th</sup> American Society for Cell Biology Meeting, San Francisco; 2000

Estradiol and SERMS Differentially Regulate Tethered ER $\alpha$ -mediated Transcription. **Suresh Pillai**, Jeffrey Weiss, Monika Jakacka, Eun Jig Lee, and J. Larry Jameson. Presented at the Endocrine Society Meeting in San Francisco, 2002

APPENDIX II  
BREAST CANCER JOURNAL CLUB

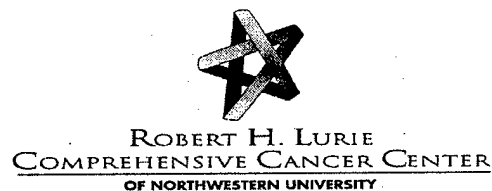
# Robert H. Lurie Comprehensive Cancer Center Breast Cancer Program Journal Club

*Vanderwicken Library  
Olson Pavilion 8260  
Tuesdays, 11 a.m.*

September	25	Barry Gehm
October	2	Sam Pappas
October	9	Robert Chatterton
October	16	Hong Liu
October	23	Clodia Osipo
October	30	Priya Gaina
November	6	Jerry Soff
November	13	Vince Cryns
November	20	Csaba Gajdos
November	27	Seema Khan
December	4	David Bentrem
December	11	Sunil Badve
December	18	Woo-Chan Park
December	25	<b>No Journal Club (X-mas)</b>
January	1	<b>No Journal Club (New Year)</b>
January	8	Sandy Pearce
January	15	Danijela Vignjevic
January	22	Mike Werner
January	29	Ana Levenson
February	5	Sudhakar Baluchamy
February	12	Peter Gann
February	19	Hao Wang
February	26	Sharon Stack

March	5	Ruth O'Regan
March	12	Yi Wu
March	19	Bin Chen
March	26	Toshio Ishikawa
April	2	MinSun Chang
April	9	<b>No Journal Club</b> (AACR)
April	16	Sue Gapstur
April	23	Suresh Pillai
April	30	Bayar Thimmapaya
May	7	Jennifer MacGregor Schafer
May	14	Boris Pasche
May	21	Meri Kamradt

APPENDIX III  
ADVANCED TOPICS IN BREAST CANCER



## Advanced Topics in Breast Cancer Course

**V. Craig Jordan, Ph.D., D.Sc.**  
Course Director

Advanced Topics in Breast Cancer will consist of eight classes taught by members of the Robert H. Lurie Comprehensive Cancer Center Breast Cancer Program. All sessions will be held on Wednesdays in the Vanderwicken Library, Olson 8260, from 9 am to 10:30 am. The final class will present current controversies in breast cancer.

DATE	FACULTY	TOPIC
January 9, 2002	Susan Gapstur, Ph.D.	Epidemiology of Breast Cancer
February 13, 2002	Monica Morrow, M.D.	Surgical Management of Breast Cancer
March 13, 2002	Sunil Badve, M.D.	Pathology of Breast Cancer
April 10, 2002	Gerald Soff, M.D.	Angiogenesis and Breast Cancer
May 8, 2002	V. Craig Jordan, Ph.D.	Endocrine Therapy of Breast Cancer
June 12, 2002	William Gradishar, M.D.	Medical Oncology of Breast Cancer
July 10, 2002	Boris Pasche, M.D., Ph.D.	Genetics of Breast Cancer
August 14, 2002	V. Craig Jordan, Ph.D.	Controversies in Breast Cancer

APPENDIX IV  
PUBLICATIONS

Submitted: July 9, 2002

**Collagen Binding Properties of the MT1-MMP Hemopexin C Domain: The  
Ectodomain of the 44-kDa Autocatalytic Fragment of  
MT1-MMP Inhibits Cell Invasion by Disrupting Native Type I Collagen Cleavage**

**Eric Tam<sup>‡</sup>, Yi I. Wu<sup>¶</sup>, Georgina S. Butler<sup>§</sup>, M. Sharon Stack<sup>¶</sup>, and Christopher M.  
Overall<sup>‡</sup> <sup>§</sup> <sup>‡‡</sup>**

*From the Departments of <sup>‡</sup>Biochemistry and Molecular Biology, <sup>§</sup>Oral Biological and  
Medical Sciences, University of British Columbia, Vancouver, Canada, <sup>¶</sup>Department of  
Cell and Molecular Biology, Northwestern University Medical School, Chicago, USA*

<sup>‡‡</sup> To whom correspondence should be addressed:

Christopher M. Overall  
University of British Columbia  
2199 Wesbrook Mall  
J.B. Macdonald Building  
Vancouver, B.C.  
V6T 1Z3  
Canada

Email: [chris.overall@ubc.ca](mailto:chris.overall@ubc.ca)

Fax: 604-822-3562

Tel: 604-822-2958

**Running Title:** The role of collagen binding by the MT1-MMP hemopexin C domain

<sup>1</sup>The abbreviations used are: MMP, matrix metalloproteinase; MT, membrane type; TIMP, tissue inhibitor of metalloproteinases; DMEM, Dulbecco's modified essential medium; BSA, bovine serum albumin; ConA, concanavalin A.



## SUMMARY

Upregulation of the collagenolytic membrane type-1 matrix metalloproteinase (MT1-MMP) leads to increased MMP-2 (gelatinase A) activation and MT1-MMP autolysis. The autocatalytic degradation product is a cell surface 44-kDa fragment (Gly<sup>285</sup>-Val<sup>582</sup>) of MT1-MMP in which the ectodomain consists of only the linker, hemopexin C domain and the stalk segment found before the transmembrane sequence. In the collagenases, hemopexin C domain exosites bind native collagen which is required for triple helicase activity during collagen cleavage. We investigated the collagen binding properties and the role of the hemopexin C domain of MT1-MMP and of the 44-kDa MT1-MMP ectodomain in collagenolysis. Recombinant proteins, MT1-LCD (Gly<sup>285</sup>-Cys<sup>508</sup>), consisting of the linker and the hemopexin C domain, and MT1-CD (Gly<sup>315</sup>-Cys<sup>508</sup>), which consists of the hemopexin C domain only, were found to bind native type I collagen but not gelatin. Functionally, MT1-LCD inhibited collagen-induced MMP-2 activation in fibroblasts, suggesting that interactions between collagen and endogenous MT1-MMP directly stimulate the cellular activation of pro-MMP-2. MT1-LCD, but not MT1-CD, also blocked the cleavage of native type I collagen by MT1-MMP *in vitro*, indicating an important role for the MT1-MMP linker region in triple helicase activity. Similarly, soluble MT1-LCD, but not MT1-CD or peptide analogs of the MT1-MMP linker, reduced the invasion of type I collagen matrices by MDA-MB-231 cells as did the expression of recombinant 44-kDa MT1-MMP. Together, these studies demonstrate that generation of the 44-kDa MT1-MMP autolysis product regulates collagenolytic activity and subsequent invasive potential, suggesting a novel feedback mechanism for the control of pericellular proteolysis.

## INTRODUCTION

Type I collagen is the most abundant protein of the extracellular matrix and is an important structural component in blood vessels, skin, tendons, ligaments, and bone (1). Accordingly, the synthesis and degradation of type I collagen is tightly regulated. Disruptions in this homeostasis can lead to diseases such as pulmonary fibrosis, scleroderma, arthritis, and osteoporosis, which if untreated, can result in loss of tissue function and integrity. In a number of cancer cells the capacity to degrade type I collagen and invade through type I collagen matrices often correlates with metastatic potential (2)—a characteristic that is as important for the local dissemination of tumor cells that type IV collagen degradation and basement membrane penetration is for metastasis (3). Despite the importance of maintaining correct collagen homeostasis in tissues, the proteases responsible for type I collagen degradation *in vivo* remain unclear. An intracellular pathway may play an important role in collagen degradation (4) that, in bone, utilizes the cysteine protease cathepsin K at low pH (5). Extracellularly, fibrillar type I collagen may be degraded at neutral pH by several matrix metalloproteinases (MMPs), a 24-member family of zinc-dependent endopeptidases in man (2). The major collagenolytic MMPs are the secreted collagenases MMP-1, -8, and -13 (6), and the cell surface membrane type (MT)1-MMP (7,8). MT1-MMP also activates collagenase-2 (MMP-13) (9) and is the primary activator of MMP-2 (10), a gelatinase that exhibits weak native type I collagenolytic activity (11-13).

MMPs share a common overall structure consisting of a propeptide, catalytic domain, linker (also called a hinge), and a hemopexin C domain (14). While the majority of MMPs are secreted as latent zymogens, MT-MMPs, the largest subgroup of MMPs, are membrane anchored by the presence of a type I transmembrane sequence and cytoplasmic tail (MT1-, MT2-, MT3-, and MT5-MMP) or by glycosylphosphatidylinositol linkage (MT4- and MT6-MMP) (14). MT1-MMP is activated intracellularly by proprotein convertase-dependent or independent pathways (15,16) and is expressed as an active protease on the surface of many normal and pathological cell types (10,17). The importance of MT1-MMP is indicated by its requirement for the invasion of endothelial and cancer cells through type I collagen matrices (18-20). Moreover, mice deficient in MT1-

MMP developed severe aberrations in type I collagen-abundant tissues, such as bone and skin, and the mice exhibited arthritis and scleroderma (21,22). In man, homoallelic loss-of-function mutations in the MMP-2 gene result in excessive bone resorption and arthritis (23). This condition resembles the phenotype of the MT1-MMP knockout mouse supporting the close functional connection of MMP-2 and MT1-MMP in regulating pericellular collagen homeostasis in the mouse and man.

Native type I collagen consists of two  $\alpha 1(I)$  chains and one  $\alpha 2(I)$  chain interwound in a right-handed triple helix that is resistant to cleavage by most proteinases at neutral pH with the exception of the MMP collagenases (14). Because the active site of collagenolytic MMPs can only accommodate a single  $\alpha$ -chain, cleavage of the three  $\alpha$ -chains occurs sequentially at the single collagenase-susceptible site, Gly<sup>775</sup>-Ile/Leu<sup>776</sup>, to generate 3/4- and 1/4-collagen fragments. To achieve this, the collagen helix must be initially unwound by a triple helicase mechanism in order to expose the scissile bonds. This critical step requires the presence of collagen binding exosites (14), in addition to elements within the active site (24-26). In MMP-1, -8, and -13, the hemopexin C domain supports binding to collagen and is required for native collagen cleavage (27-32). Deletion or mutation of the MMP-8 linker also reduces collagenolysis (33,34). Furthermore, synthetic peptide analogs of the MMP-1 linker bound collagen and inhibited collagen cleavage (35). Interestingly, the 35-amino acid residue linker of MT1-MMP is twice the length of other collagenase linkers (18 residues), however, the significance of this and its role in collagen cleavage has yet to be examined.

The regulation of MT1-MMP activity, MMP-2 activation and pericellular type I collagen levels is complex. In a variety of cells, stimulation by fibrillar type I collagen has been shown to increase the cell surface expression of MT1-MMP and induce the cellular activation of pro-MMP-2 (36-42). This response is in part dependent on  $\beta 1$  integrin clustering (40,42,43) and is potentially self regulating as type I collagen is susceptible to MT1-MMP and MMP-2 proteolysis (44). Concentration of MT1-MMP by overexpression (45,46) or clustering interactions favors MMP-2 activation (47-49) and collagenolysis (50). Concomitant with increased MT1-MMP expression and MMP-2 activation is the

autocatalytic processing of MT1-MMP at Gly<sup>284</sup>-Gly<sup>285</sup> to shed the catalytic domain from the hemopexin C domain, which is retained on the cell membrane (40,46,51). Hence, the ectodomain of the residual 44-kDa MT1-MMP fragment (Gly<sup>285</sup>-Val<sup>582</sup>) on the cell surface consists of the linker, hemopexin C domain and stalk segment only (see Fig. 1A) and so is catalytically inactive. The significance of the 44-kDa MT1-MMP *in vivo* is not clear. In addition to being present at increased levels following cell binding to type I collagen, the 44-kDa MT1-MMP has also been detected on the surface of tumor cells (44,51). During MMP-2 activation, TIMP-2-free MT1-MMP must be in close proximity to a trimeric complex of MT1-MMP/TIMP-2/pro-MMP-2 in order to activate the bound pro-MMP-2 (52). The mechanisms of MT1-MMP oligomerization are not clear. Recombinant hemopexin C domain of MT1-MMP did not form oligomers in solution nor modulate MMP-2 activation when added to cells (47). Recent reports using transmembrane MT1-MMP chimera and deletion mutants have suggested that the hemopexin C domain can mediate homophilic complex formation of cellular MT1-MMP for efficient MMP-2 activation (48,49). Expression of a transmembrane tethered MT1-MMP hemopexin C domain lacking the linker, termed PEX (Thr<sup>313</sup>-Val<sup>582</sup>), in HT1080 cells inhibited MT1-MMP oligomerization, the cellular activation of pro-MMP-2 and Matrigel invasion (48), a function previously attributed to MMP-2 proteolytic activity against type IV collagen (53).

Considering that MT1-MMP is a collagenase, we hypothesized that exosites on the hemopexin C domain would bind to type I collagen and be essential for collagenolytic activity. Thus, the autolytically generated 44-kDa MT1-MMP ectodomain would be predicted to modulate pericellular collagenolysis on the membrane through dominant-negative interactions. Since native type I collagen stimulates MMP-2 activation, we also hypothesized that collagen binding by the hemopexin C domain of MT1-MMP would modulate MMP-2 activation with 44-kDa MT1-MMP opposing these effects *in vivo*. Experiments reported here demonstrate that collagen binding by the MT1-MMP hemopexin C domain is essential for collagenolytic activity and enhancement of MMP-2 activation by MT1-MMP. Inhibition of this interaction either *in vitro* or on the cell surface inhibits collagen degradation. Together, these studies suggest a novel feedback

mechanism through which generation of the 44-kDa MT1-MMP autolysis product regulates pericellular collagenolytic activity and subsequent invasive potential.

## EXPERIMENTAL PROCEDURES

**Materials**—Rat-tail type I collagen was prepared as previously described (54). Vitrogen® was purchased from Cohesion (Palo Alto, CA). Biotin-labeled type I collagen was prepared as previously described (55). Human placental type I collagen was purchased from Sigma (Saint Louis, MS). The triple helical nature of collagen was confirmed by the absence of trypsin sensitivity at an enzyme/substrate ratio of 1:10 over 3 h. The general hydroxamate inhibitor BB2116 was provided by British Biotech Pharmaceuticals (Oxford, UK). Hydroxamate inhibitor GM6001 and AB8102 (blocking antibody raised against the human MT1-MMP catalytic domain) were purchased from Chemicon (Temecula, CA). The polyclonal antibody RP1MMP-14 (raised against the MT1-MMP linker) was purchased from Triple Point Biologics (Portland, OR). The affinity-purified polyclonal antibodies,  $\alpha$ MT1-CD and  $\alpha$ His<sub>6</sub> were described previously (47).

**Synthetic Peptides and Recombinant Proteins**—The following MT1-MMP linker peptide analogs were synthesized: MT1-L18 (R<sup>302</sup>PSVPDKPKNPTYGPNIC<sup>319</sup>) (University of Victoria, Canada) and MT1-L35 (G<sup>285</sup>ESGFPTKMPPQPRTTSRPSVPDKPKNP TYGPNIC<sup>319</sup>) (Tufts University, MA), and verified by mass spectrometry. Recombinant domains of human MT1-MMP and MMP-2 were expressed in *E. coli* as N-terminal His-tagged proteins. The MT1-MMP hemopexin C domain (CD) with or without the linker (L) (MT1-LCD, Gly<sup>285</sup>-Cys<sup>508</sup> and MT1-CD, Gly<sup>315</sup>-Cys<sup>508</sup>) (see Fig. 1A) and the MMP-2 hemopexin C domain with the linker (MMP2-LCD, Gly<sup>446</sup>-Cys<sup>660</sup>) were prepared as previously described (47). Recombinant human MMP2-CBD (Val<sup>220</sup>-Gln<sup>393</sup>) (collagen binding domain consisting of three fibronectin type II modules) was prepared previously (54). Any bacterial endotoxins in purified recombinant protein preparations were removed by polymyxin B agarose columns (Sigma). The fidelity of purified recombinant proteins was confirmed by electrospray ionization mass spectrometry and N-terminal Edman sequencing of protein bands cut from the membrane of Western blots. Human soluble (s) MT1-MMP, truncated C-terminal to the hemopexin C domain (sMT1-MMP), was kindly provided by British Biotech Pharmaceuticals (Oxford, UK). Recombinant human MMP-2, TIMP-1 and TIMP-2 were expressed in a mammalian cell system and purified as

previously described (56) or kindly provided by Dr. H. Nagase (Imperial College School of Medicine, UK).

*Electrophoretic Techniques*—Samples in reducing (65 mM dithithreitol) or non-reducing sample buffer (125 mM Tris-HCl, pH 6.8, 2.0 % SDS, 2.0 M urea, 0.05 % bromophenol blue) were separated on 15% SDS-PAGE gels and analyzed by either silver nitrate staining or by Western blotting using  $\alpha$ MT1-CD and  $\alpha$ His<sub>6</sub> antibodies. Enhanced chemiluminescence (ECL) detection was performed according to manufacturer's instructions (Amersham Pharmacia Biotech). For zymographic analysis, samples were separated under non-reducing conditions on 10% SDS-PAGE gels co-polymerized with 0.5 mg/ml gelatin. Gels were washed for 30 min with 2.5 % Triton X-100, rinsed with deionized water, and incubated with assay buffer (100 mM Tris, pH 8.0, 30 mM CaCl<sub>2</sub>, 0.05 % Brij, 0.025% NaN<sub>3</sub>) at 37 °C for 4 h before staining with Coomassie Brilliant Blue G250.

*Gel-filtration chromatography*—Purified MT1-LCD (0.5 mg) was subjected to gel-filtration chromatography on a Superdex 75 column equilibrated with PBS (10 mM Na<sub>2</sub>HPO<sub>4</sub>, 1.8 mM NaH<sub>2</sub>PO<sub>4</sub>, 2.7 mM KCl, 140 mM NaCl, pH 7.4) and run on an AKTA Purifier (Amersham Pharmacia Biotech). Protein elution was monitored at 215 nm. Molecular weight standards used were BSA (67 kDa), ovalbumin (43 kDa), chymotrypsin A (25 kDa) and ribonuclease A (13.7 kDa).

*Solid-Phase Binding Assays*—Native and heat-denatured type I collagen (rat tail) (5  $\mu$ g/ml) were diluted in 15 mM Na<sub>2</sub>CO<sub>3</sub>, 35 mM NaHCO<sub>3</sub>, 0.02% NaN<sub>3</sub>, pH 9.6 (100  $\mu$ l) and coated onto 96-microwell plates (Falcon) overnight at 4 °C as described previously (54,57). Wells coated with myoglobin served as a control for non-specific binding. The coated wells were blocked with 1% BSA to which serially diluted recombinant proteins in PBS (100  $\mu$ l total volume) were added and incubated for 1 h at room temperature. After extensive washes, bound proteins were quantitated using affinity-purified polyclonal antibodies followed by incubation with goat anti-rabbit alkaline phosphatase-conjugated secondary antibody. Substrate, *p*-nitrophenyl phosphate disodium (Sigma), was added to the wells and color development was monitored at 405 nm in a Thermomax plate reader (Molecular Devices).

*Ligand Blot Assays*—Proteins (5  $\mu$ g) in 50 mM Tris-HCl, pH 8.0, 150 mM NaCl were filtered onto an Immobilon-P® membrane (Millipore) by vacuum. Membranes were blocked with 1% BSA in PBS and incubated with biotin-labeled native type I collagen in PBS/Tween 20 for 1 h. Bound collagen was visualized using horseradish peroxidase (HRP)-conjugated streptavidin and ECL detection.

*Enzyme Assays*—Biotin-labeled type I collagen (0.025 pmol) was incubated with either sMT1-MMP or MMP-2 in assay buffer (50 mM Tris-HCl, pH 7.4, 200 mM NaCl, 5 mM  $\text{CaCl}_2$ , 3.8 mM  $\text{NaN}_3$ , 0.05 % Brij) for 18 h at 28 °C. MMPs were activated with 2 mM 4-aminophenylmercuric acetate. Recombinant proteins and BB2116 in assay buffer were added to the reactions where indicated. Following digestion, samples were separated by 7.5 % SDS-PAGE and analyzed by Western blotting using streptavidin-HRP and ECL detection.  $\alpha 1(I)$  and  $\alpha 2(I)$  chains were quantitated by scanning densitometry and the percentage of native collagen cleavage was calculated as previously described (58). Cleavage of the quenched fluorescent substrate, Mca-Pro-Leu-Gly-Dpa-Ala-Arg-NH<sub>2</sub>, was performed as described previously (56). MT1-LCD and MT1-CD in assay buffer (100 mM Tris-HCl, pH 7.4, 100 mM NaCl, 10 mM  $\text{CaCl}_2$ , 0.05 % Brij) were added to the reaction where indicated.

*Transmembrane MT1-MMP and MT1-MMP Hemopexin C Domain Constructs*—The mammalian expression vector pCR3.1-Uni (Invitrogen) carrying human MT1-MMP cDNA was the generous gift of Dr. D. Pei (University of Minnesota, MN). To express cell (c) surface transmembrane MT1-MMP deletion mutants, cMT1-CD ( $\Delta 112$ -315) and cMT1-LCD ( $\Delta 112$ -284), two-step overlapping PCR using high-fidelity PCR enzyme Pfx (Invitrogen) was performed with T7 and 5'-ATATGTCGACCGGCCGCTCCCGATGGGC-3', reverse primer (Invitrogen) as external primers, and 5'-CGAAGGAAGCGCCCCAACATCTGTGACGGGAAC-3' and 5'-ACAGATGTTGGGGCGCTTCCTTCGAACATTGGC-3' (cMT1-CD,  $\Delta 112$ -315), or 5'-CGAAGGAAGCGCGGTGAGTCAGGGTTCCTCCACC-3' and 5'-CCCTGACTCACCGCGCTTCCTTCGAACATTGGCC-3' (cMT1-LCD,  $\Delta 112$ -284), as



internal primer pairs. The catalytically inactive MT1-MMP (Glu240Ala) mutant construct was generated using 5'-GGTGGCTGTGCACGCGCTGGGCCATGCC-3' and 5'-GGCATGGCCCAGCGCGTGCACAGCCACC-3' (Glu240Ala) primers. Full-length constructs were synthesized by PCR with T7 and reverse primers, digested with Hind III and EcoR I, ligated back to pCR3.1-Uni vector and fully sequenced.

*Cell Culture and Stable Transfection*—Early passage human gingival fibroblasts were kindly provided by Dr. D. Brunette (University of British Columbia, Canada) and maintained in Dulbecco's modified essential medium (DMEM) containing 10% newborn calf serum (Life Technologies). MDA-MB-231 breast carcinoma cells were kindly provided by Dr. V.G. Jordan (Northwestern University, IL) and cultured in DMEM (Cellgro) supplemented with 10% fetal bovine serum (U.S. Bio-technologies Inc). MDA-MB-231 cells were transfected with MT1-MMP cDNA constructs using FuGENE 6 (Roche) according to manufacturer's instructions. Stable cell lines were clonal-selected and maintained in medium containing 1 mg/ml G418 (Mediatech Inc). For each line, 5 clones were pooled and used in the experiments.

*Transwell Invasion and Migration Assay*—MDA-MB-231 cell invasion and migration assays through type I collagen (human placental) were performed as described previously (42). Endotoxin-free recombinant proteins, linker peptide analogs and antibodies in PBS were added to the cell media with BSA or IgG as controls. GM6001 was added to the cells in DMSO.

*Collagen Gels*—To prepare collagen gels, 8 volumes of Vitrogen was neutralized with 1 volume of 10× concentrated PBS and 1 volume of 0.1 M NaOH. Fibroblasts were detached with PBS containing 0.54 mM EDTA and 1.1 mM glucose, and resuspended in a neutralized Vitrogen solution (2.0 mg/ml) containing 11.3% DMEM and 2.5% new born calf serum. The cell/collagen solution (75 µl) was then transferred into 96-well tissue culture plates and incubated at 37 °C for 1 h to allow for collagen polymerization. Cells were supplemented with DMEM containing 2.5% new born calf serum for 18 h. Collagen gels were then rinsed with DMEM and cells were cultured under serum-free conditions with or

without MT1-LCD (endotoxin-free, in PBS) for the duration of the experiment. Cell conditioned media was replaced every 24 h and analyzed by gelatin zymography after 72 h.

*Latex Beads*—Native and denatured type I collagen (100 µg/ml) were incubated with latex beads (1%) (Sigma) for 1 h at room temperature to allow for adsorption. The beads were then washed with PBS and blocked with 1% BSA for 1 h. Beads not absorbed with collagen served as a control. Blocked beads were rinsed with PBS and resuspended in DMEM at a concentration of 0.2% (v/v). Fibroblasts cultured in 96-well tissue culture plates were rinsed and incubated in serum-free medium for 1 h prior to incubation with the latex beads in DMEM (100 µl). Endotoxin-free MT1-LCD in PBS was added the latex bead preparations where indicated. Cells were cultured for 24 h after which the conditioned cell media was analyzed by gelatin zymography.

## RESULTS

*Recombinant Protein Expression*—To characterize the MT1-MMP hemopexin C domain and the ectodomain of 44-kDa MT1-MMP, two forms of the MT1-MMP hemopexin C domain were cloned and expressed in *E. coli* as previously described (47). MT1-LCD (Gly<sup>285</sup>-Cys<sup>508</sup>) corresponds to the N-terminus of 44-kDa MT1-MMP and includes both the linker and the hemopexin C domain (Fig. 1Aiv). MT1-CD (Gly<sup>315</sup>-Cys<sup>508</sup>) consists of the hemopexin C domain only (Fig. 1Aiv). Yields of purified protein were typically ~20 mg from 3 L of liquid culture. The identities of the purified proteins were confirmed by Western blotting with  $\alpha$ MT1-CD antibody (Fig. 1B) and  $\alpha$ His<sub>6</sub> (data not shown). Non-reducing SDS-PAGE analysis demonstrated the absence of dimeric intermolecular disulfide cross-linked aggregates. Reducing SDS-PAGE and electrospray mass spectrometry determination of the purified protein masses were consistent with the predicted masses. As shown in Fig. 1B, both MT1-LCD (27,894 Da) and MT1-CD (24,612 Da) were within 1-2 Da of the predicted mass after accounting for the removal of the N-terminal methionine and hydrogen atoms after disulfide bond formation. Edman sequencing confirmed N-terminal methionine processing and the presence of the N-terminal His<sub>6</sub> tag (Fig. 1B). MT1-LCD did not form non-covalent multimeric complexes under native conditions as shown by the elution of a single peak at 28 kDa corresponding to the monomeric form of MT1-LCD upon gel filtration chromatography (Fig 1C).

*Collagen Binding Properties of the MT1-MMP Hemopexin C Domain*—We first assessed the collagen binding properties of the MT1-MMP hemopexin C domain by performing solid-phase binding assays with type I collagen, the preferred collagen substrate of MT1-MMP. As shown in Fig 2A, binding of MT1-CD and MT1-LCD to native collagen was similar indicating that the linker had little apparent effect on collagen binding affinity. Unlike MMP2-CBD, both MT1-CD and MT1-LCD did not bind denatured collagen (Fig. 2B). MMP2-LCD did not bind native or denatured type I collagen as shown previously (57). Binding of native type I collagen to MT1-CD and MT1-LCD was confirmed by ligand blot analysis with MMP2-LCD and BSA serving as negative controls (Fig. 2C).

*Collagen/MT1-MMP Hemopexin C Domain Interactions during Collagen-Induced MMP-2 Activation*— Physical clustering of MT1-MMP was previously shown to facilitate the pro-MMP-2 activation reaction by increasing the proximity of catalytically active MT1-MMP to the trimeric activation complex (52). Owing to the collagen binding properties of the MT1-MMP hemopexin C domain, we postulated that type I collagen may function as an *in vivo* mechanism to directly bind and concentrate cell surface MT1-MMP to facilitate the cellular activation of pro-MMP-2. To test this, human gingival fibroblasts were cultured in three-dimensional type I collagen gels for 72 h to stimulate the activation of pro-MMP-2. Soluble MT1-LCD was added to the cultures to compete with endogenous MT1-MMP for collagen binding. As shown in Fig. 3A, activation of pro-MMP-2 in the cell cultures was reduced with increasing concentrations of MT1-LCD. Control cells cultured on plastic did not activate pro-MMP-2. To confirm this response, latex beads coated with type I collagen were found to stimulate pro-MMP-2 activation in fibroblasts cultured on plastic (Fig. 3B). Consistent with our observations, induction of pro-MMP-2 activation by native collagen-adsorbed beads was reduced by the presence of MT1-LCD to the levels seen with BSA-adsorbed beads (Fig. 3B). The requirement for fibrillar collagen was confirmed as gelatin-adsorbed beads did not stimulate pro-MMP-2 activation. In the absence of latex beads, the addition of soluble native collagen to fibroblasts cultured on plastic produced inconsistent and variable levels of activation (data not shown). Together, these results demonstrate that native type I fibrillar collagen interactions with the MT1-MMP hemopexin C domain in fibroblasts may concentrate cell surface MT1-MMP to stimulate the cellular activation of pro-MMP-2.

*Effect of Exogenous MT1-MMP Hemopexin C Domain on Collagenolysis by sMT1-MMP and MMP-2*— Studies of collagenases have shown that the hemopexin C domain is required to support binding to and cleavage of collagen (27-29,31,32,59). To examine the role of the hemopexin C domain in MT1-MMP collagenolysis, recombinant hemopexin C domain constructs were incubated with sMT1-MMP and biotin-labeled type I collagen. Reactions were performed at 28 °C to maintain collagen triple helicity, as confirmed by the lack of collagen cleavage in the presence of trypsin even at a 1:10 enzyme/substrate mole ratio (data not shown). sMT1-MMP cleaved native type I collagen (Fig. 4A) and was

inhibited by TIMP-2 and BB2116 (data not shown). As seen in Fig. 4A (*left panel*), the sMT1-MMP cleavage of native type I collagen was inhibited by the presence of MT1-LCD in a concentration-dependent manner. In contrast, neither MT1-CD (Fig. 4A, *right panel*) nor the control protein, MMP2-LCD, had any effect on cleavage. The percentage of  $\alpha$ -chain cleavage for each reaction was quantitated by scanning densitometry and graphically plotted against the amount of MT1-LCD or MT1-CD added (Fig. 4B). The presence of hemopexin C domain proteins at the end of each reaction was confirmed by Western blot analysis (Fig. 4C). In contrast, MT1-CD and MT1-LCD did not affect sMT1-MMP activity against the quenched fluorescent substrate, Mca-Pro-Leu-Gly-Dpa-Ala-Arg-NH<sub>2</sub> (Table I), indicating that cleavage is independent of the hemopexin C domain. Owing to the unique association between MT1-MMP and MMP-2 *in vivo*, we assessed whether the MT1-MMP hemopexin C domain may affect MMP-2 collagenolysis. Similar to that observed for MT1-MMP, MT1-LCD, but not MT1-CD, disrupted MMP-2 cleavage of native type I collagen (Fig. 5).

*Collagen Binding Properties of MT1-MMP Linker Peptide Analogs and the Effect on Collagenolysis*—Although both MT1-MMP hemopexin C domain constructs share similar binding properties, only MT1-LCD disrupted collagenolysis. Since this result indicated an important role for the linker in native collagen cleavage, we generated two synthetic peptide analogs to further study the effect of the MT1-MMP linker on MT1-MMP collagenolysis. Using clustal alignments, we designed the peptide analog, MT1-L18 (Arg<sup>302</sup>-Cys<sup>319</sup>), to match an 18-amino acid residue region of similarity possessed by the collagenolytic MMPs, MMP-1, -2, -8, and -13 (Fig. 6A). MT1-L35 (Gly<sup>285</sup>-Cys<sup>319</sup>) encompasses the entire MT1-MMP linker and includes the unique 17-amino acid residue region that is N-terminal to the homologous 18-amino acid residue region (Fig. 6A). As shown in Fig. 6B, neither MT1-L18 nor MT1-L35 showed affinity for native (Fig. 6B*i*) or denatured type I collagen (Fig. 6B*ii*), indicating that the MT1-MMP linker alone does not contribute to collagen binding or that the collagen binding site spans the junction of the linker and hemopexin C domain. Similarly, both peptide analogs did not disrupt native type I collagen cleavage by sMT1-MMP, even at 1000-fold molar excess (Fig 6C). To determine if either linker peptide sequence could confer regulatory activity on the MT1-CD

polypeptide, MT1-L18 or MT1-L35 were added to the reaction mixture containing MT1-CD. As shown in Figure 6C, no inhibition of collagenolysis was observed. In a second set of experiments, MT1-LCD inhibited collagen cleavage as previously observed (Fig. 4), regardless of whether MT1-L18 or MT1-L35 was added. Since the presence of the linker sequence and the hemopexin C domain together as separate polypeptides is not sufficient for disrupting cleavage, these data suggest that the ability of the MT1-LCD to inhibit collagenolysis is context and/or conformation specific.

*Cellular Invasion of Type I Collagen is Inhibited by a 44-kDa MT1-MMP Ectodomain Fragment* — Active MT1-MMP is efficiently processed to a 44-kDa ectodomain fragment containing the MT1-LCD sequence (Gly<sup>285</sup>-Cys<sup>508</sup>) that is retained on the cell membrane (40,46,51). Since the soluble MT1-LCD inhibits native collagen cleavage by sMT1-MMP, we hypothesized that 44-kDa MT1-MMP may also function in a similar manner at the cell surface to modulate the collagenolytic activity of transmembrane MT1-MMP. To test this hypothesis, we used MDA-MB-231 breast carcinoma cells, which express endogenous MT1-MMP in the absence of detectable levels of MMP-2. Invasion of 3-dimensional collagen gels overlaid onto a porous polycarbonate filter requires collagenolytic activity (42). In control experiments, MDA-MB-231 cellular invasive activity was inhibited by the hydroxamate inhibitor GM6001, indicating a requirement for metalloproteinase activity (Fig. 7A). TIMP-2 significantly reduced invasion ( $p < 0.05$ ) whereas TIMP-1 had no effect (60), confirming the dependence for MT-MMPs in MDA-MB-231 cell invasion. A blocking antibody against the MT1-MMP active site (Fig. 7A, *anti-MT1*) also reduced invasion compared to IgG controls ( $p < 0.05$ ), identifying MT1-MMP as the critical protease in this process. Indeed, overexpression of MT1-MMP on MDA-MB-231 cells increased collagen invasion approximately 2.5-fold compared to vector transfectants ( $p < 0.05$ , Fig. 7A *black bars*). Furthermore, expression of the inactive mutant, MT1-MMP (Glu240Ala), on MDA-MB-231 cells resulted in inhibition of invasion to below control values and suggesting that this species may function as a dominant negative mutant.

To determine whether the MT1-LCD could inhibit cell-associated collagenolytic activity, cells were incubated with either BSA, MT1-LCD, or MT-L35. At low concentrations

(4  $\mu$ M), the invasion of MT1-MMP transfected (Fig. 7B) or parental (data not shown) MDA-MB-231 cells was unaffected. MT-L35 did not affect invasion at any concentration tested (data not shown). However, since MT1-LCD binds native collagen, the effective concentration of free protein available to the cells may be reduced by binding to the collagen filters. Therefore, the highest concentration possible with these protein preparations (30  $\mu$ M) was used to ensure saturation of binding sites within the collagen-coated filters and availability of free protein at the cell surface to interact with MT1-MMP. Collagen invasion was significantly reduced ( $p < 0.05$ , Fig. 7B) demonstrating inhibition of cell-associated MT1-MMP collagenolytic activity and confirming the *in vitro* analysis of MT1-LCD inhibiting collagen cleavage.

Because autolysis of transmembrane MT1-MMP leads to the accumulation of a cell surface 44-kDa MT1-MMP ectodomain fragment containing the hemopexin domain and linker and lacking the active site, the effect of this cell-associated fragment on cellular MT1-MMP-mediated collagenolysis was assessed. For this experiment, transmembrane cellular constructs of MT1-LCD (Gly<sup>285</sup>-Val<sup>582</sup>, designated cMT1-LCD) and MT1-CD (Pro<sup>316</sup>-Val<sup>582</sup>, designated cMT1-CD) (Fig. 8A) were expressed in MDA-MB-231 cells and type I collagen invasion assessed relative to vector transfected controls. Intracellular furin processing of these constructs at R<sup>111</sup> generates the 44-kDa MT1-MMP and the linker-deleted form thereof. Expression of cMT1-LCD significantly reduced invasion compared to cells expressing cMT1-CD ( $p < 0.05$ , Fig 8B), confirming the *in vitro* biochemical results and indicating the importance of the MT1-MMP linker-hemopexin domain in native collagen cleavage by cells. In control experiments, migration of MDA-MB-231 cells toward type I collagen, a process independent of collagenase activity (42, 61) was unaffected by expression of cMT1-LCD or cMT1-CD (Fig. 8C). As these data clearly demonstrate the ability of cMT1-LCD to modulate type I collagen cleavage by transmembrane MT1-MMP, our results suggest that a function of endogenous MT1-MMP autolysis to produce 44-kDa MT1-MMP is to regulate pericellular collagenolytic activity.

## DISCUSSION

As an integral membrane protein, MT1-MMP appears suited for coordinating the homeostatic catabolism of pericellular type I collagen under the guide of the cell (62-64, 65). MT1-MMP mediates collagen degradation directly by cleaving native collagen and, indirectly, by activating the gelatinase and weak collagenase, MMP-2 (11-13). Spatially and temporally, these two distinct activities of MT1-MMP regulate collagenolytic and gelatinolytic activities on the cell surface. The studies reported here have revealed the importance of the MT1-MMP hemopexin C domain and linker in the mechanism collagen cleavage, and demonstrated the role of collagen binding to MT1-MMP in stimulating MMP-2 activation by cells. Moreover, these actions may be modulated in a dominant negative manner by the 44-kDa remnant form of MT1-MMP on the cell surface, revealing a novel regulatory function in proteolysis for an autolytic fragment of a protease.

The structure of collagen presents a challenge for proteolytic cleavage as indicated by the low  $k_{cat}/K_m$  values for collagenases (66). Despite several studies from a number of laboratories, the triple helix mechanism remains enigmatic (14). Our use of recombinant domains and polypeptides to probe the exosite requirements of MT1-MMP for collagenolysis revealed similar domain requirements for triple helix activity as the secreted collagenases. The binding of the MT1-MMP hemopexin C domain, with or without the linker, to native collagen is consistent with previous reports for the collagenolytic MMPs (27, 30-32). Interestingly, the MT1-MMP hemopexin C domain does not bind denatured collagen. This suggests that following cleavage, subsequent denaturation of the collagen would result in the release of MT1-MMP from the cleaved substrate facilitating turnover.

Inhibition of sMT1-MMP collagen cleavage using MT1-MMP hemopexin C domain constructs required the presence of the linker indicating that collagen binding, by the hemopexin C domain alone, is not sufficient to disrupt collagenolysis. This requirement was also observed in MMP-2 collagenolysis as MT1-LCD, but not MT1-CD, blocked MMP-



2 cleavage of native collagen. Protein engineering studies of MMP-1 and MMP-8 have previously shown a role for the linker in triple helicase activity (33-35); however, our studies have revealed some unique features of the MT1-MMP linker. Souza *et al* proposed that the MMP-1 collagenase linker, owing to its proline content, intercalates with the collagen triple helix, thereby displacing individual  $\alpha$ -chains for cleavage (67). We found that MT1-MMP linker peptide analogs of either the full-length 35-amino acid residue linker or the 18-amino acid residue region corresponding to that found in the collagenases, did not bind native or denatured type I collagen. These results indicate that the MT1-MMP linker may not bind or intercalate with the collagen triple helix as proposed for the MMP-1 linker. Potentially, the full collagen binding exosite of the MT1-MMP hemopexin C domain that recognizes the 3/4-1/4-collagen site may span the linker/hemopexin C domain junction, thereby accounting for the lack of collagen binding by the linker analogs alone. The MT1-MMP linker, when connected to the hemopexin C domain, may act as a specificity determinant directing binding of the protease to the 3/4-1/4-collagen cleavage site. Thus, competition from MT1-LCD, but not MT1-CD, may block MT1-MMP from binding collagen here and so inhibit cleavage. Topographically, the MT1-MMP, and other collagenase linkers, may also correctly configure the catalytic domain relative to the hemopexin C domain for collagenolytic competence. Indeed the MT1-MMP linker has predicted rigidity due to the presence of 9 proline residues, with the X-ray crystallographic structure of the MMP-1 linker also indicating that the collagenase linker is not flexible (68). Hence, MT1-LCD binding of collagen may sterically disrupt the collagenolytic configuration of sMT1-MMP at the 3/4-1/4 collagen cleavage site, thereby inhibiting cleavage.

The importance of MT1-MMP in collagen homeostasis is supported by the finding that fibrillar type I collagen stimulates cell surface expression of MT1-MMP and subsequent MMP-2 activation (36,37,39,40,41). In these events, induction of MT1-MMP transcription is dependent on  $\beta_1$  integrin receptors and actin cytoskeleton rearrangement (43, 38). Clustering of  $\beta_1$  integrins by collagen ligation or antibody crosslinking induces *de novo* expression of MT1-MMP and subsequent MMP-2 activation (37,40,42). In addition to these transcriptional events, collagen-induced MMP-2 activation also involves an uncharacterized nontranscriptional response (69). Interestingly, our data reveals that

collagen may assemble MT1-MMP on the cell surface via binding to the hemopexin C domain, thereby increasing the local concentration of MT1-MMP for collagenolysis and efficient MMP-2 activation. In view of the demonstrated absence of oligomer formation by the MT1-LCD used here, we interpret the reduction in collagen-induced MMP-2 activation by MT1-LCD to be the result of competitive binding for collagen between the exogenous MT1-LCD and cell surface MT1-MMP, rather than competitively disrupting any MT1-MMP/MT1-MMP binding interactions. Indeed this observation may represent a biological mechanism similar to that obtained *in vitro* with ConA, which also clusters cell surface MT1-MMP (47). As previously shown, ConA increases the matrix degradative phenotype of the cell through transcriptional and post-transcriptional regulation of MMP and TIMP genes that was reflected by extensive endogenous collagen degradation in the conditioned media (50). Cleavage of cell surface collagen also releases collagen-bound pro-MMP-2, which can now enter the activation pathway, but when bound to collagen is recalcitrant to activation (70). Hence, pericellular collagen has multiple effects in binding and regulating the activities of collagenolytic MMPs.

MT1-MMP activity on the cell surface is also regulated by endocytosis (71,72), TIMP binding (56,73) and trimolecular complex formation (74,56), as well as the autolytic shedding of the catalytic domain to yield 44-kDa MT1-MMP (46,51,75). Currently, the role of 44-kDa MT1-MMP *in vivo* is not clear. It has been reported recently that the hemopexin C domain and the cytoplasmic tail of MT1-MMP mediate homophilic interactions that increase MMP-2 activation (48,49). Using HT1080 cells Itoh *et al* (48) reported that expression of MT1-MMP PEX (Thr<sup>313</sup>-Val<sup>582</sup>), a truncated form of 44-kDa MT1-MMP that lacks most of the linker and hence is similar to cMT1-CD used here, reduced MMP-2 activation and subsequent Matrigel invasion, presumably by disrupting the formation of oligomeric MT1-MMP complexes—PEX is unfortunately a confusing designation for the MT1-MMP hemopexin C domain as PEX was already the name of a cell surface zinc metallopeptidase belonging to the neprilysin family (76-78). As reported here and previously (47), we have found no evidence for oligomerization using MT1-LCD or MT1-CD, emphasizing the importance of the stalk segment, transmembrane sequence and cytoplasmic tail in these proposed complexes. Unlike the effects of MT1-LCD in disrupting

the collagen-induced activation of MMP-2, the inability of soluble MT1-LCD or MT1-CD to competitively block MMP-2 activation in cells cultured on plastic reported previously (47), indicates the importance of cellular context for these effects and highlights the difference in collagen-mediated activation of MMP-2, which is blocked by MT1-LCD, from activation induced by MT1-MMP overexpression or ConA, which is not.

In our previous studies of chemokine cleavage by MMP-2 we found that chemokine binding to the hemopexin C domain markedly improved the catalytic efficiency of cleavage (79,80). Notably, addition of recombinant MMP-2 hemopexin C domain to incubation mixtures of chemokine and active MMP-2 in enzyme assays could totally block substrate cleavage (80). Therefore, the presence of the entire 35-amino acid residue linker and hemopexin C domain in the 44-kDa MT1-MMP ectodomain suggested to us that this autolytic product has the potential to antagonize the proteolytic activity of MT1-MMP in a dominant-negative manner by interacting with extracellular substrates. Our data demonstrates that expression of cMT1-LCD (Gly<sup>285</sup>-Val<sup>582</sup>), representing the 44-kDa MT1-MMP in its entirety (46), on MDA-MB-231 cells inhibits MT1-MMP-mediated type I collagen cleavage and cell invasion. The inhibitory effect of cMT1-LCD expression on cell invasion was confirmed by the addition of soluble MT1-LCD to MT1-MMP-transfected cells. This process is distinct from that reported previously (48) and discussed above as MDA-MB-231 cells, unlike HT1080 cells, do not express MMP-2. Nonetheless, the capacity of MT1-LCD to also block MMP-2 native collagen cleavage may amplify the downregulation of collagenolysis by blocking MMP-2 in addition to MT1-MMP. Invasion was also inhibited with the expression of catalytically inactive MT1-MMP (Glu240Ala) further supporting the role of MT1-MMP in collagen invasion and of the hemopexin C domain in collagen binding and triple helical collagen cleavage. Consistent with our biochemical analysis, neither the expression of cMT1-CD nor the addition of soluble MT1-CD affected cell invasion to a significant degree, confirming the importance of the MT1-MMP linker in context with the hemopexin C domain in collagenolysis. In view of these effects, it is also likely that 44-kDa MT1-MMP may reduce MMP-2 activation by reducing MT1-MMP clustering by pericellular collagen. However, this could not be directly tested since MDA-MB-231 cells do not

express MMP-2. Together, these results clearly reveal the 44-kDa MT1-MMP as a novel inhibitor of pericellular type I collagen cleavage by MT1-MMP and MMP-2 activities.

We have previously proposed models regarding the regulation of pericellular type I collagen levels upon  $\beta_1$  integrin induction of MT1-MMP and MMP-2 activity (14,40,70). Our collaborative investigation into the role of the 44-kDa MT1-MMP ectodomain adds a new dimension to this homeostatic process. As shown in Figure 9, fibrillar type I collagen induces a  $\beta_1$  integrin-dependent increase in MT1-MMP expression on the cell surface. Our data shows that the collagen binding properties of the MT1-MMP hemopexin C domain are necessary for native collagen cleavage and potentiates MMP-2 activation, most likely by concentrating MT1-MMP/TIMP-2/MMP-2 complexes with TIMP-free MT1-MMP (Fig 9A). In the MMP-2 activation process, MT1-MMP collagenolytic activities are suppressed by TIMP-2 binding to form the trimolecular pro-MMP-2 complex, and by MT1-MMP autolysis—converting the proteolytic signature of the cell from collagenolytic to gelatinolytic. Following pro-MMP-2 activation and MT1-MMP autolytic shedding, the accumulation of 44-kDa MT1-MMP further reduces pericellular collagenolysis by MT1-MMP and MMP-2 (Fig. 9B). Overall, these intimately related and complex events allow for a conversion of proteolytic activity to take place on the cell surface. This shift from a collagenolytic to a gelatinolytic profile is likely important for maintaining collagen homeostasis. Hence, the studies reported here reveal several new aspects in the biology of MT1-MMP as a consequence of native type I collagen binding by the hemopexin C domain. This also provides a novel explanation for the generation of MT1-MMP clusters on the cell surface and adds a new layer of control to the complex regulation of focal proteolysis by MT1-MMP and MMP-2.

## REFERENCES

1. Vuorio, E., and de Crombrughe, B. (1990) *Annu. Rev. Biochem* **59**, 837-872
2. Egeblad, M., and Werb, Z. (2002) *Nature Rev Cancer* **2**, 161-74.
3. Stetler-Stevenson, W. G., and Yu, A. E. (2001) *Semin Cancer Biol* **11**, 143-52.
4. Overall, C. M., and Sodek, J. (1988) *Matrix degradation in hard and soft connective tissues*. The Biological Mechanisms of Tooth Eruption and Root Resorption (Davidovitch, Z., Ed.), EBSCO Media, Birmingham, Alabama
5. Saftig, P., Hunziker, E., Wehmeyer, O., Jones, S., Boyde, A., Rommerskirch, W., Moritz, J. D., Schu, P., and von Figura, K. (1998) *Proc Natl Acad Sci U S A* **95**, 13453-8.
6. Nagase, H., and Woessner, J. F., Jr. (1999) *J Biol Chem* **274**, 21491-4.
7. Pei, D., and Weiss, S. J. (1996) *J Biol Chem* **271**, 9135-40.
8. Ohuchi, E., Imai, K., Fujii, Y., Sato, H., Seiki, M., and Okada, Y. (1997) *J Biol Chem* **272**, 2446-51.
9. Cowell, S., Knauper, V., Stewart, M. L., D'Ortho, M. P., Stanton, H., Hembry, R. M., Lopez-Otin, C., Reynolds, J. J., and Murphy, G. (1998) *Biochem J* **331**, 453-8.
10. Sato, H., Takino, T., Okada, Y., Cao, J., Shinagawa, A., Yamamoto, E., and Seiki, M. (1994) *Nature* **370**, 61-5.
11. Sodek, J., and Overall, C. M. (1992) *Matrix Suppl* **1**, 352-62
12. Aimes, R. T., and Quigley, J. P. (1995) *J Biol Chem* **270**, 5872-6.
13. Patterson, M. L., Atkinson, S. J., Knauper, V., and Murphy, G. (2001) *FEBS Lett* **503**, 158-62.
14. Overall, C. M. (2001) *Methods Mol Biol* **151**, 79-120
15. Yana, I., and Weiss, S. J. (2000) *Mol Biol Cell* **11**, 2387-401.
16. Rozanov, D. V., Deryugina, E. I., Ratnikov, B. I., Monosov, E. Z., Marchenko, G. N., Quigley, J. P., and Strongin, A. Y. (2001) *J Biol Chem* **276**, 25705-14.
17. Takino, T., Sato, H., Yamamoto, E., and Seiki, M. (1995) *Gene* **155**, 293-8.
18. Galvez, B. G., Matias-Roman, S., Albar, J. P., Sanchez-Madrid, F., and Arroyo, A. G. (2001) *J Biol Chem* **276**, 37491-500.
19. Belien, A. T., Paganetti, P. A., and Schwab, M. E. (1999) *J Cell Biol* **144**, 373-84.

20. Aznavoorian, S., Moore, B. A., Alexander-Lister, L. D., Hallit, S. L., Windsor, L. J., and Engler, J. A. (2001) *Cancer Res* **61**, 6264-75.
21. Holmbeck, K., Bianco, P., Caterina, J., Yamada, S., Kromer, M., Kuznetsov, S. A., Mankani, M., Robey, P. G., Poole, A. R., Pidoux, I., Ward, J. M., and Birkedal-Hansen, H. (1999) *Cell* **99**, 81-92.
22. Zhou, Z., Apte, S. S., Soininen, R., Cao, R., Baaklini, G. Y., Rauser, R. W., Wang, J., Cao, Y., and Tryggvason, K. (2000) *Proc Natl Acad Sci U S A* **97**, 4052-7.
23. Martignetti, J. A., Aqeel, A. A., Sewairi, W. A., Boumah, C. E., Kambouris, M., Mayouf, S. A., Sheth, K. V., Eid, W. A., Dowling, O., Harris, J., Glucksman, M. J., Bahabri, S., Meyer, B. F., and Desnick, R. J. (2001) *Nat Genet* **28**, 261-5.
24. Knauper, V., Patterson, M. L., Gomis-Ruth, F. X., Smith, B., Lyons, A., Docherty, A. J., and Murphy, G. (2001) *Eur J Biochem* **268**, 1888-96.
25. Chung, L., Shimokawa, K., Dinakarpanian, D., Grams, F., Fields, G. B., and Nagase, H. (2000) *J Biol Chem* **275**, 29610-7.
26. Brandstetter, H., Grams, F., Glitz, D., Lang, A., Huber, R., Bode, W., Krell, H. W., and Engh, R. A. (2001) *J Biol Chem* **276**, 17405-12.
27. Allan, J. A., Hembry, R. M., Angal, S., Reynolds, J. J., and Murphy, G. (1991) *J Cell Sci* **99**, 789-95.
28. Clark, I. M., and Cawston, T. E. (1989) *Biochem J* **263**, 201-6.
29. Windsor, L. J., Birkedal-Hansen, H., Birkedal-Hansen, B., and Engler, J. A. (1991) *Biochemistry* **30**, 641-7.
30. Murphy, G., Allan, J. A., Willenbrock, F., Cockett, M. I., O'Connell, J. P., and Docherty, A. J. (1992) *J Biol Chem* **267**, 9612-8.
31. Knauper, V., Osthues, A., DeClerck, Y. A., Langley, K. E., Blaser, J., and Tschesche, H. (1993) *Biochem J* **291**, 847-54.
32. Knauper, V., Cowell, S., Smith, B., Lopez-Otin, C., O'Shea, M., Morris, H., Zardi, L., and Murphy, G. (1997) *J Biol Chem* **272**, 7608-16.
33. Hirose, T., Patterson, C., Pourmotabbed, T., Mainardi, C. L., and Hasty, K. A. (1993) *Proc Natl Acad Sci U S A* **90**, 2569-73.
34. Knauper, V., Docherty, A. J., Smith, B., Tschesche, H., and Murphy, G. (1997) *FEBS Lett* **405**, 60-4.

35. de Souza, S. J., and Brentani, R. (1992) *J Biol Chem* **267**, 13763-7.
36. Azzam, H. S., and Thompson, E. W. (1992) *Cancer Res* **52**, 4540-4.
37. Gilles, C., Polette, M., Seiki, M., Birembaut, P., and Thompson, E. W. (1997) *Lab Invest* **76**, 651-60.
38. Tomasek, J. J., Halliday, N. L., Updike, D. L., Ahern-Moore, J. S., Vu, T. K., Liu, R. W., and Howard, E. W. (1997) *J Biol Chem* **272**, 7482-7.
39. Haas, T. L., Davis, S. J., and Madri, J. A. (1998) *J Biol Chem* **273**, 3604-10.
40. Ellerbroek, S. M., Fishman, D. A., Kearns, A. S., Bafetti, L. M., and Stack, M. S. (1999) *Cancer Res* **59**, 1635-41.
41. Ruangpanit, N., Chan, D., Holmbeck, K., Birkedal-Hansen, H., Polarek, J., Yang, C., Bateman, J. F., and Thompson, E. W. (2001) *Matrix Biol* **20**, 193-203.
42. Ellerbroek, S. M., Wu, Y. I., Overall, C. M., and Stack, M. S. (2001) *J Biol Chem* **276**, 24833-42.
43. Seltzer, J. L., Lee, A. Y., Akers, K. T., Sudbeck, B., Southon, E. A., Wayner, E. A., and Eisen, A. Z. (1994) *Exp Cell Res* **213**, 365-74.
44. Ellerbroek, S. M., and Stack, M. S. (1999) *Bioessays* **21**, 940-9.
45. Butler, G. S., Butler, M. J., Atkinson, S. J., Will, H., Tamura, T., van Westrum, S. S., Crabbe, T., Clements, J., d'Ortho, M. P., and Murphy, G. (1998) *J Biol Chem* **273**, 871-80.
46. Hernandez-Barrantes, S., Toth, M., Bernardo, M. M., Yurkova, M., Gervasi, D. C., Raz, Y., Sang, Q. A., and Fridman, R. (2000) *J Biol Chem* **275**, 12080-9.
47. Overall, C. M., Tam, E., McQuibban, G. A., Morrison, C., Wallon, U. M., Bigg, H. F., King, A. E., and Roberts, C. R. (2000) *J Biol Chem* **275**, 39497-506.
48. Itoh, Y., Takamura, A., Ito, N., Maru, Y., Sato, H., Suenaga, N., Aoki, T., and Seiki, M. (2001) *Embo J* **20**, 4782-4793.
49. Lehti, K., Lohi, J., Juntunen, M. M., Pei, D., and Keski-Oja, J. (2002) *J Biol Chem* **277**, 8440-8.
50. Overall, C. M., and Sodek, J. (1990) *J Biol Chem* **265**, 21141-51.
51. Lehti, K., Lohi, J., Valtanen, H., and Keski-Oja, J. (1998) *Biochem J* **334**, 345-53.
52. Kinoshita, T., Sato, H., Okada, A., Ohuchi, E., Imai, K., Okada, Y., and Seiki, M. (1998) *J Biol Chem* **273**, 16098-103.

53. Albini, A., Melchiori, A., Santi, L., Liotta, L. A., Brown, P. D., and Stetler-Stevenson, W. G. (1991) *J Natl Cancer Inst* **83**, 775-9.
54. Steffensen, B., Wallon, U. M., and Overall, C. M. (1995) *J Biol Chem* **270**, 11555-66.
55. Mancini, S., Romanelli, R., Laschinger, C. A., Overall, C. M., Sodek, J., and McCulloch, C. A. (1999) *J Periodontol* **70**, 1292-302.
56. Bigg, H. F., Morrison, C. J., Butler, G. S., Bogoyevitch, M. A., Wang, Z., Soloway, P. D., and Overall, C. M. (2001) *Cancer Res* **61**, 3610-8.
57. Wallon, U. M., and Overall, C. M. (1997) *J Biol Chem* **272**, 7473-81.
58. Overall, C. M., and Sodek, J. (1987) *J Dent Res* **66**, 1271-82.
59. d'Ortho, M. P., Will, H., Atkinson, S., Butler, G., Messent, A., Gavrilovic, J., Smith, B., Timpl, R., Zardi, L., and Murphy, G. (1997) *Eur J Biochem* **250**, 751-7.
60. Strongin, A. Y., Marmer, B. L., Grant, G. A., and Goldberg, G. I. (1993) *J Biol Chem* **268**, 14033-9.
61. Fishman, D. A., Liu, Y., Ellerbroek, S. M., and Stack, M. S. (2001) *Cancer Res* **61**, 3194-9.
62. Nakahara, H., Howard, L., Thompson, E. W., Sato, H., Seiki, M., Yeh, Y., and Chen, W. T. (1997) *Proc Natl Acad Sci U S A* **94**, 7959-64.
63. Nabeshima, K., Inoue, T., Shimao, Y., Okada, Y., Itoh, Y., Seiki, M., and Kono, M. (2000) *Cancer Res* **60**, 3364-9.
64. Lehti, K., Valtanen, H., Wickstrom, S., Lohi, J., and Keski-Oja, J. (2000) *J Biol Chem* **275**, 15006-13.
65. Hotary, K., Allen, E., Punturieri, A., Yana, I., and Weiss, S. J. (2000) *J Cell Biol* **149**, 1309-23.
66. Welgus, H. G., Jeffrey, J. J., Stricklin, G. P., Roswit, W. T., and Eisen, A. Z. (1980) *J Biol Chem* **255**, 6806-13.
67. De Souza, S. J., Pereira, H. M., Jacchieri, S., and Brentani, R. R. (1996) *Faseb J* **10**, 927-30.
68. Li, J., Brick, P., O'Hare, M. C., Skarzynski, T., Lloyd, L. F., Curry, V. A., Clark, I. M., Bigg, H. F., Hazleman, B. L., Cawston, T. E., and et al. (1995) *Structure* **3**, 541-9.



69. Ruangpanit, N., Price, J. T., Holmbeck, K., Birkedal-Hansen, H., Guenzler, V., Huang, X., Chan, D., Bateman, J. F., and Thompson, E. W. (2002) *Exp Cell Res* **272**, 109-18.
70. Steffensen, B., Bigg, H. F., and Overall, C. M. (1998) *J Biol Chem* **273**, 20622-8.
71. Jiang, A., Lehti, K., Wang, X., Weiss, S. J., Keski-Oja, J., and Pei, D. (2001) *Proc Natl Acad Sci U S A* **98**, 13693-8.
72. Uekita, T., Itoh, Y., Yana, I., Ohno, H., and Seiki, M. (2001) *J Cell Biol* **155**, 1345-56.
73. Will, H., Atkinson, S. J., Butler, G. S., Smith, B., and Murphy, G. (1996) *J Biol Chem* **271**, 17119-23.
74. Strongin, A. Y., Collier, I., Bannikov, G., Marmer, B. L., Grant, G. A., and Goldberg, G. I. (1995) *J Biol Chem* **270**, 5331-8.
75. Stanton, H., Gavrilovic, J., Atkinson, S. J., d'Ortho, M. P., Yamada, K. M., Zardi, L., and Murphy, G. (1998) *J Cell Sci* **111**, 2789-98.
76. Consortium, T. H. (1995) *Nat Genet* **11**, 130-6.
77. Lipman, M. L., Panda, D., Bennett, H. P., Henderson, J. E., Shane, E., Shen, Y., Goltzman, D., and Karaplis, A. C. (1998) *J Biol Chem* **273**, 13729-37.
78. Turner, A. J., Isaac, R. E., and Coates, D. (2001) *Bioessays* **23**, 261-9.
79. McQuibban, G. A., Gong, J. H., Tam, E. M., McCulloch, C. A., Clark-Lewis, I., and Overall, C. M. (2000) *Science* **289**, 1202-6.
80. McQuibban, G. A., Butler, G. S., Gong, J. H., Bendall, L., Power, C., Clark-Lewis, I., and Overall, C. M. (2001) *J Biol Chem* **276**, 43503-8.

## FOOTNOTES

This study was supported by grants from the National Cancer Institute of Canada and the National Institutes of Health Research. E. Tam is supported by a Roman Babicki Scholarship and Canadian Arthritis Network Trainee Award. Y. Wu is supported by a United States Army MRMC Training Grant. C.M. O is supported by a Canada Research Chair in Metalloproteinase Biology.

## FIGURE LEGENDS

FIG. 1. **MT1-MMP hemopexin C domain constructs and linker peptide analogs.** A, the domain structures of (i) pro-MT1-MMP and (ii) 44-kDa MT1-MMP are shown in a linear diagram. The signal sequence (SS), propeptide domain (PRO), stalk segment (ST), transmembrane sequence (TM), and cytoplasmic tail (CYT) of MT1-MMP are indicated. Schematic representations of (iii) MT1-MMP linker peptide analogs, MT1-L18 and MT1-L35, and (iv) hemopexin C domain constructs, MT1-CD and MT1-LCD, are shown with N and C terminal residues indicated. B, purified MT1-CD and MT1-LCD (0.1  $\mu$ g) were electrophoresed on 15 % SDS-PAGE gels under reducing (+DTT) and non-reducing (-DTT) conditions. Gels were analyzed by either silver staining or by Western blotting using  $\alpha$ MT1-CD antibody. Protein masses measured by electrospray injection mass spectrometry (Mass), predicted masses, and N-terminal Edman sequence analysis are indicated. C, MT1-LCD was subjected to FPLC gel filtration chromatography on a Superdex 75 column and elution was monitored at 215 nm. The elution volumes of the void volume ( $V_0$ ) and column volume ( $V_t$ ) and molecular weight standards are indicated.

FIG. 2. **Type I collagen binding properties of MT1-MMP hemopexin C domain constructs.** Serial dilutions of MT1-CD and MT1-LCD were incubated in 96-microwell plates coated with native (A) or heat-denatured (65 °C for 1 h) (B) type I collagen (0.5  $\mu$ g/well) as described under solid phase assays in "Experimental Procedures". MMP2-CBD and MMP2-LCD were included as positive and negative controls, respectively. Bound recombinant domains were detected using  $\alpha$ -His<sub>6</sub> antibody. C, ligand blot assay. Immobilized MT1-CD and MT1-LCD, and control proteins, BSA and MMP2-LCD, (5  $\mu$ g each) were incubated with biotin-labeled type I collagen (0.1  $\mu$ g/ml) in PBS as described in "Experimental Procedures". Bound collagen was detected using streptavidin-HRP.

FIG. 3. **Recombinant MT1-MMP hemopexin C domain reduces collagen-induced activation of MMP-2.** A, fibroblasts ( $1 \times 10^4$ ) grown on tissue culture plastic or within type I collagen gels (2.0 mg/ml) were incubated with or without MT1-LCD (0.05 - 5  $\mu$ M) in DMEM for 72 h. MMP-2 in the conditioned cell media was visualized by gelatin

zymography. *B*, fibroblasts ( $1 \times 10^4$ ) grown on plastic were incubated with latex beads adsorbed with type I collagen (native or denatured) or BSA in DMEM for 24 h. Exogenous MT1-LCD (5  $\mu$ M) was added to the cultures where indicated. Conditioned cell media was analyzed by gelatin zymography. Lanes presented in both *A* and *B* are from the same zymogram.

**FIG. 4. Recombinant MT1-MMP hemopexin C domain reduces MT1-MMP collagenolysis.** *A*, biotin-labeled type I collagen was incubated in the absence (C) or presence of sMT1-MMP (1 pmol) for 18 h at 28 °C. Recombinant proteins, MT1-LCD, MT1-CD and MMP2-LCD were added at the indicated mole equivalents relative to sMT1-MMP. Reactions were separated by SDS-PAGE (7.5 %), followed by Western blotting using streptavidin-HRP. *B*, percentage of  $\alpha$ -chain cleavage was determined by densitometric analysis as described in "Experimental Procedures" and plotted against the amount of soluble recombinant hemopexin C domain added. *C*, MT1-LCD and MT1-CD were detected in reaction samples by SDS-PAGE (15 %) and Western blotting using the  $\alpha$ MT1-CD antibody.

**FIG. 5. Recombinant MT1-MMP hemopexin C domain blocks MMP-2 cleavage of native collagen.** *A*, biotin-labeled type I collagen was incubated in absence (C) or presence of MMP-2 (0.84 pmol) for 18 h at 28 °C. MT1-LCD and MT1-CD (0.1-100-fold mole equivalents) were added to the reaction where indicated. Following digestion, samples were separated by SDS-PAGE (7.5 %), followed by Western blotting using streptavidin-HRP.

**FIG. 6. Characterization of MT1-MMP peptide linker analogs.** *A*, sequence alignment of collagenolytic MMP linkers using Megalign (DNASTAR Inc.) (Clustal method). Conserved residues are denoted with (\*). Sequences of the peptide analogs of MT1-MMP are indicated. *B*, 96-well plate was coated with either native (i) or denatured (ii) type I collagen (rat tail) (0.5  $\mu$ g/well). Serial dilutions of MT1-LCD, MT1-L18, and MT1-L35 were added and bound protein/peptide was detected using RP1MMP-14 antibody, which recognizes the linker. *C*, biotin-labeled type I collagen was incubated in the absence (C)

or presence of sMT1-MMP (1 pmol) for 18 h at 28 °C. Mole excesses of MT1-MMP hemopexin C domain constructs (CD and LCD) (100-fold) and linker peptide analogs (L18 and L35)(1000-fold) were added to the reaction where indicated. Reactions were separated by SDS-PAGE (7.5 %), followed by Western blotting using streptavidin-HRP.

**FIG. 7. Invasion of MDA-MB-231 cells is MT1-MMP-dependent and is inhibited by recombinant MT1-MMP hemopexin C domain.** *A* and *B*, invasion of type I collagen. Cells ( $2.5 \times 10^5$ ) were seeded onto Transwell filters (8  $\mu$ m pore) coated with a type I collagen gel (20  $\mu$ g) and allowed to invade for 24 h as described under "Experimental Procedures". Non-invading cells were removed from the upper chamber with a cotton swab. Filters were then stained and cells, adherent to the underside of the filter, were enumerated using an ocular micrometer. The average of triplicate experiments were normalized to corresponding controls (designated 100%) and are presented with standard deviation being shown (\*  $p < 0.05$ ). *A*, parental MDA-MB-231 cells (white) were allowed to invade in the presence of Me<sub>2</sub>SO (DMSO), GM6001 (10  $\mu$ M), BSA (10 nM), TIMP-1 (10 nM), TIMP-2 (10 nM), purified rabbit IgG (IgG, 10  $\mu$ g/ml), or AB8102 antibody (anti-MT1, 10  $\mu$ g/ml). MDA-MB-231 cells expressing MT1-MMP or MT1-MMP(E240A) (black) were also analyzed. Results are expressed as % of control invasion (versus BSA and Vector). *B*, MDA-MB-231 cells expressing MT1-MMP ( $2.5 \times 10^5$ ) were incubated with DMSO, GM6001 (10  $\mu$ M) and MT1-LCD, MT1-CD, and BSA (4  $\mu$ M and 30  $\mu$ M) and allowed to invade for 24 h. Results are expressed as % of control invasion (versus BSA).

**FIG. 8. Recombinant 44-kDa MT1-MMP inhibits MDA-MB-231 cell invasion.** *A*, linear diagram of MT1-MMP and deletion mutants, cMT1-LCD ( $\Delta$ 112-284) and cMT1-CD ( $\Delta$ 112-315). The signal sequence (SS), propeptide domain (PRO), stalk segment (ST), transmembrane sequence (TM) and, cytoplasmic tail (CYT) are indicated. Invasion of type I collagen (*B*) and migration (*C*) of MDA-MB-231 cells expressing MT1-MMP deletion mutants, cMT1-LCD and cMT1-CD, were assessed. *B*, cells ( $2.5 \times 10^5$ ) were seeded onto Transwell filters (8  $\mu$ m pore) coated with a type I collagen gel (20  $\mu$ g) and allowed to invade for 24 h as described under "Experimental Procedures". *C*, cells ( $2.5 \times 10^5$ ) were seeded onto Transwell filters coated with a thin layer of collagen on the underside and

incubated for 1.5 h to permit migration. In both assays, non-invading or non-migrating cells were removed from the upper chamber with a cotton swab. Filters were then stained and cells, adherent to the underside of the filter, were enumerated using an ocular micrometer. The average of triplicate experiments were normalized to the vector control (designated 100%) and are presented with standard deviation as shown (\*  $p < 0.05$ ).

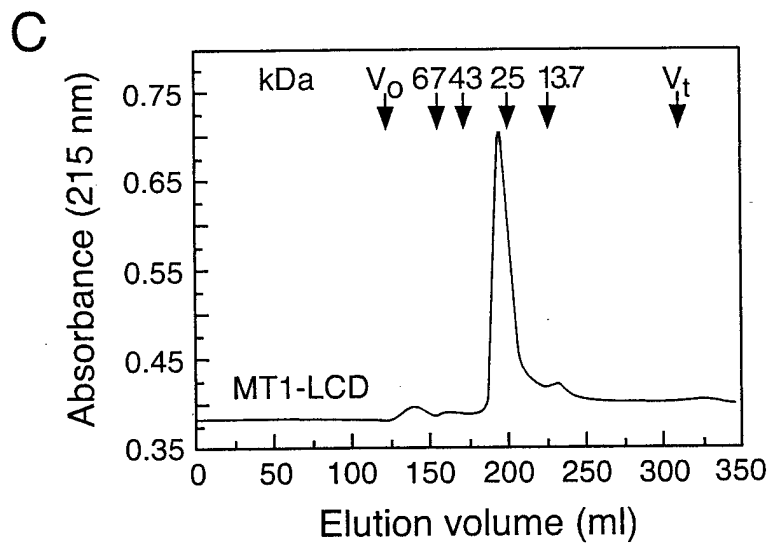
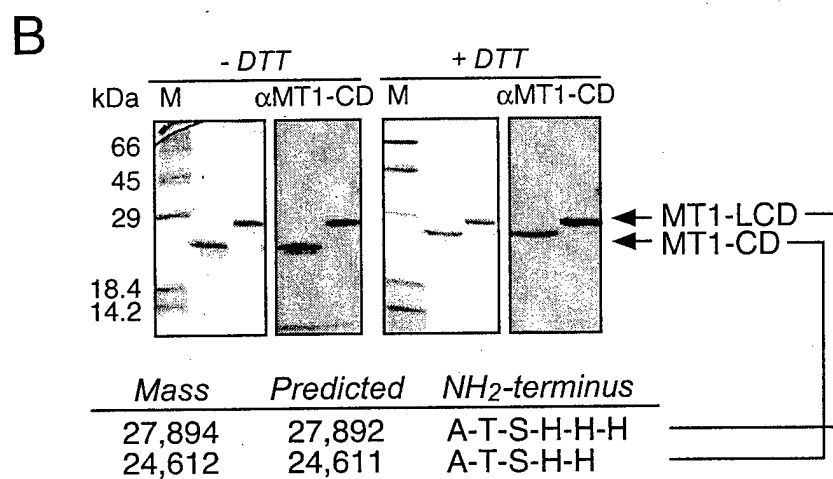
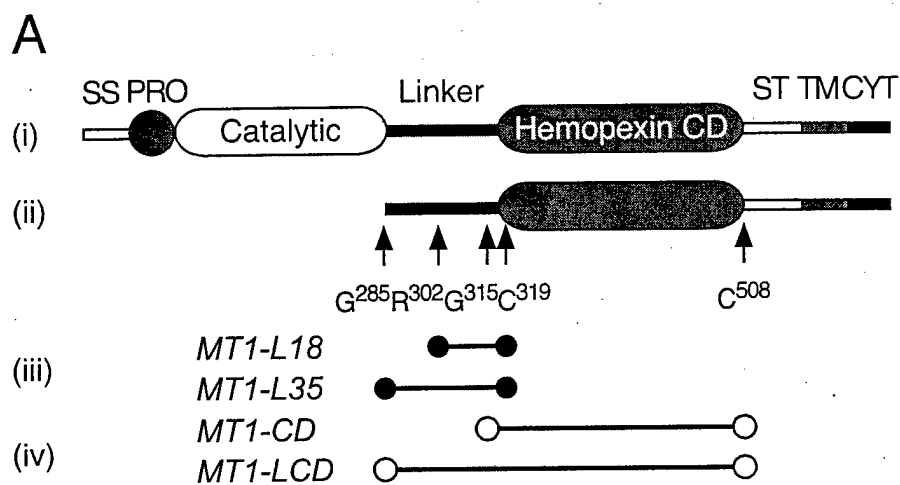
**FIG. 9. Potential role of the 44-kDa MT1-MMP in pericellular collagen degradation.** A, collagenolytic cell profile. Upon collagen-induced engagement of  $\beta_1$  integrins and intracellular signaling, expression of MT1-MMP is upregulated on the cell surface. Increased MT1-MMP expression promotes the cleavage of native collagen (1) and the release of collagen-bound pro-MMP-2 (2), which now enters into the activation pathway. The conversion from collagenolysis to gelatinolysis initiates with the formation of the trimolecular complex (3), which reduces MT1-MMP collagenolytic activity, and the activation of pro-MMP-2, which is enhanced by the collagen-mediated assembly of MT1-MMP (4). B, gelatinolytic cell profile. Following pro-MMP-2 activation and MT1-MMP autocatalytic degradation, the 44-kDa MT1-MMP accumulates on the cell surface and contributes to the proteolytic conversion by inhibiting MT1-MMP (5) and MMP-2 (6) collagenolysis, but not MMP-2 gelatinolysis (7). The absence of native collagen and  $\beta_1$  integrin engagement also reduces MT1-MMP expression on the cell surface.

Table I

## Quenched fluorescent peptide cleavage by sMT1-MMP

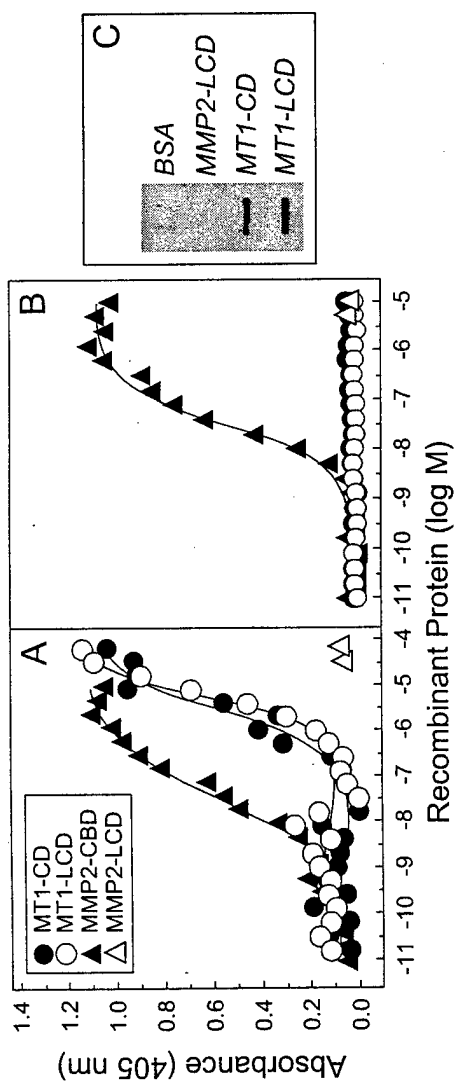
Mca-Pro-Leu-Gly-Dpa-Ala-Arg-NH<sub>2</sub> (0.1 nmol) was incubated with (control) or without (buffer) sMT1-MMP (0.035 pmol) for 1 h at 37 °C (control). MT1-LCD and MT1-CD were added to the reaction at 100-fold mole excess to sMT1-MMP.

	Buffer	Control	MT1-LCD	MT1-CD
Rate of cleavage (RFU $\times 10^{-3} \cdot s^{-1}$ )	0.05	6.7	7.0	7.0

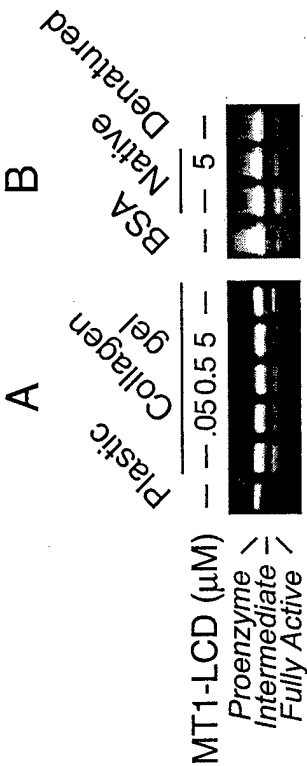




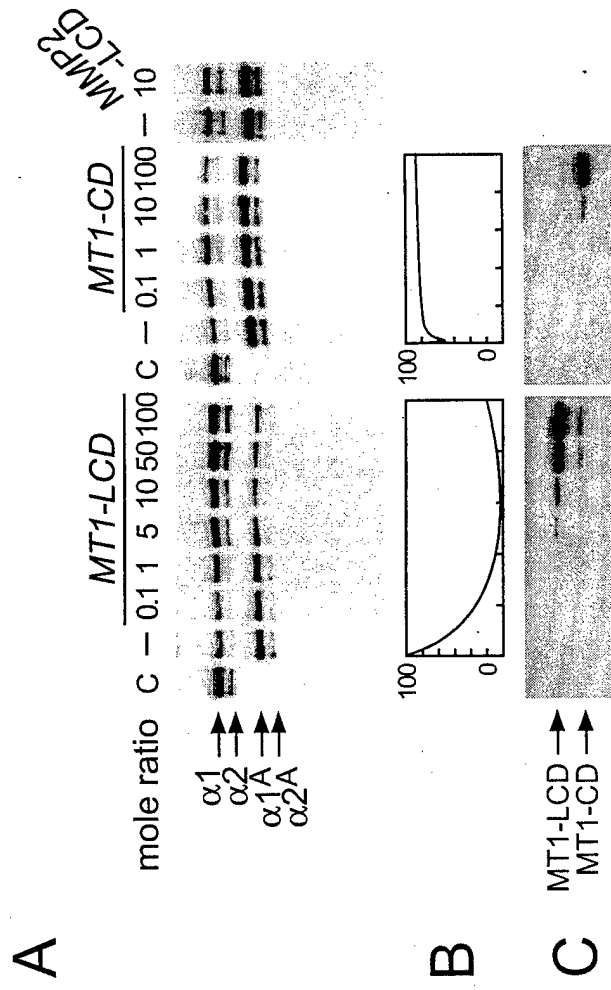
Tam et al Fig. 2



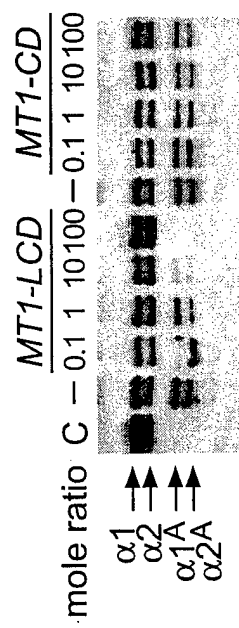
Tam et al, Fig. 3



Tam et al, Fig. 4

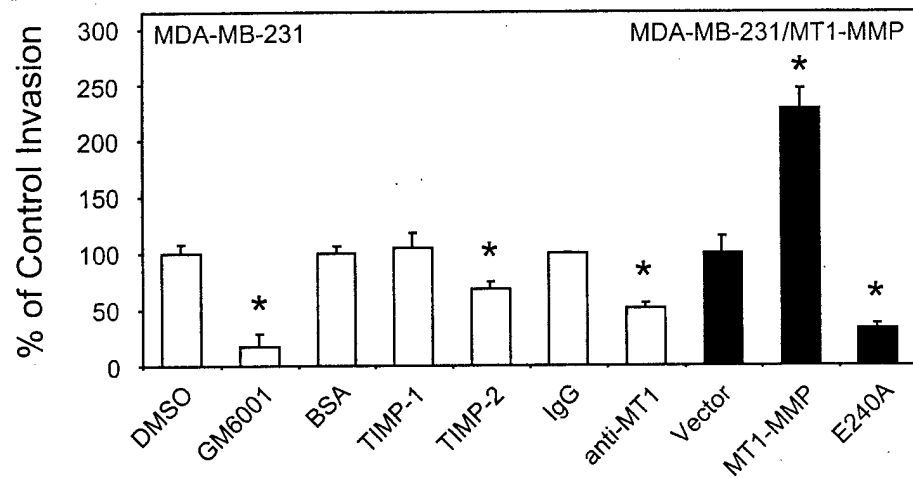


Tam et al, Fig. 5

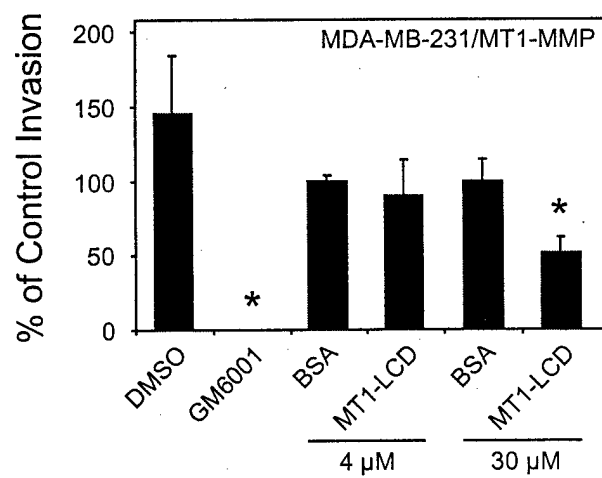




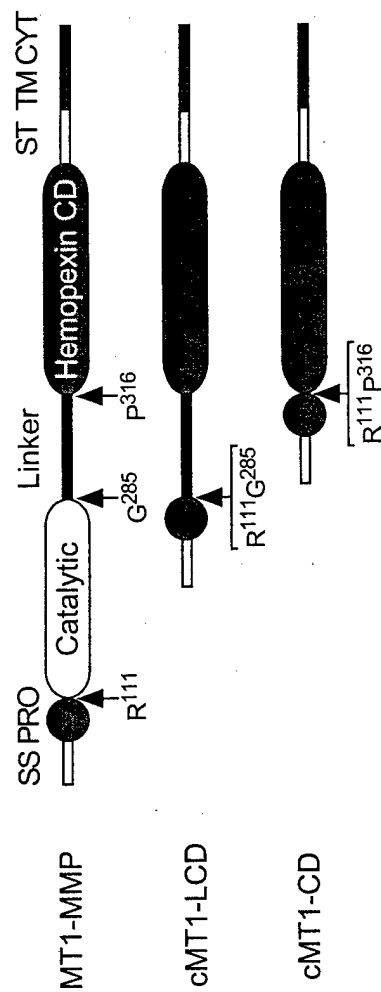
**A**



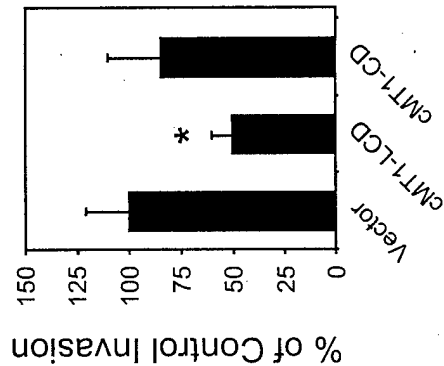
**B**



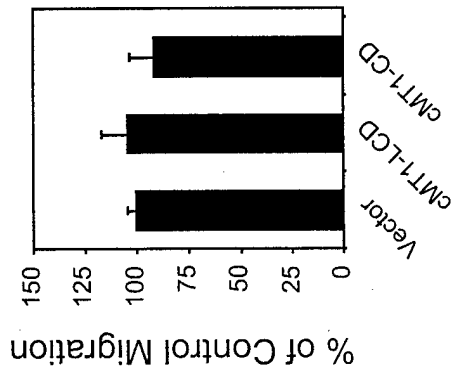
A

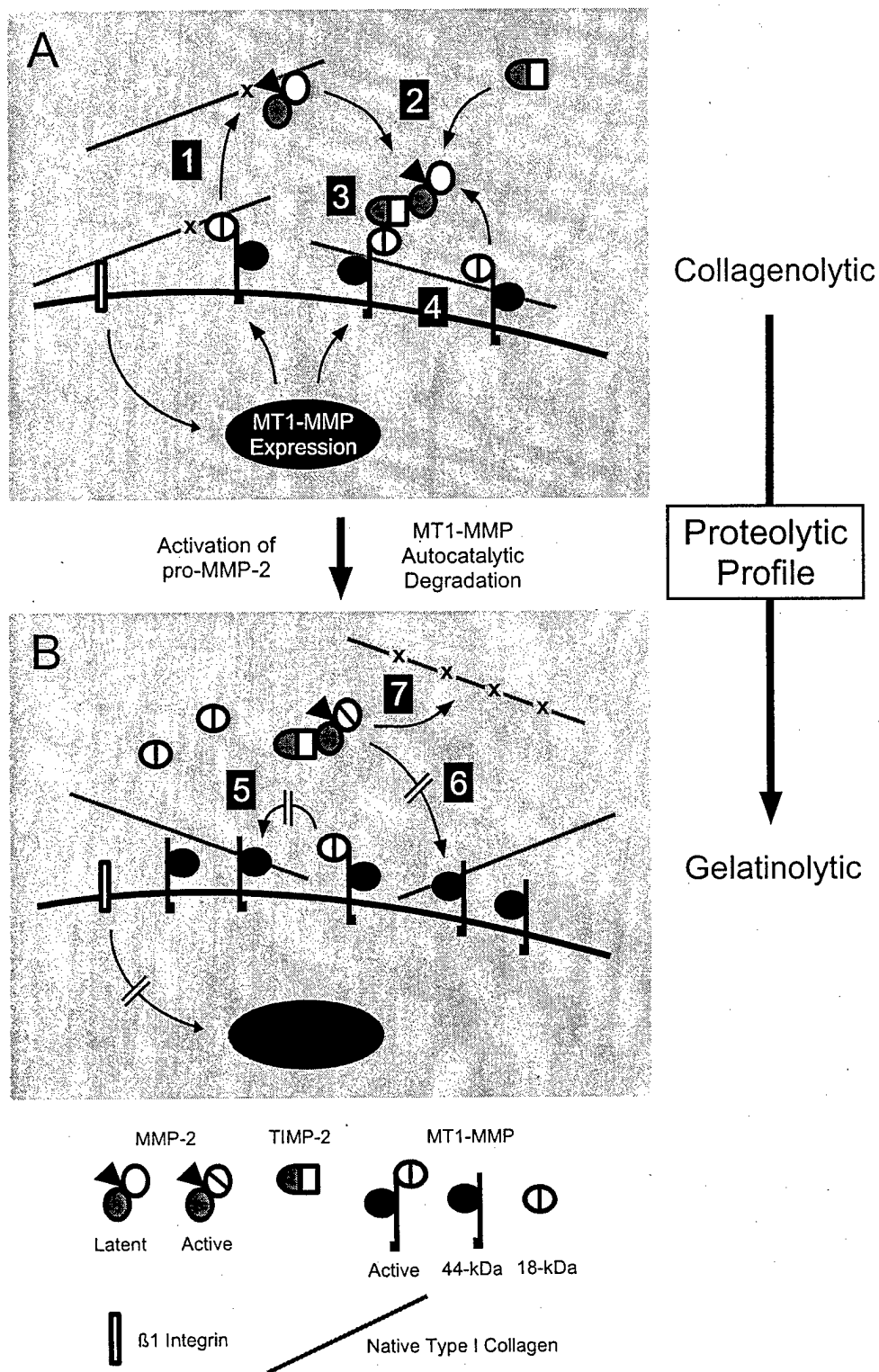


B



C







**Calcium Regulation of Matrix Metalloproteinase-Mediated Migration in  
Oral Squamous Cell Carcinoma Cells.**

H.G. Munshi, Y.I. Wu, E.V. Ariztia and M.S. Stack

Division of Hematology/Oncology, Department of Medicine (H.G.M.); and Department of Cell & Molecular Biology (Y.I.W., E.V.A. and M.S.S.), Feinberg School of Medicine, Northwestern University; and the Robert H. Lurie Comprehensive Cancer Center of Northwestern University (H.G.M. and M.S.S.), Chicago, IL 60611.

Running Title: Calcium regulates matrix metalloproteinase-2 activation.

Key Words: Calcium, MMP-2, MT1-MMP, TIMP-2, keratinocytes, endocytosis, migration

Address for correspondence: M. Sharon Stack, Ph.D.  
Northwestern University Medical School  
Department of Cell and Molecular Biology  
303 E. Chicago Ave., Tarry 8-715  
Chicago IL 60611, USA  
Tel: (312)908-8216  
Fax: (312)503-7912  
e-mail: [mss130@northwestern.edu](mailto:mss130@northwestern.edu)

## ABSTRACT

Activation of matrix metalloproteinase 2 (MMP-2) has been shown to play a significant role in the behavior of cancer cells, affecting both migration and invasion. The activation process requires multimolecular complex formation involving proMMP-2, membrane type 1-MMP (MT1-MMP) and tissue inhibitor of metalloproteinases-2 (TIMP-2). Because calcium is an important regulator of keratinocyte function, we evaluated the effect of calcium on MMP regulation in an oral squamous cell carcinoma line (SCC25). Increasing extracellular calcium (0.09-1.2 mM) resulted in a dose-dependent increase in MT1-MMP-dependent proMMP-2 activation. Despite the requirement for MT1-MMP in the activation process, no changes in MT1-MMP expression, cell surface localization or endocytosis were apparent. However, increased generation of the catalytically inactive 43kDa MT1-MMP autolysis product and decline in the TIMP-2 levels in conditioned media were observed. The decrease in TIMP-2 levels in the conditioned media was prevented by a broad-spectrum MMP inhibitor, suggesting that calcium promotes recruitment of TIMP-2 to MT1-MMP on the cell surface. Despite the decline in soluble TIMP-2, no accumulation of TIMP-2 in cell lysates was seen. Blocking TIMP-2 degradation with bafilomycin A1 significantly increased cell associated TIMP-2 levels in the presence of high calcium. These data suggest that the decline in TIMP-2 is due to increased calcium-mediated MT1-MMP-dependent degradation of TIMP-2. In functional studies, increasing calcium enhanced MMP-dependent cellular migration on laminin-5-rich matrix using an *in vitro* colony dispersion assay. Taken together, these results suggest that changes in extracellular calcium can regulate post-translational MMP dynamics and thus affect the cellular behavior of oral squamous cell carcinoma.

Oral squamous cell carcinoma (OSCC) is characterized by local, regional, and distant spread of the disease; however, the cellular and molecular events that control the invasive behavior are poorly understood (1,2). Immunohistochemical studies have implicated enzymes belonging to the matrix metalloproteinase (MMP) family in basement membrane proteolysis and tissue invasion in OSCC (3). MMPs are a large family of metallo-endopeptidases with activity directed against a variety of extracellular matrix substrates (4-7). Expression of MMP-2 (gelatinase A, a 72 kD type IV collagenase) is observed in invasive and metastatic cases of OSCC (3,8). Furthermore, increased expression of MMP-2 is associated with decreased staining of extracellular matrix in OSCC, suggesting that MMP-2 promotes matrix breakdown (3,8). MMP-2 is secreted from cells as a zymogen (proMMP-2) and is activated post-translationally by a trans-membrane MMP designated as membrane type 1-MMP (MT1-MMP) (9-11). MT1-MMP is also upregulated in OSCC and increased expression is observed in highly invasive and metastatic cases (3,8). ProMT1-MMP is synthesized as a 63-66 kDa zymogen and is activated intracellularly to a 55kDa specie by the serine proteinase furin, a member of the proprotein convertase family (12-14).

The activation of proMMP-2 is regulated by a complex mechanism involving formation of a trimolecular complex with MT1-MMP and tissue inhibitor of metalloproteinase-2 (TIMP-2) (10, 15-17). In this model, TIMP-2 plays a dual role in the regulation of MMP-2 activation, functioning both to promote and to inhibit the activation process in a concentration-dependent manner (16,18). TIMP-2 bridges the interaction between the MMP-2 zymogen and MT1-MMP, via N-terminal binding to the active site of MT1-MMP with the concomitant C-terminal binding to the proMMP-2 hemopexin domain (10, 15-20). Thus, at low TIMP-2 concentration, an adjacent TIMP-2-free MT1-MMP can effectively process the cell-surface bound proMMP-2 to a 68kDa intermediate specie, which undergoes autolytic processing to the mature 62kDa active specie. However at high TIMP-2 concentration, all of the cell surface MT1-MMP undergo complex formation with TIMP-2, thereby inhibiting proMMP-2 activation (10, 15-20).

As stringent control of MMP activity plays an important role in keratinocyte behavior (21-23) and dysregulation of MMP activity has been correlated with metastatic progression, factors that control acquisition of net MMP activity in OSCC were evaluated. Of the many agents that are known to affect keratinocyte behavior, calcium is one of the key factors (24-27). There is a steep calcium gradient within the epidermis, with higher calcium present in the uppermost layers (28-30). Moreover, altering extracellular calcium has been used to effectively model *in vitro* physiologic changes in keratinocytes that occur within the epidermis as cells migrate from the basal to the uppermost layers. Interestingly, recent studies have demonstrated a relationship between extracellular calcium and enhanced matrix metalloproteinase gene expression in primary human keratinocytes (31-33).

Since calcium is an important regulator of keratinocyte function, we evaluated the effect of calcium on MMP regulation in an oral squamous cell carcinoma line (SCC25). Increasing extracellular calcium resulted in a dose-dependent increase in proMMP-2 activation, accompanied by enhanced MT1-MMP autolytic processing and a decline in the levels of soluble TIMP-2. The decrease in TIMP-2 levels in the conditioned media was prevented by a broad-spectrum MMP inhibitor, suggesting that calcium promotes recruitment of TIMP-2 to MT1-MMP on the cell surface. Despite the decline in soluble TIMP-2, no accumulation of TIMP-2 in cell lysates was seen. However, blocking TIMP-2 degradation with bafilomycin A1 significantly increased cell associated TIMP-2 levels in the presence of high calcium. These data suggest that the decline in TIMP-2 is due to increased calcium-mediated MT1-MMP-dependent degradation of TIMP-2. Moreover, calcium enhanced MMP-dependent cellular migration on laminin-5-rich matrix. These results suggest that changes in extracellular calcium can regulate post-translational MMP dynamics and thus affect the cellular behavior of OSCC.

## EXPERIMENTAL PROCEDURES

*Materials* – Gelatin, type I collagen, cell culture reagents, chelex 100, mercaptoethane sulfonic acid (MESNA), peroxidase conjugated secondary antibodies and the MT1-MMP antibody directed against the hinge region were purchased from Sigma (St Louis, MO). Phorbol-12-myristate-13-acetate (PMA),

epidermal growth factor (EGF) and bafilomycin A1 were from Calbiochem (La Jolla, CA). Dulbecco's Modified Eagle Media (DMEM), DMEM without calcium, Ham's F12, G418, Trizol and One-Step RT-PCR kits were purchased from Gibco (Grand Island, NY). Purified TIMP-1 and TIMP-2 proteins, rabbit polyclonal TIMP-2 antibody, and the broad spectrum MMP inhibitor GM6001 were purchased from Chemicon (Temecula, CA). TIMP-2 ELISA kit was from Oncogene Research Products (Boston, MA). Supersignal enhanced chemiluminescence (ECL) reagent, EZ-Link Sulfo-NHS-LC-Biotin, EZ-Link Sulfo-NHS-SS-Biotin and UltraLink Immobilized Streptavidin Gel were obtained from Pierce (Rockford, IL). The furin inhibitor decanoly-Arg-Val-Lys-Arg-chloromethylketone (RVKR) was from Alexis Biochemicals (San Diego, CA). Microcon 10 microconcentrators and polyvinylidene difluoride (PVDF) membranes were purchased from Millipore (Bedford, MA). FuGene-6 was obtained from Roche Molecular Biochemicals (Indianapolis, IN). RQ1 DNase was from Promega (Madison, WI).

*Cell cultures* – SCC25 cells were obtained from American Type Culture Collection (ATCC). SCC25 cells were routinely maintained in DMEM: Ham's F12 = 1:1 media containing 10% fetal calf serum and supplemented with 100 units/ml penicillin. SCC25 and SCC25-MT (defined below) cells were plated in DMEM media containing 0.09 mM calcium and supplemented with chelex treated 10% fetal calf serum. After overnight serum starvation, the cells were switched to serum-free DMEM containing the indicated calcium concentration. In additional experiments, inhibitors or other chemical reagents were added 30 min prior to the medium change.

In some experiments, cells were cultured on thin layer or 3-dimensional collagen surfaces (34). Briefly, acid solubilized rat tail type I collagen was diluted to 50  $\mu$ g/ml in 0.02 N acetic acid and added to the tissue culture plate for 1 h at 18 °C. The solution was aspirated and the plate was rinsed three times with PBS. Three dimensional collagen gels were prepared by diluting acid solubilized type I collagen to a concentration of 1 mg/ml in cold DMEM (calcium-free), neutralizing with sodium hydroxide and then allowing to gel (700  $\mu$ l in 12-well plates) for 30 min at 37 °C prior to plating cells.

*Generation of SCC25-MT cells* – Human MT1-MMP cDNA (a kind gift from Duanqing Pei, University of Minnesota) was cloned into pCR3.1-Uni (Invitrogen, Carlsbad, CA) mammalian expression vector. SCC25 cells were stably transfected using FuGene-6 according to the manufacturer's instructions. Cell clones resistant to 0.8 mg/ml G418 were chosen and screened for MMP-2 activation by zymography as described below and for MT1-MMP expression by western blotting using antibody directed against the hinge region. Six different clones with high levels of MT1-MMP expression were selected for subsequent experiments. The cells were then maintained in DMEM: Ham's F12 media = 1:1 supplemented with 10% fetal calf serum, 100 units/ml penicillin and 0.65 mg/ml G418.

*Analysis of MMP-2 and TIMP-2 expression* – Gelatinase activities in 24 h serum-free conditioned media were determined using SDS-PAGE gelatin zymography as previously described (34). Briefly, SDS-PAGE gels (9% acrylamide) were co-polymerized with 0.1% gelatin and samples were electrophoresed without reduction or boiling using 5X Laemmli sample buffer (35). SDS was removed through a 30 min incubation in 2.5% Triton X-100 and gels were incubated in 20 mM Glycine (pH 8.3), 10 mM CaCl<sub>2</sub>, 1  $\mu$ M ZnCl<sub>2</sub> at 37 °C for 24-36 h. The gels were stained with Coomassie Blue to visualize zones of gelatinolytic activity. The conditioned media were concentrated 15-20 fold using Microcon 10 microconcentrators, boiled in Laemmli sample dilution buffer (35) and analyzed for TIMP-2 by SDS-PAGE (15% gels), and immunoblotted with rabbit polyclonal antibody (Chemicon). Levels of TIMP-2 protein in the cell lysates were quantified by ELISA (Oncogene Research Products) according to the manufacturer's specifications.

*MT1-MMP and TIMP-2 RNA levels* - Total RNA was isolated from SCC25 and SCC25-MT cells using Trizol reagent according to manufacturer's instructions. Following digestion with RQ1 DNase for 30 min at 37 °C, the total RNA concentration was determined by spectrophotometric measurement. Primer pairs for human MT1-MMP, human TIMP-2 and human GAPDH were as follows: forward primer 5'-GCCCATTTGGCCAGTTCTGGCGGG-3' and reverse primer 5'-CCTCGTCCACCTCAATGATGATC-3'

for MT1-MMP; forward primer 5'-GGCGTTTTGCAATGCAGATGTAG-3' and reverse primer 5'-CACAGGAGCCGTCACTTCTCTTG-3' for TIMP-2; forward primer 5'-CGGAGTCAACGGATTTGGT CGTAT-3' and reverse primer 5'-AGCCTTCTCCATGGTGGTGAAGAC-3' for GAPDH (36). The length of the MT1-MMP, TIMP-2 and GAPDH amplicons were 530, 497 and 307 base pairs respectively. RT-PCR was performed using the One Step RT-PCR kit where reverse transcription and DNA amplification occur in the same reaction. Briefly, 1 µg of total RNA was used as template in a reaction that included the appropriate primers in the presence of both reverse transcriptase and Taq polymerase. The mixture was incubated at 45°C for 30 min and cycled 30 times at 94°C for 30 sec, 55°C for 30 sec and 72°C for 2 min. Appropriate negative controls of amplification included reactions without reverse transcriptase. PCR products were visualized by UV transillumination of 1.5% agarose gels stained with ethidium bromide.

*Cell surface biotinylation* – To label cell surface proteins, SCC25-MT cells were grown to confluence in a 6-well plate, washed with ice-cold PBS, and incubated at 4 °C with gentle shaking for 30 min with 0.5 mg/ml cell-impermeable Sulfo-NHS-LC-Biotin in ice cold PBS; followed by washing with 100 mM glycine to quench free biotin. Cells were detached by scraping, lysed in modified RIPA buffer (50 mM tris, pH 7.4, 150 mM NaCl, 5 mM EDTA, 1% Triton X-100 and 0.1% SDS) with proteinase inhibitors (1 µg/ml aprotinin, 1 µM pepstatin, and 10 µM leupeptin), and clarified by centrifugation. To isolate biotinylated cell-surface proteins, equal amounts of protein from each sample were incubated with streptavidin beads at 4 °C for 14 hours, followed by centrifugation. After boiling in Laemmli sample dilution buffer (35) to dissociate streptavidin bead-biotin complexes, the biotin-labeled samples were analyzed by SDS-PAGE (9% gels), and immunoblotted for MT1-MMP.

*MT1-MMP endocytosis* - To determine whether calcium affects MT1-MMP endocytosis, SCC25-MT cells grown to confluence in a 6-cm dish were washed with ice-cold PBS and then incubated with cleavable cell-impermeable sulfo-NHS-SS-biotin (1mg/ml) for 20 min in an ice bath. Biotinylation was

stopped by washing with ice-cold PBS followed by 100mM glycine in PBS to quench free biotin. Cells were then incubated with DMEM containing either 0.09 mM or 1.2 mM calcium at 37 °C for 40 min to initiate endocytosis. Endocytosis of cell surface proteins was then stopped by placing the cells on ice and washing them with ice cold PBS. Biotin was then cleaved off the exposed cell surface by incubating the cells with membrane impermeable reducing agent MESNA (100 mM) for 30 min at 4 °C (37). The cells were lysed in modified RIPA buffer with proteinase inhibitors (1 µg/ml aprotinin, 1 µM pepstatin, and 10 µM leupeptin), and clarified by centrifugation. To isolate biotinylated proteins (representing endocytosed surface labeled species), equal amounts of protein from each of the samples were incubated with streptavidin beads at 4 °C for 14 hours, followed by centrifugation. After boiling in Laemmli sample dilution buffer (35) to dissociate streptavidin bead-biotin complexes, the samples were analyzed by SDS-PAGE (9% gels), and immunoblotted for MT1-MMP. In control experiments to determine the efficiency of surface stripping with MESNA, cells were maintained on ice for the duration of the experiment and were not induced to undergo endocytosis via a temperature shift. In additional control experiments, the MESNA stripping step was omitted such that total labeled protein (endocytosed and the cell surface pool) was analyzed.

*Generation of laminin-5 enriched matrix and cell dispersion assays* - The extracellular matrix deposited by SCC25 cells was generated as described previously (34,38). Briefly, SCC25 cells were grown in 12-well plates to 48-72 hours post confluence prior to treatment for 7 min with 20 mM ammonium hydroxide to remove cells. After 3 rapid washes each in sterile distilled water and PBS, the laminin-5 enriched matrix was then used for *in vitro* migration assays. The effect of calcium on laminin-5 induced migration was assessed using a cell dispersion assay as previously described (39). Briefly, SCC25 and SCC25-MT cells ( $3 \times 10^4$ ) were plated in DMEM (0.09 mM calcium) inside a cloning cylinder placed in the middle of 12-well plate coated with laminin-5 enriched matrix. After the cells have attached and spread, the cloning cylinder was removed, cells washed twice with DMEM media containing 0.09 mM calcium and serum starved for three additional hours. The media was then switched to DMEM containing either 0.09 mM or



1.2 mM calcium supplemented with 20 ng/ml EGF. In selected experiments, the proteinase-dependence of migration was determined by adding the MMP inhibitor GM6001 (10  $\mu$ M). To quantify the relative motility, the migratory front was photographed every 12 h for 48 h and the percentage of cells crossing a line designated 'migratory max' was enumerated.

## RESULTS

### *Extracellular calcium regulates proMMP-2 activation*

MMP activity is subject to complex post-translational regulation by a number of processes including zymogen activation, enzyme-inhibitor binding, endocytosis and shedding (4-7,40,41); however, the biologic factors that control and coordinate these processes are poorly understood. As keratinocytes are subjected to fluctuations in extracellular calcium in the epidermal milieu, the effect of calcium on MMP activation was evaluated in SCC25 cells. The predominant soluble MMP expressed by SCC25 cells is MMP-2, with low-level expression of MMP-9. SCC25 cells were plated in low calcium media (0.09 mM), serum starved, and incubated with fresh serum-free media containing increasing calcium. Conditioned media were collected at 24 h and analyzed for MMP activity by gelatin zymography. While cells cultured in 0.09 mM calcium concentration expressed proMMP-2 (Fig 1 A, lane 1), increasing calcium concentration resulted in a dose-dependent MMP-2 activation (Fig 1A, lanes 2-4). There was no change in MMP-9 expression with increasing calcium concentration in these cells (data not shown). Since collagen has been shown to affect MMP-2 expression and/or processing (42-48), the effect of calcium on collagen-induced MMP-2 activation was examined. Similar to the results obtained with SCC25 cells on plastic (Fig 1A), cells plated on thin layer collagen demonstrated MMP-2 activation with increasing calcium concentration (Fig 1B, lanes 1-3). Although cells cultured on 3-dimensional collagen gels had a more pronounced baseline MMP-2 activation (Fig 1B, lane 4), a calcium dependent increase in MMP-2 activation was observed (Fig 1B, lanes 5-6). These data indicate that extracellular calcium-mediated

regulation of MMP-2 activation in SCC25 cells may act in synergy with collagen induced proMMP-2 processing.

To investigate the proteolytic process leading to MMP-2 activation, SCC25 cells were treated with a broad-spectrum MMP inhibitor GM6001, or vehicle (DMSO) control. GM6001 inhibited calcium induced proMMP-2 activation, demonstrating the involvement of an MMP in the activation process (Fig 2A, lanes 3 and 4). To further investigate MMP-dependence, SCC25 cells were treated with TIMP-1 and TIMP-2. TIMP-2 blocks both MMP-2 and MT1-MMP activities, whereas MT1-MMP activity is not inhibited by TIMP-1 (49,50). TIMP-1 had no effect on calcium induced MMP-2 activation (Fig 2A, lanes 5 and 6), while TIMP-2 completely abrogated the response (Fig 2A, lanes 7 and 8), implicating MT1-MMP in the calcium-induced proMMP-2 activation reaction.

To further investigate the involvement of MT1-MMP in calcium-dependent proMMP-2 activation, SCC25 cells were treated with a furin inhibitor decanoly-Arg-Val-Lys-Arg-chloromethylketone (RVKR), which has been shown to block activation of proMT1-MMP (51). Treatment of SCC25 cells with RVKR inhibited calcium mediated MMP-2 activation, further implicating MT1-MMP in the calcium induced proMMP-2 activation (compare Fig 2B, lanes 1 and 3 with Fig 2B, lanes 5 and 7). To determine whether calcium can act in synergy with PMA, another agent that has been shown to induce MMP-2 activation via MT1-MMP (11,52), cells were cultured in low versus high calcium concentration in the presence of PMA and various proteinase inhibitors. As previously reported PMA induced proMMP-9 expression (52,53), irrespective of calcium concentration (Fig 2C, compare lanes 1, 2, and lanes 5, 6). In contrast, expression of proMMP-2 was not affected; however activation was stimulated (Fig 2C, lanes 1,2 and lanes 5,6). Addition of calcium further increased PMA-induced proMMP-2 activation (compare Fig 2C, lanes 2 and 6), indicative of synergistic stimulation of MMP processing. In control experiments, activation was blocked by both RVKR and GM6001 (Fig 2C, lanes 3,7 and 4, 8, respectively).

#### *Overexpression of MT1-MMP in SCC25 cells*

To further investigate the involvement of MT1-MMP in calcium-dependent proMMP-2 activation, SCC25 cells overexpressing MT1-MMP (designated SCC25-MT) were generated (Fig 3A). Overexpression of MT1-MMP in SCC25-MT cells was verified by western blotting of whole cell lysates, indicating the presence of the 55kDa active specie and the 43kDa catalytically inactive autolysis product (Fig 3A). As it has been previously reported (54,55), GM6001 prevents autolysis of MT1-MMP and thus increases the accumulation of the 55kDa specie (Fig 3A, lane 2). Correlating with the enhanced MT1-MMP expression in SCC25-MT cells (Fig 3A, lane 4), a significantly increased MMP-2 activation is observed (Fig 3A, lower panel lane 4). Similar to wild-type SCC25 cells, calcium increased proMMP-2 activation by SCC25-MT cells in a dose dependent manner (Fig 3B). Activation was inhibited by the broad spectrum MMP inhibitor GM6001 (Fig 3C) and by TIMP-2 (Fig 3D).

#### *Effect of extracellular calcium on MT1-MMP*

To determine whether the calcium-induced increases in proMMP-2 activation are the result of enhanced MT1-MMP expression, the MT1-MMP mRNA levels from SCC25 and SCC25-MT cells were analyzed by RT-PCR. Changes in the message levels for GAPDH were used as internal control. SCC25-MT cells expressed higher levels of MT1-MMP message compared to SCC25 cells; however, calcium did not alter the steady state levels of MT1-MMP mRNA (Fig 4A).

As the RT-PCR data indicated that MT1-MMP expression levels were unaffected by calcium, post-translational mechanisms of MT1-MMP regulation were investigated. To evaluate the effect of calcium on MT1-MMP processing, SCC25-MT cells were plated in low calcium, serum starved, and incubated in fresh medium containing low (0.09 mM) or high (1.2 mM) calcium concentration in the presence or absence of GM6001 to prevent autocatalytic processing of MT1-MMP to the 43kDa specie. After 24 h, the cell lysates were probed for MT1-MMP by western blotting. In agreement with the RT-PCR data, no significant change in overall MT1-MMP protein expression was observed (Fig 4B, upper panel). However, increased processing of MT1-MMP to the 43kDa autolysis product was observed in

high calcium, indicative of enhanced MT1-MMP activity, as further supported by zymogram data showing increased proMMP-2 activation (Fig 4B, lower panel, lane 3).

To determine whether MT1-MMP activity is enhanced via increased cell surface association, surface biotinylation was used to probe calcium-induced changes in the cell surface MT1-MMP species. Serum-starved SCC25-MT cells were maintained in low or high calcium for 24 h as indicated, then incubated with cell impermeable NHS-biotin to label cell surface proteins, and lysed in modified RIPA buffer. Following precipitation of surface-labeled proteins with streptavidin beads, samples were electrophoresed and probed for MT1-MMP by immunoblotting. Similar to the results obtained with whole cell lysates, calcium had no effect on the surface expression of MT1-MMP (Fig 4C). Enhanced surface levels of 43kDa autolysis product were also observed, providing additional evidence for increased cell surface MT1-MMP activity.

#### *Rapid kinetics of calcium-induced proMMP-2 activation.*

To evaluate the kinetics of proMMP-2 activation, serum-starved SCC25 and SCC25-MT cells were first incubated in low calcium medium (0.09 mM) to accumulate proMMP-2 and TIMP-2 in the conditioned media. After 24h, activation was initiated by the addition of calcium from a concentrated stock solution to a final concentration of 1.2 mM. At various time points, conditioned media and cell lysates were collected and the relative kinetics of proMMP-2 activation were analyzed by gelatin zymography. Rapid MMP-2 activation was detected at the cell surface within 30 min following calcium restoration in both wild type and MT1-MMP overexpressing SCC25 cells (Figs 5A and 5B). Surface activation was followed by a more gradual release of MMP-2 as evidenced by accumulation of activated MMP-2 in the conditioned media (Figs 5C and 5D). The rapid calcium induced activation of proMMP-2 was blocked by GM6001 (data not shown).

Since MMP-2 activation occurs rapidly following calcium addition, two distinct approaches were utilized to address the potential for rapid calcium induced changes in the surface localization of MT1-

MMP. In initial experiments, cells were cultured in low calcium medium (0.09 mM), switched to high calcium (1.2 mM), and at the indicated times cell surface proteins were labeled with NHS-biotin followed by lysis in modified RIPA buffer. The surface labeled proteins were immunoprecipitated with streptavidin beads and probed for MT1-MMP by immunoblotting. No significant changes in the surface levels of the 55kDa MT1-MMP specie were induced by calcium supplementation (Fig 6A), although GM6001 stabilized cell-surface MT1-MMP against autolysis (Fig 6B).

Recent data demonstrate that MT1-MMP can be regulated post translationally via internalization from the cell surface (56,57). To determine whether calcium induces dynamic turnover of MT1-MMP and thereby regulates MMP-2 activation, we evaluated MT1-MMP endocytosis in SCC25-MT cells. SCC25-MT cells were surface biotinylated with cleavable cell-impermeable NHS-SS-Biotin at 4 °C to block endocytosis, and then transferred to 37 °C in 0.09 or 1.2 mM calcium containing medium to allow for internalization (Fig 7A, [1]). Control cells were maintained at 4 °C to prevent internalization [2]. After a 40-min incubation at 37 °C, the cells were returned to 4 °C to stabilize surface protein profiles and block further internalization [3]. Biotin on the remaining cell surface proteins was then removed using the reducing agent MESNA [4]. In control experiments, MESNA was omitted to enable evaluation of total labeled proteins (i.e. surface and internalized) [5]. Cells were washed with ice-cold PBS, lysed, and labeled proteins were precipitated with streptavidin beads [6-8], electrophoresed and probed for MT1-MMP by immunoblotting. In cells not subject to the temperature shift prior to reduction (Fig 7A, [a]), no MT1-MMP was detected, demonstrating the efficacy of MESNA in removing the biotin from surface labeled MT1-MMP (Fig 7B, lanes 1 and 4). In contrast, cells incubated at 37 °C contained a protected, MESNA-resistant pool of MT1-MMP (Fig 7A, [b]), demonstrating internalization of MT1-MMP in SCC25-MT cells (Fig 7B, lanes 2 and 5). Treatment of cells with GM6001 for 40 min did not affect internalization of the 55kDa MT1-MMP specie (data not shown). To evaluate the effect of calcium on MT1-MMP endocytosis, calcium levels in the medium were modulated at the time of temperature shift. MT1-MMP was effectively internalized in both low (0.09) and high (1.2 mM) calcium conditions (Fig 7B, lanes 2 and 5). Analysis of total cellular MT1-MMP (Fig 7A, [c]; surface and internalized) confirmed

previous results and indicated no change in the overall expression levels (Fig 7B, lanes 3 and 6). Together, these data demonstrate that MT1-MMP is regulated by endocytosis under both low and high calcium conditions. However, the rapid calcium-induced changes in proMMP-2 activation kinetics are not mirrored by corresponding changes in surface MT1-MMP expression or endocytosis.

#### *Calcium regulates TIMP-2 levels*

TIMP-2 plays an important role in proMMP-2 activation (10,15-20); at low concentration it facilitates activation by bridging trimolecular-activation complex formation whereas at higher concentrations the activation is inhibited via interaction of TIMP-2 with the catalytically competent MT1-MMP active site. Because the calcium-induced proMMP-2 activation could not be attributed to changes in either MT1-MMP expression or to surface localization, the remaining component of the trimolecular complex, TIMP-2, was evaluated. Following serum starvation in low calcium, SCC25-MT cells were maintained in medium containing the indicated calcium concentration in the presence or absence of GM6001. Conditioned media were collected at 24 h, concentrated 15-20 fold and TIMP-2 analyzed by western blotting. A dose-dependent decrease in soluble TIMP-2 was observed (Fig 8A, lanes 1-4). To determine whether the calcium-induced decrease in soluble TIMP-2 results from decreased expression, the TIMP-2 message levels from SCC25 and SCC25-MT cells were analyzed by RT-PCR. No calcium-induced changes in TIMP-2 message levels were observed either in SCC25 or SCC25-MT cells (Fig 8B). However, analysis of soluble TIMP-2 protein levels in cells cultured with GM6001 indicated that GM6001 blocked the calcium-mediated decline in soluble TIMP-2 (Fig 8A, lanes 5-8). Together, these data suggest that blocking the MT1-MMP active site with GM6001 may prevent the loss of soluble TIMP-2 by affecting recruitment of TIMP-2 to the cell surface-activation complex, providing evidence that calcium regulates TIMP-2 at the post-translational level.

To determine whether the rapid calcium-mediated induction of proMMP-2 activation reflects changes in surface-associated TIMP-2 levels, the effect of calcium on the kinetics of TIMP-2 loss from the conditioned media was examined. SCC25-MT cells were incubated in low calcium (0.09 mM)

medium to accumulate pro-MMP-2 and TIMP-2 in the conditioned media. After 24h, calcium from a concentrated stock solution was added to a final concentration of 1.2 mM. At the indicated times, the conditioned media were collected, concentrated and TIMP-2 analyzed by western blotting. TIMP-2 levels in the conditioned media changed with time, with the decrease apparent at 2h following calcium restoration (Fig 8C, upper panel). The presence of GM6001 blocked the decline (Fig 8C, lower panel), further supporting the hypothesis that calcium promotes MT1-MMP dependent recruitment of TIMP-2 to the cell surface trimolecular activation complex.

To differentiate whether the calcium-induced decrease in soluble TIMP-2 levels reflected enhanced surface accumulation versus increased degradation of TIMP-2, the vacuolar ATPase inhibitor bafilomycin A1 was utilized. The rationale for this experiment was based on previous studies showing that PMA-induced stimulation of proMMP-2 activation and corresponding loss of soluble TIMP-2 resulted from MT1-MMP mediated TIMP-2 internalization and subsequent intracellular degradation in endosomal and/or lysosomal compartments (58). Increasing the pH of these compartments with bafilomycin A1 blocked TIMP-2 degradation, leading to a build-up of cellular TIMP-2 levels (58). Thus, SCC25-MT cells were cultured in 0.09 or 1.2 mM calcium for 24 h in the presence or absence of bafilomycin A1 (75 nM), and conditioned media were collected, concentrated 15-20 fold, and evaluated for TIMP-2 by western blotting. In addition, the cell lysates at 24 h were collected and analyzed for TIMP-2 by ELISA. As shown above (Fig 8A), calcium decreased the TIMP-2 levels in the conditioned media (Fig 9A, lanes 1,3), but did not affect the levels of TIMP-2 in the cell lysates (Fig 9B). Together, these data indicate that the calcium-mediated decline in soluble TIMP-2 is not due to cell surface accumulation of the inhibitor and suggest that TIMP-2 degradation is increased in high calcium. This is supported by experiments using bafilomycin A1, which partially blocked the calcium-mediated decline in soluble TIMP-2 (Fig 9A, lane 4). Since bafilomycin A1 blocks TIMP-2 degradation (58), these data support the hypothesis that the decline in soluble TIMP-2 observed under high calcium conditions reflects increased degradation of TIMP-2.

### *Calcium promotes SCC25 cell migration*

To evaluate the functional consequences of calcium-induced MMP-2 activation, the effect of calcium on SCC25 and SCC25-MT cell migration on laminin-5 rich matrix was examined. Migration was quantified using an *in vitro* cell dispersion assay (39), in which cells are plated at high density in a glass ring and allowed to migrate after removal of the ring (Fig 10A). After the cells have attached and spread, the ring is removed, serum-starved for 3h and the media switched to either low (0.09 mM) or high (1.2 mM) calcium supplemented with 20 ng/ml EGF, and migration is quantified at 12-48 h. In a representative experiment quantified at 24 h, SCC25 cells migrated on laminin 5-rich matrix, with SCC25-MT cells displaying increased migration relative to wild-type cells (Fig 10B). Calcium enhanced the motility of both wild-type and MT1-MMP overexpressing SCC25 cells. Calcium-induced migration was blocked by GM6001, indicating that the enhanced migration observed can be attributed to increased MMP activity.

## DISCUSSION

Studies using multiple cancer models have shown that MMP-2 activation is important in cellular behavior (59-62). The activation of MMP-2 *in vitro* is associated with increased migration and invasiveness of cancer cells (63-65). Further, there is increased MMP-2 activation with lymph node metastasis in a number of different cancers, including OSCC (3,8,66). Hence, the regulation of MMP-2 activation has been extensively studied. Previously, it was shown that MMP-2 activation could be promoted with non-physiological agents like PMA (11,52) and concanavalin A (67,68) and also by proteins of the extracellular matrix such as collagen and fibronectin (42-48,69,70). In this study, we show that calcium also regulates proMMP-2 activation without altering expression of the zymogen. Increasing extracellular calcium resulted in a dose-dependent activation of proMMP-2, accompanied by enhanced generation of 43kDa catalytically inactive MT1-MMP species and a decline in the levels of soluble TIMP-2. Calcium did not affect the steady state levels of TIMP-2 in the cell lysates, suggesting that calcium induces TIMP-2 degradation. As a functional consequence, calcium promoted cellular migration,



suggesting that calcium may control keratinocyte migration via regulation of MMP-2 activation.

Calcium-mediated MMP-2 activation was MT1-MMP dependent; however calcium did not affect MT1-MMP message or cell surface protein levels, consistent with the observation that calcium-mediated activation of MMP-2 occurs rapidly at the cell surface. Increased generation of the catalytically inactive 43kDa MT1-MMP specie autolysis product was also observed. These data are in agreement with the recent reports showing that MMP-2 activation induced by fibronectin and PMA increased accumulation of the 43kDa MT1-MMP specie without affecting the levels of the 55kDa MT1-MMP specie (58,69,70). Despite the rapid activation of MMP-2 at the cell surface, calcium did not affect MT1-MMP endocytosis.

Calcium-induced MMP-2 activation was associated with a MT1-MMP-dependent decline in soluble TIMP-2. A similar phenomenon has been recently reported in other model systems (58,69,71). For example, PMA and type IV collagen-induced MMP-2 activation in HT1080 cells is coupled with TIMP-2 degradation (58,69). In SCC25 cells, the calcium-induced decline in TIMP-2 also likely results from degradation as treatment with bafilomycin A1, a highly specific inhibitor of vacuolar ATPase that was previously shown to block MT1-MMP-mediated degradation of TIMP-2 (58), restored soluble TIMP-2 levels. This is in contrast to the loss of soluble TIMP-2 that accompanies concanavalin A-induced proMMP-2 activation, which results from enhanced cell surface binding rather than degradation (58,69,72). The mechanism by which changes in extracellular calcium promote TIMP-2 internalization and degradation is currently under investigation. Nevertheless, it is interesting to note that an inverse relationship between MMP-2 activation and soluble TIMP-2 has been observed in many human cancer cell lines (51,72,73).

The calcium-induced changes in post-translational MMP regulation correlated with increased migration over laminin-5 enriched matrix. Several reports have demonstrated involvement of active MMP-2 in cellular migration (63,64,74,75), including laminin-5-driven motility (76,77). MT1-MMP has also been implicated in epithelial cell migration over laminin-5 matrix (39,77). Our data demonstrate that migration on laminin-5 is enhanced both in MT1-MMP overexpressing cells and under conditions that promote MMP-2 activation. Since calcium is a key regulator of keratinocyte function, these data suggest

that localized changes in calcium in the extracellular milieu may function as a fine regulatory mechanism for post-translational control of MMP activity and MMP-influenced cellular behaviors such as migration and invasion.

#### ACKNOWLEDGEMENTS

This research was supported in part by grant PO1 DE12328 (M.S.S.) from the National Institute for Dental and Craniofacial Research. H.G.M. was supported in part by a grant from the National Institute of Health to the RHL Comprehensive Cancer Center's Training Program in Signal Transduction and Cancer (5T32 CA70085). H.G.M is a recipient of the 2002 American Society of Clinical Oncology Young Investigator Award.

#### FOOTNOTES

The abbreviations used are: MMP, matrix metalloproteinase; MT1-MMP, membrane type 1-MMP; TIMP, tissue of inhibitor of metalloproteinases; RVKR, decanoly-Arg-Val-Lys-Arg-chloromethylketone; DMEM, Dulbecco's Modified Eagle Media.

## REFERENCES

1. Liotta, L. A., Tryggvason, K., Garbisa, S., Hart, I., Foltz, C. M., and Shafie, S. (1980) *Nature* **284**(5751), 67-8.
2. Forastiere, A., Koch, W., Trotti, A., and Sidransky, D. (2001) *N Engl J Med* **345**(26), 1890-900.
3. Kurahara, S., Shinohara, M., Ikebe, T., Nakamura, S., Beppu, M., Hiraki, A., Takeuchi, H., and Shirasuna, K. (1999) *Head Neck* **21**(7), 627-38.
4. Werb, Z. (1997) *Cell* **91**(4), 439-42.
5. Nagase, H., and Woessner, J. F., Jr. (1999) *J Biol Chem* **274**(31), 21491-4.
6. Sternlicht, M. D., and Werb, Z. (2001) *Annu Rev Cell Dev Biol* **17**, 463-516
7. Egeblad, M., and Werb, Z. (2002) *Nature Rev Cancer* **2**(3), 161-74.
8. Shimada, T., Nakamura, H., Yamashita, K., Kawata, R., Murakami, Y., Fujimoto, N., Sato, H., Seiki, M., and Okada, Y. (2000) *Clin Exp Metastasis* **18**(2), 179-88
9. Sato, H., Takino, T., Okada, Y., Cao, J., Shinagawa, A., Yamamoto, E., and Seiki, M. (1994) *Nature* **370**(6484), 61-5.
10. Butler, G. S., Butler, M. J., Atkinson, S. J., Will, H., Tamura, T., van Westrum, S. S., Crabbe, T., Clements, J., d'Ortho, M. P., and Murphy, G. (1998) *J Biol Chem* **273**(2), 871-80.
11. Lehti, K., Lohi, J., Valtanen, H., and Keski-Oja, J. (1998) *Biochem J* **334**(Pt 2), 345-53.
12. Sato, H., Kinoshita, T., Takino, T., Nakayama, K., and Seiki, M. (1996) *FEBS Lett* **393**(1), 101-4.
13. Maquoi, E., Noel, A., Frankenhe, F., Angliker, H., Murphy, G., and Foidart, J. M. (1998) *FEBS Lett* **424**(3), 262-6.
14. Yana, I., and Weiss, S. J. (2000) *Mol Biol Cell* **11**(7), 2387-401.
15. Strongin, A. Y., Collier, I., Bannikov, G., Marmer, B. L., Grant, G. A., and Goldberg, G. I. (1995) *J Biol Chem* **270**(10), 5331-8.
16. Itoh, Y., Ito, A., Iwata, K., Tanzawa, K., Mori, Y., and Nagase, H. (1998) *J Biol Chem* **273**(38), 24360-7.
17. Zucker, S., Drews, M., Conner, C., Foda, H. D., DeClerck, Y. A., Langley, K. E., Bahou, W. F.,

- Docherty, A. J., and Cao, J. (1998) *J Biol Chem* **273**(2), 1216-22.
18. Jo, Y., Yeon, J., Kim, H. J., and Lee, S. T. (2000) *Biochem J* **345 Pt 3**, 511-9.
  19. Overall, C. M., King, A. E., Sam, D. K., Ong, A. D., Lau, T. T., Wallon, U. M., DeClerck, Y. A., and Atherstone, J. (1999) *J Biol Chem* **274**(7), 4421-9.
  20. Toth, M., Bernardo, M. M., Gervasi, D. C., Soloway, P. D., Wang, Z., Bigg, H. F., Overall, C. M., DeClerck, Y. A., Tschesche, H., Cher, M. L., Brown, S., Mobashery, S., and Fridman, R. (2000) *J Biol Chem* **275**(52), 41415-23.
  21. Madlener, M., Parks, W. C., and Werner, S. (1998) *Exp Cell Res* **242**(1), 201-10.
  22. Baumann, P., Zigrino, P., Mauch, C., Breitkreutz, D., and Nischt, R. (2000) *Br J Cancer* **83**(10), 1387-93.
  23. Nagavarapu, U., Relloma, K., and Herron, G. S. (2002) *J Invest Dermatol* **118**(4), 573-81.
  24. Hennings, H., Michael, D., Cheng, C., Steinert, P., Holbrook, K., and Yuspa, S. H. (1980) *Cell* **19**(1), 245-54.
  25. Hennings, H., and Holbrook, K. A. (1983) *Exp Cell Res* **143**(1), 127-42.
  26. Yuspa, S. H., Kilkenny, A. E., Steinert, P. M., and Roop, D. R. (1989) *J Cell Biol* **109**(3), 1207-17.
  27. Bikle, D. D., Ng, D., Tu, C. L., Oda, Y., and Xie, Z. (2001) *Mol Cell Endocrinol* **177**(1-2), 161-71.
  28. Menon, G. K., Grayson, S., and Elias, P. M. (1985) *J Invest Dermatol* **84**(6), 508-12.
  29. Menon, G. K., Price, L. F., Bommannan, B., Elias, P. M., and Feingold, K. R. (1994) *J Invest Dermatol* **102**(5), 789-95.
  30. Mauro, T., Bench, G., Sidderas-Haddad, E., Feingold, K., Elias, P., and Cullander, C. (1998) *J Invest Dermatol* **111**(6), 1198-201.
  31. Kobayashi, T., Hattori, S., Nagai, Y., Tajima, S., and Nishikawa, T. (1998) *Dermatology* **197**(1), 1-5
  32. Kobayashi, T., Hattori, S., Nagai, Y., and Tajima, S. (2000) *IUBMB Life* **50**(3), 221-6.

33. Kobayashi, T., Kishimoto, J., Ge, Y., Jin, W., Hudson, D. L., Ouahes, N., Ehama, R., Shinkai, H., and Burgeson, R. E. (2001) *EMBO Rep* **2**(7), 604-8.
34. Munshi, H. G., and Stack, M. S. (2002) *Methods Cell Biol* **69**, 195-205
35. Laemmli, U. K. (1970) *Nature* **227**(259), 680-5.
36. Wong, H., Muzik, H., Groft, L. L., Lafleur, M. A., Matouk, C., Forsyth, P. A., Schultz, G. A., Wall, S. J., and Edwards, D. R. (2001) *Methods Mol Biol* **151**, 305-20
37. Neuhaus, E. M., and Soldati, T. (2000) *J Cell Biol* **150**(5), 1013-26.
38. Gospodarowicz, D. (1984) in *Methods for Preparation of Media Supplements and Substrata*. (Barnes, D.W., Sirbasku, D.A., and Stao, G.H., eds), pp 275-293, Alan R. Liss, New York.
39. Gilles, C., Polette, M., Coraux, C., Tournier, J. M., Meneguzzi, G., Munaut, C., Volders, L., Rousselle, P., Birembaut, P., and Foidart, J. M. (2001) *J Cell Sci* **114**(Pt 16), 2967-76.
40. Hernandez-Barrantes, S., Bernardo, M., Toth, M., and Fridman, R. (2002) *Semin Cancer Biol* **12**(2), 131-8.
41. Toth, M., Hernandez-Barrantes, S., Osenkowski, P., Bernardo, M. M., Gervasi, D. C., Shimura, Y., Meroueh, O., Kotra, L. P., Galvez, B. G., Arroyo, A. G., Mobashery, S., and Fridman, R. (2002) *J Biol Chem* **277**(29), 26340-50.
42. Azzam, H. S., and Thompson, E. W. (1992) *Cancer Res* **52**(16), 4540-4.
43. Seltzer, J. L., Lee, A. Y., Akers, K. T., Sudbeck, B., Southon, E. A., Wayner, E. A., and Eisen, A. Z. (1994) *Exp Cell Res* **213**(2), 365-74.
44. Gilles, C., Polette, M., Seiki, M., Birembaut, P., and Thompson, E. W. (1997) *Lab Invest* **76**(5), 651-60.
45. Haas, T. L., Davis, S. J., and Madri, J. A. (1998) *J Biol Chem* **273**(6), 3604-10.
46. Ellerbroek, S. M., Fishman, D. A., Kearns, A. S., Bafetti, L. M., and Stack, M. S. (1999) *Cancer Res* **59**(7), 1635-41.
47. Ellerbroek, S. M., Wu, Y. I., Overall, C. M., and Stack, M. S. (2001) *J Biol Chem* **276**(27), 24833-42.

48. Aznavoorian, S., Moore, B. A., Alexander-Lister, L. D., Hallit, S. L., Windsor, L. J., and Engler, J. A. (2001) *Cancer Res* **61**(16), 6264-75.
49. Strongin, A. Y., Marmer, B. L., Grant, G. A., and Goldberg, G. I. (1993) *J Biol Chem* **268**(19), 14033-9.
50. Will, H., Atkinson, S. J., Butler, G. S., Smith, B., and Murphy, G. (1996) *J Biol Chem* **271**(29), 17119-23.
51. Kurschat, P., Zigrino, P., Nischt, R., Breitkopf, K., Steurer, P., Klein, C. E., Krieg, T., and Mauch, C. (1999) *J Biol Chem* **274**(30), 21056-62.
52. Lohi, J., and Keski-Oja, J. (1995) *J Biol Chem* **270**(29), 17602-9.
53. Simon, C., Goepfert, H., and Boyd, D. (1998) *Cancer Res* **58**(6), 1135-9.
54. Yamamoto, M., Tsujishita, H., Hori, N., Ohishi, Y., Inoue, S., Ikeda, S., and Okada, Y. (1998) *J Med Chem* **41**(8), 1209-17.
55. Rozanov, D. V., Deryugina, E. I., Ratnikov, B. I., Monosov, E. Z., Marchenko, G. N., Quigley, J. P., and Strongin, A. Y. (2001) *J Biol Chem* **276**(28), 25705-14.
56. Jiang, A., Lehti, K., Wang, X., Weiss, S. J., Keski-Oja, J., and Pei, D. (2001) *Proc Natl Acad Sci USA* **98**(24), 13693-8.
57. Uekita, T., Itoh, Y., Yana, I., Ohno, H., and Seiki, M. (2001) *J Cell Biol* **155**(7), 1345-56.
58. Maquoi, E., Frankenne, F., Baramova, E., Munaut, C., Sounni, N. E., Remacle, A., Noel, A., Murphy, G., and Foidart, J. M. (2000) *J Biol Chem* **275**(15), 11368-78.
59. Brown, P. D., Bloxidge, R. E., Stuart, N. S., Gatter, K. C., and Carmichael, J. (1993) *J Natl Cancer Inst* **85**(7), 574-8.
60. Nomura, H., Fujimoto, N., Seiki, M., Mai, M., and Okada, Y. (1996) *Int J Cancer* **69**(1), 9-16.
61. Liabakk, N. B., Talbot, I., Smith, R. A., Wilkinson, K., and Balkwill, F. (1996) *Cancer Res* **56**(1), 190-6.
62. Crescimanno, C., Foidart, J. M., Noel, A., Polette, M., Maquoi, E., Birembaut, P., Baramova, E., Kaufmann, P., and Castellucci, M. (1996) *Exp Cell Res* **227**(2), 240-51.

63. Deryugina, E. I., Bourdon, M. A., Luo, G. X., Reisfeld, R. A., and Strongin, A. (1997) *J Cell Sci* **110**(Pt 19), 2473-82.
64. Makela, M., Larjava, H., Pirila, E., Maisi, P., Salo, T., Sorsa, T., and Uitto, V. J. (1999) *Exp Cell Res* **251**(1), 67-78.
65. Itoh, Y., Takamura, A., Ito, N., Maru, Y., Sato, H., Suenaga, N., Aoki, T., and Seiki, M. (2001) *Embo J* **20**(17), 4782-93.
66. Kawata, R., Shimada, T., Maruyama, S., Hisa, Y., Takenaka, H., and Murakami, Y. (2002) *Acta Otolaryngol* **122**(1), 101-6.
67. Overall, C. M., and Sodek, J. (1990) *J Biol Chem* **265**(34), 21141-51.
68. Yu, M., Sato, H., Seiki, M., and Thompson, E. W. (1995) *Cancer Res* **55**(15), 3272-7.
69. Maquoi, E., Frankenre, F., Noel, A., Krell, H. W., Grams, F., and Foidart, J. M. (2000) *Exp Cell Res* **261**(2), 348-59.
70. Stanton, H., Gavrilovic, J., Atkinson, S. J., d'Ortho, M. P., Yamada, K. M., Zardi, L., and Murphy, G. (1998) *J Cell Sci* **111**(Pt 18), 2789-98.
71. Gilles, C., Bassuk, J. A., Pulyaeva, H., Sage, E. H., Foidart, J. M., and Thompson, E. W. (1998) *Cancer Res* **58**(23), 5529-36.
72. Shofuda, K., Moriyama, K., Nishihashi, A., Higashi, S., Mizushima, H., Yasumitsu, H., Miki, K., Sato, H., Seiki, M., and Miyazaki, K. (1998) *J Biochem (Tokyo)* **124**(2), 462-70.
73. Baumann, P., Zigrino, P., Mauch, C., Breitkreutz, D., and Nischt, R. (2000) *Br J Cancer* **83**(10), 1387-93.
74. Nawrocki Raby, B., Polette, M., Gilles, C., Clavel, C., Strumane, K., Matos, M., Zahm, J. M., Van Roy, F., Bonnet, N., and Birembaut, P. (2001) *Int J Cancer* **93**(5), 644-52.
75. Takahashi, K., Eto, H., and Tanabe, K. K. (1999) *Int J Cancer* **80**(3), 387-95.
76. Giannelli, G., Falk-Marzillier, J., Schiraldi, O., Stetler-Stevenson, W. G., and Quaranta, V. (1997) *Science* **277**(5323), 225-8.
77. Koshikawa, N., Giannelli, G., Cirulli, V., Miyazaki, K., and Quaranta, V. (2000) *J Cell Biol*



148(3), 615-24.

## FIGURE LEGENDS

**Fig. 1. Extracellular calcium regulates proMMP-2 activation.** A. SCC25 cells were plated on plastic in medium containing 0.09 mM calcium. Following overnight serum starvation, cells were transferred to medium containing the indicated calcium concentration (0.09 mM to 1.2 mM). The conditioned media were collected at 24 h and analyzed for MMP activity by gelatin zymography. B. SCC25 cells were plated in medium containing 0.09 mM calcium on thin layer or three-dimensional (3-D) collagen as described in Experimental Procedures. Following serum starvation, media were replaced with serum-free medium at the indicated calcium concentration. The conditioned media were collected at 24 h and analyzed for MMP activity by gelatin zymography. The results are representative of at least four independent experiments.

**Fig. 2. Calcium-induced proMMP-2 activation involves MT1-MMP.** A. SCC25 cells were plated on plastic in medium containing 0.09 mM calcium, subjected to overnight serum starvation, and transferred to fresh medium at the indicated calcium concentration. At the time of calcium switch, the cells were treated with DMSO (vehicle control), MMP inhibitor GM6001 (10  $\mu$ M), TIMP-1 (20 ng/ml) or TIMP-2 (20 ng/ml). The conditioned media were collected at 24 h and analyzed for MMP activity by gelatin zymography. B. SCC25 cells were plated on plastic in medium containing 0.09 mM calcium, subjected to overnight serum starvation, and transferred to fresh medium at the indicated calcium concentration. At the time of calcium switch, the cells were treated with PMA (20 nM), MMP inhibitor GM6001 (10  $\mu$ M), and/or furin inhibitor decanoly-Arg-Val-Lys-Arg-chloromethylketone (RVKR, 20  $\mu$ M). The conditioned media were collected at 24 h and analyzed for MMP activity by gelatin zymography. The results are representative of three independent experiments.

**Fig. 3. Overexpression of MT1-MMP in SCC25 cells.** A. SCC25 cells overexpressing MT1-MMP (SCC25-MT) were generated as described in Experimental Procedures. At 24 h the cell lysates from wild type SCC25 and SCC25-MT cells were analyzed for MT1-MMP expression by western blotting and the conditioned media for MMP-2 activity by gelatin zymography. The membranes were immunoblotted with

anti-MT1-MMP antibody followed by peroxidase-conjugated secondary antibody and enhanced chemiluminescence detection. B. SCC25-MT cells were plated on plastic in medium containing 0.09 mM calcium. Following overnight serum starvation, cells were transferred to medium containing the indicated calcium concentration (0.09 mM to 1.2 mM). Conditioned media were collected at 24 h and analyzed for MMP activity by gelatin zymography. C, D. SCC25-MT cells were plated on plastic in medium containing 0.09 mM calcium and following overnight serum starvation, the media was changed to either 0.09 mM or to 1.2 mM calcium concentration. At the time of calcium switch, the cells were treated with DMSO (vehicle control), MMP inhibitor GM6001 (10  $\mu$ M), TIMP-1 (20 ng/ml) or TIMP-2 (20 ng/ml). The conditioned media were collected at 24 h and analyzed for MMP activity by gelatin zymography. The results are representative of two independent experiments.

**Fig. 4. Effect of extracellular calcium on MT1-MMP.** A. SCC25 (lanes 1-3) and SCC25-MT (lanes 4-6) cells were cultured for 24 h in medium at the indicated calcium concentration. Total RNA was isolated using Trizol reagent, quantified, and RT-PCR for MT1-MMP message was performed using primers as detailed in the Experimental Procedures. As loading control, amplification primers for GAPDH were used. PCR products were visualized by UV transillumination of 1.5% agarose gels stained with ethidium bromide. B. SCC25-MT cells were cultured in calcium-containing medium as indicated in the presence or absence of GM6001 (10  $\mu$ M). Cells were lysed at 24 h in modified RIPA buffer containing proteinase inhibitors. Equal amounts of cell lysates were separated by SDS-PAGE and the membranes were immunoblotted with anti-MT1-MMP antibody followed by peroxidase-conjugated secondary antibody and enhanced chemiluminescence detection (upper panel). The conditioned media was analyzed for MMP-2 activation using gelatin zymography (lower panel). C. SCC25-MT cells were cultured in calcium-containing medium as indicated in the presence or absence of GM6001 (10  $\mu$ M). After 24 h the cells were surface-biotinylated and lysed. Samples were immunoprecipitated with streptavidin beads at 4 °C for 14 h to isolate cell-surface (biotinylated) proteins, and electrophoresed on a 9% SDS-polyacrylamide gel. The membranes were immunoblotted with anti-MT1-MMP antibody followed by peroxidase-conjugated

secondary antibody and enhanced chemiluminescence detection. The results are representative of at least two independent experiments.

**Fig. 5. Calcium induces rapid surface activation of proMMP-2.** SCC25 and SCC25-MT cells were serum starved overnight, and incubated for an additional 24 h in medium containing 0.09 mM calcium. Calcium from a concentrated solution was added to the conditioned media to a final concentration of 1.2 mM, and at the indicated times (in hours) the cell lysates and conditioned media (CM) from SCC25 (A, C) and SCC25-MT (B, D) cells were analyzed for MMP-2 activation by gelatin zymography. The results are representative of four independent experiments.

**Fig. 6. Calcium does not affect cell surface MT1-MMP levels.** SCC25-MT cells were serum starved overnight and then incubated for an additional 24 h with DMSO or GM6001 (10  $\mu$ M) in medium containing 0.09 mM calcium. Calcium from a concentrated solution was added to the conditioned media to a final concentration of 1.2 mM, and at the indicated times the samples were surface labeled with biotin, immunoprecipitated with streptavidin and electrophoresed on a 9% SDS-polyacrylamide gel as described in Experimental Procedures. The membranes were immunoblotted with anti-MT1-MMP antibody, followed by peroxidase-conjugated secondary antibody and enhanced chemiluminescence detection. The results are representative of three independent experiments.

**Fig 7. Calcium does not affect MT1-MMP endocytosis.** A. Schematic of endocytosis protocol. [1] SCC25-MT cells were surface biotinylated on ice to block endocytosis with cleavable Sulfo-NHS-SS-biotin and transferred to 37 °C in medium containing 0.09 or 1.2 mM calcium. [2] Control cells were maintained at 4 °C. [3] After a 40-min incubation, cells were returned to 4 °C to block further internalization. [4] Surface biotin was removed with 100 mM MESNA. [5] In control experiments, MESNA was omitted to assess total labeled protein (surface and internalized). [6-8] Cells were washed with ice cold PBS, lysed, and labeled proteins precipitated at 4 °C for 14 h with streptavidin beads to

isolate labeled proteins. B. Samples prepared as described above were boiled, electrophoresed on a 9% SDS-polyacrylamide gel and immunoblotted with anti-MT1-MMP antibody, followed by peroxidase-conjugated secondary antibody and enhanced chemiluminescence detection. The results are representative of three independent experiments.

**Fig 8. Calcium decreases soluble TIMP-2.** A. SCC25-MT cells were cultured for 24 h in medium at the indicated calcium concentration in the presence or absence of GM6001 (10  $\mu$ M). The conditioned media were collected at 24 h, concentrated 15-20 fold using Micron 10 microconcentrators, electrophoresed on a 15% SDS-polyacrylamide gel and immunoblotted with anti-TIMP-2 antibody followed by peroxidase-conjugated secondary antibody and enhanced chemiluminescence detection. B. SCC25 (lanes 1-3) and SCC25-MT (lanes 4-6) cells were cultured for 24h in medium at the indicated calcium concentrations. Total RNA was isolated using Trizol reagent, quantified, and RT-PCR for TIMP-2 message was performed using primers described in Experimental Procedures. As loading control, amplification primers for GAPDH were used. The samples were electrophoresed on a 1.5% agarose gel, stained with ethidium bromide and visualized by UV transillumination. C. SCC25-MT cells were serum starved overnight, and incubated for an additional 24 h in medium containing 0.09 mM calcium in the presence or absence of GM6001 (10  $\mu$ M). Calcium from a concentrated solution was added to the conditioned media to a final concentration of 1.2 mM, and at the indicated times the conditioned medium was harvested, concentrated 15-20 fold, electrophoresed on a 15% SDS-polyacrylamide gel and immunoblotted with anti-TIMP-2 antibody followed by peroxidase-conjugated secondary antibody and enhanced chemiluminescence detection. The results are representative of at least three independent experiments.

**Fig 9. Calcium promotes degradation of TIMP-2.** SCC25-MT cells were serum-starved overnight and incubated for an additional 24 h at the indicated calcium concentration in the presence or absence of bafilomycin A1 (75 nM). A. Conditioned media were concentrated 15-20 fold using Micron 10 microconcentrators, and electrophoresed on a 15% SDS-polyacrylamide gel. The membranes were

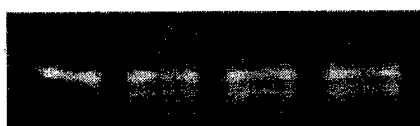
immunoblotted with anti-TIMP-2 antibody followed by peroxidase-conjugated secondary antibody and enhanced chemiluminescence detection. B. TIMP-2 levels in the cell lysates were quantified using ELISA according to the manufacturer's specifications. The results are representative of at least two independent experiments. \*, significantly different from control ( $\text{Ca}^{2+}$  0.09, Baf -) with  $p < 0.05$ .

Fig 10. **Calcium promotes cell migration.** A. Schematic of migration protocol. Cells were plated in medium containing 0.09 mM calcium on laminin-5 enriched matrix inside a glass ring. After removal of the ring, the cells were serum-starved for 3 h and then fresh serum-free medium containing either 0.09 mM or 1.2 mM calcium supplemented with 20 ng/ml EGF was added. Cells were allowed to migrate for 12-48 h. To quantify the relative motility, the migratory front was photographed every 12 h for 48 h and the percentage of cells crossing a line designated 'migratory max' was enumerated. B. SCC25 and SCC25-MT cells were allowed to migrate as described above in the presence or absence of GM6001 (10  $\mu\text{M}$ ). In a representative experiment, the relative motility at 24 h was quantified by determining the percentage of the SCC25 and SCC25-MT cells crossing the 'migratory max' line. The results are representative of three independent experiments.

**Fig 1**

**A**

**Ca<sup>2+</sup>**    0.09   0.4    0.8    1.2



**B**

**Collagen**

**Thin Layer**

**3D**

**Ca<sup>2+</sup>**   0.09   0.4   1.2    0.09   0.4   1.2



**Fig 2**

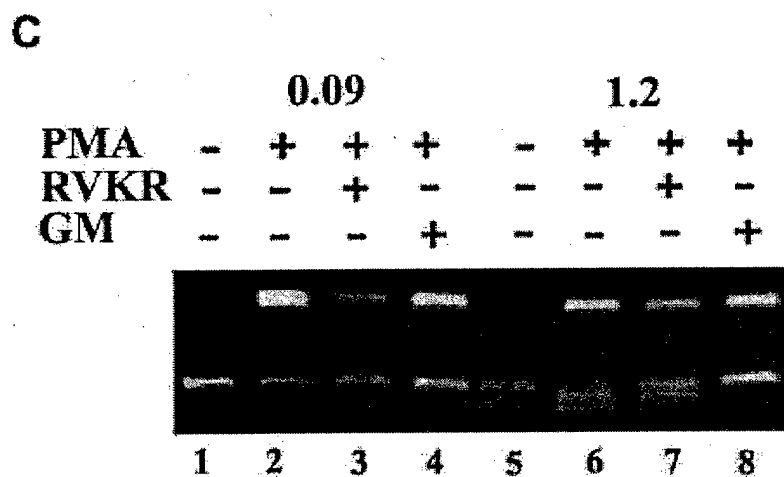
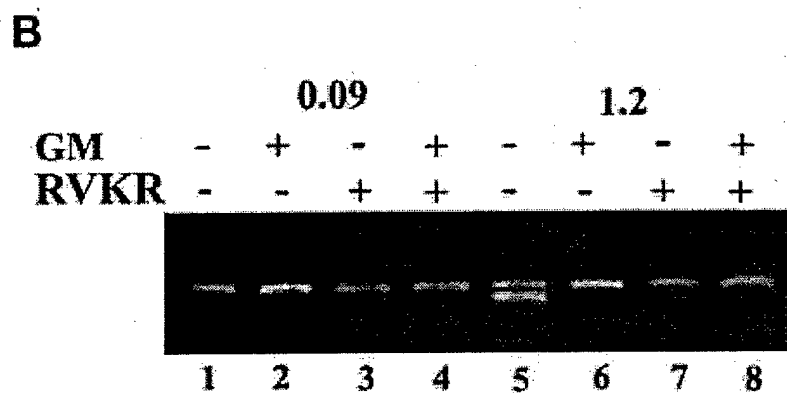
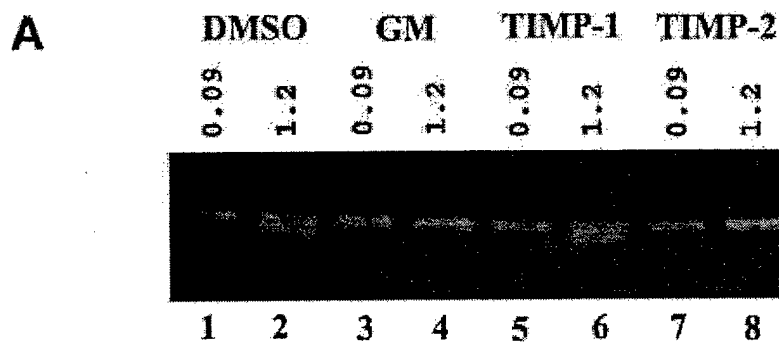




Fig 3

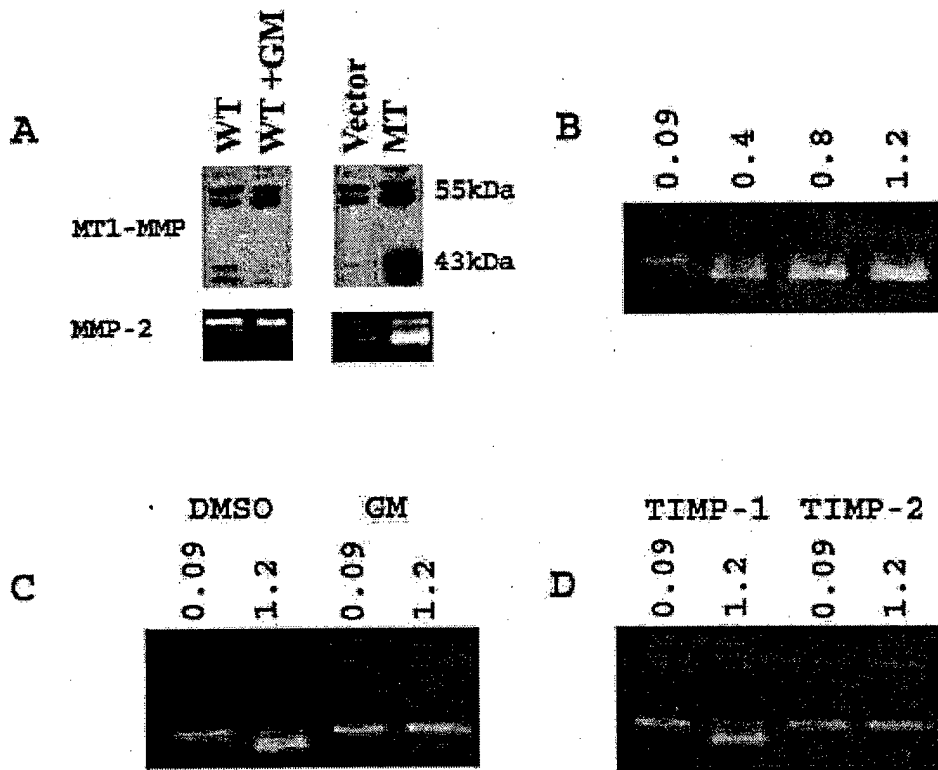


Fig 4

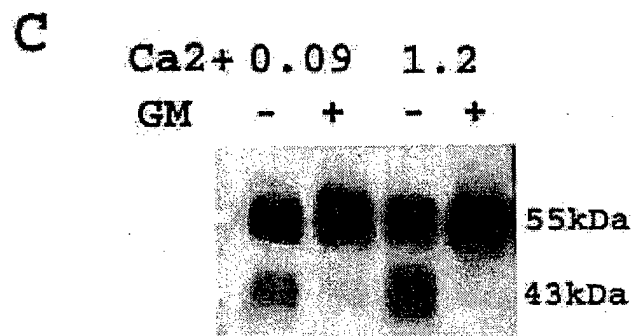
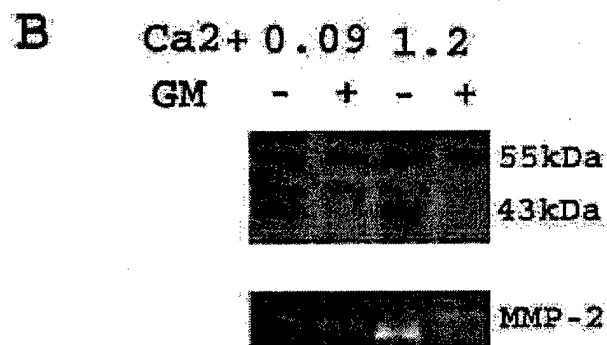
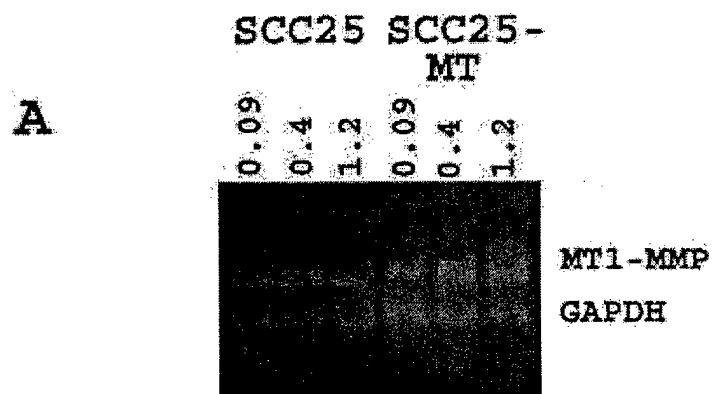


Fig 5

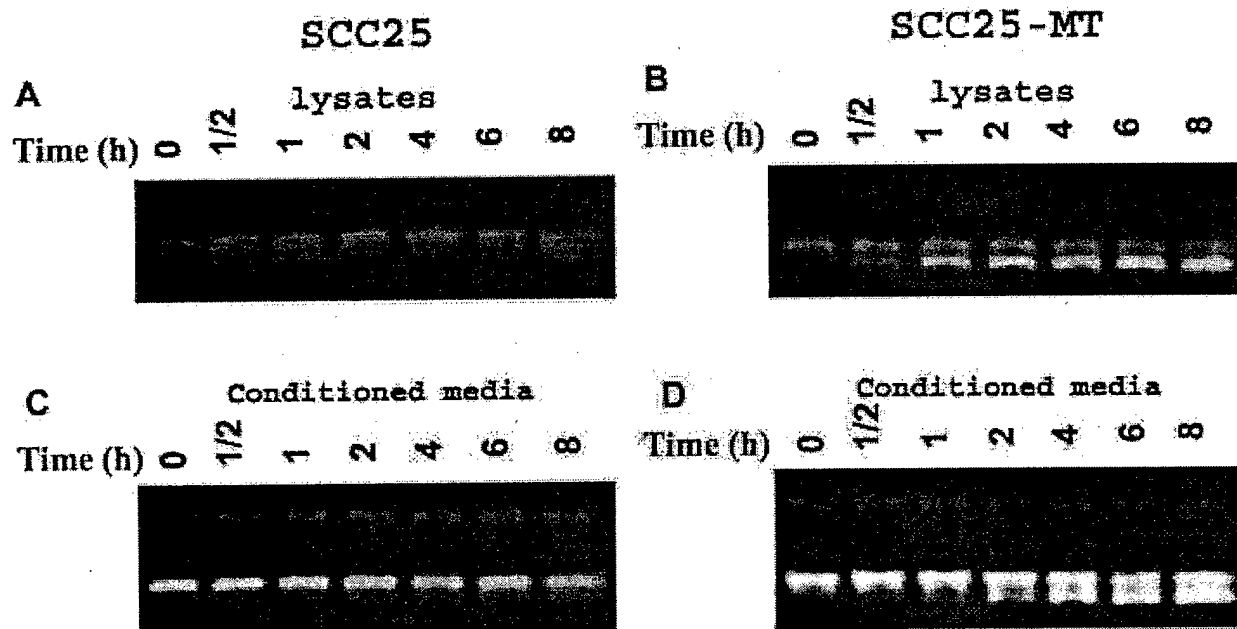
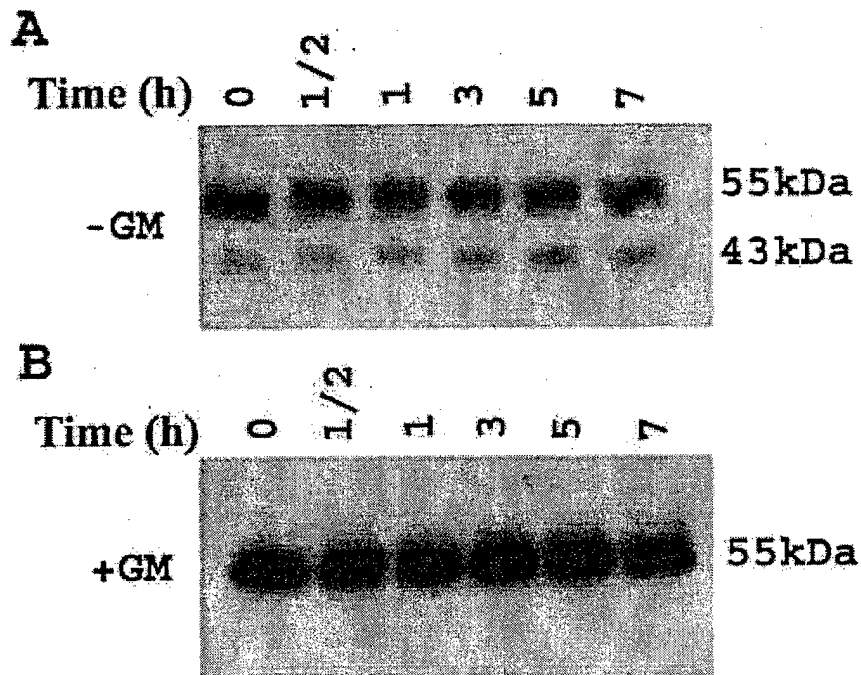
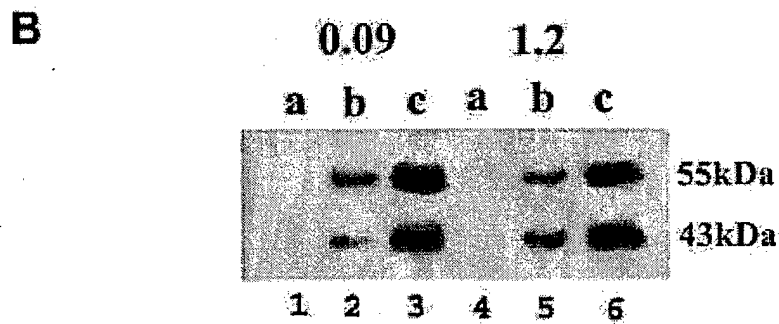
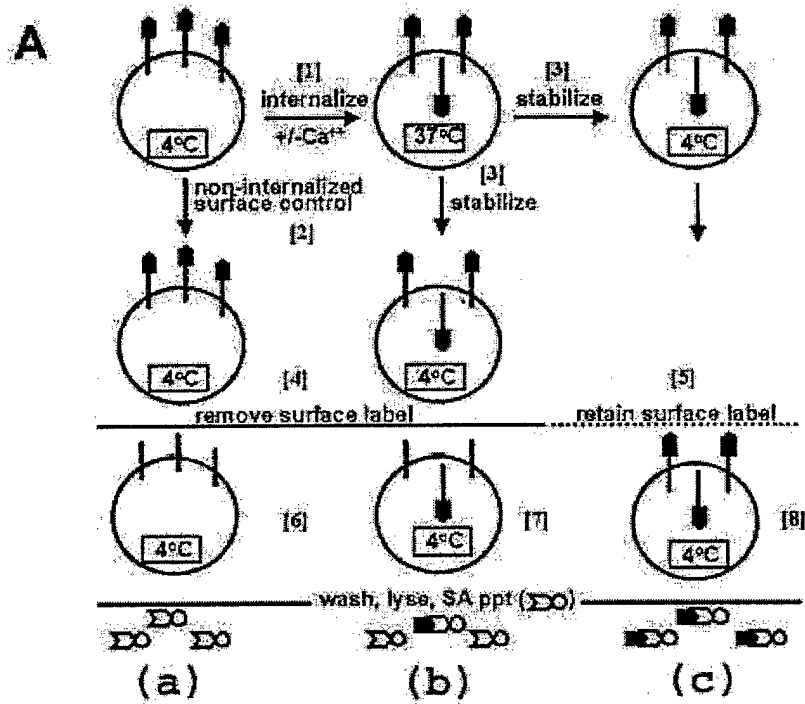


Fig 6



**Fig 7**



**Fig 8**

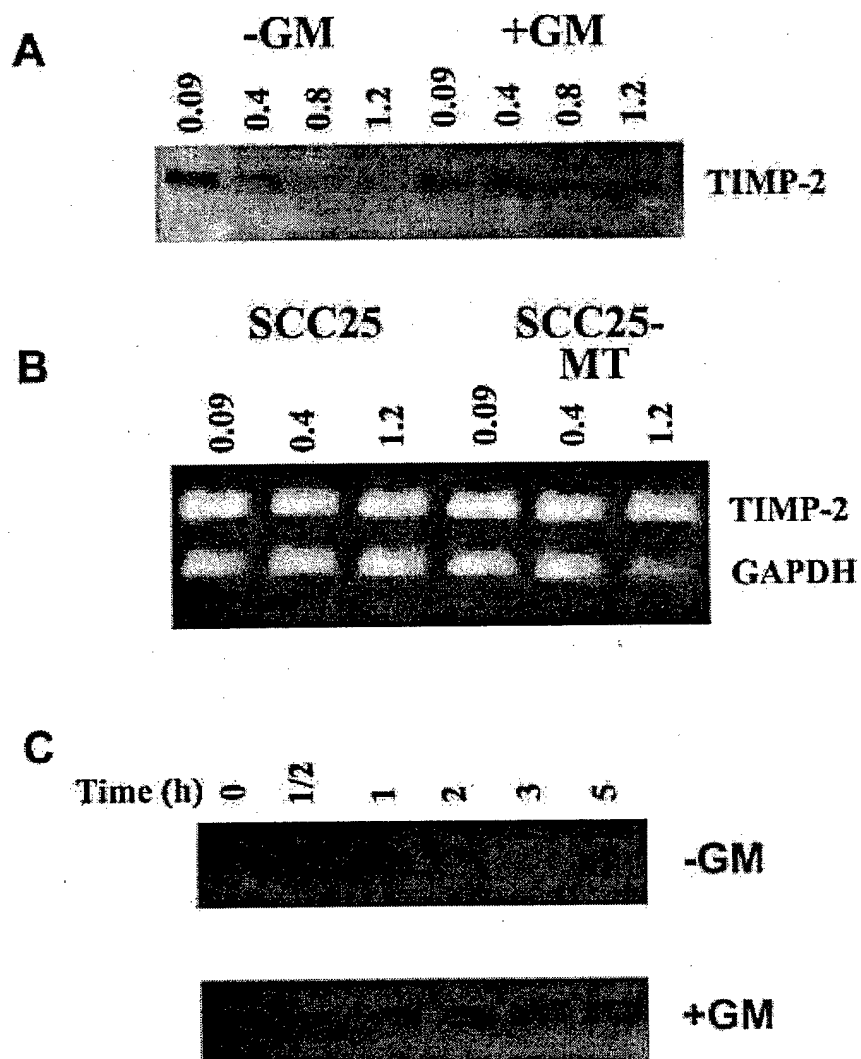
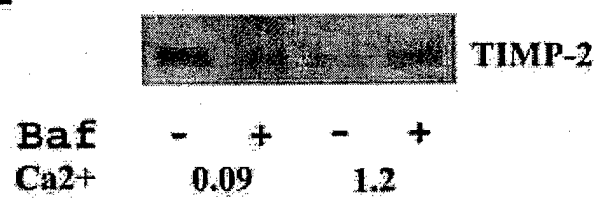
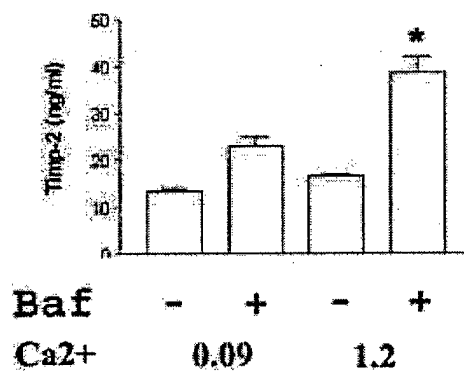


Fig 9

A



B



**Fig 10**

**A**

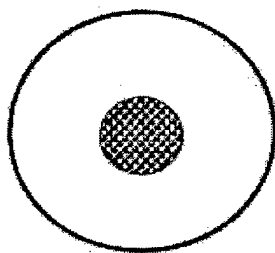
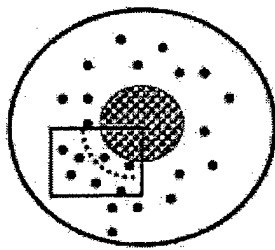


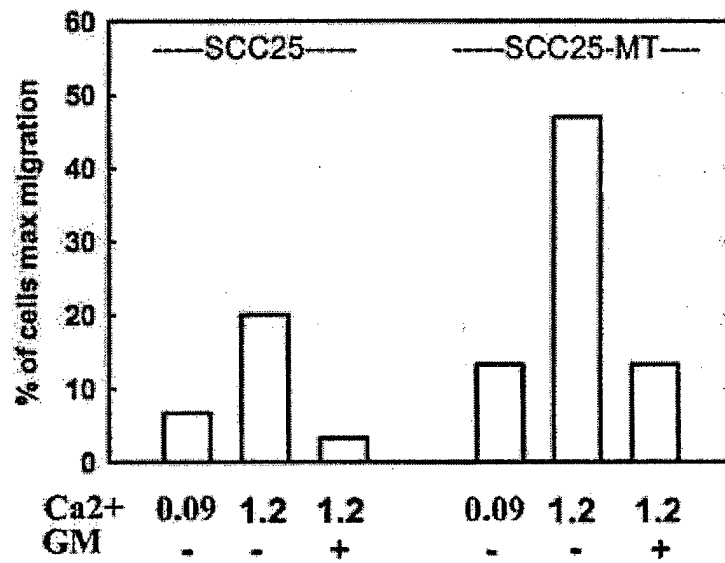
plate in cloning cylinder  
on matrix-coated dish

↓ 12-48h



photo, designate migration<sub>max</sub>,  
enumerate

**B**





## Type I Collagen Stabilization of Matrix Metalloproteinase-2

S. M. Ellerbroek,\* Y. I. Wu,\* and M. S. Stack\*<sup>†,1</sup>\*Department of Cell and Molecular Biology, and <sup>†</sup>Department of Obstetrics and Gynecology, Northwestern University Medical School, Chicago, Illinois 60611

Received November 30, 2000, and in revised form March 1, 2001; published online May 8, 2001

The activity of matrix metalloproteinase-2 (MMP-2) is regulated stringently on the posttranslational level. MMP-2 efficiently undergoes autolysis into inactive polypeptides *in vitro*, prompting the hypothesis that MMP-2 autolysis may function as an alternative mechanism for posttranslational control of MMP-2 *in vivo*. Moreover, MMP-2 binds to intact type I collagen fibrils; however, the functional consequences of this interaction have not been fully elucidated. To test the hypothesis that MMP-2 binding to type I collagen functions as a positive regulator of MMP-2 proteolytic potential, the effect of type I collagen on MMP-2 activity, inhibition by tissue inhibitor of metalloproteinase-2 (TIMP-2), and enzyme stability was examined. Here, we report that purified MMP-2 binds but does not cleave intact type I collagen. The presence of type I collagen affects neither enzymatic activity against a quenched fluorescent peptide substrate nor the kinetics of inhibition by TIMP-2. However, MMP-2 is stabilized from autolysis in the presence of type I collagen, but not by elastin, fibrinogen, or laminin. These data provide biochemical evidence that MMP-2 exosite interactions with type I collagen may function in the posttranslational control of MMP-2 activity by reducing the rate of autolytic inactivation. © 2001 Academic Press

**Key Words:** type I collagen; matrix metalloproteinase-2; gelatinase A; proteinase.

Matrix metalloproteinase-2 (MMP-2,<sup>2</sup> gelatinase A) is a member of a family of zinc-dependent metallo-endopeptidases that functions in the degradation of

collagen types IV, V, VII, X, and XIV, gelatins, elastin, fibronectin, and aggrecan (1–3). The proteinase is composed of five structural domains including an amino-terminal propeptide, a zinc-binding catalytic domain, fibronectin type II (FNII) repeats, a hinge region, and a carboxyl-terminal hemopexin-like domain (1–3). Both the fibronectin type II repeats and the hemopexin-like domain have been implicated in substrate recognition and targeting (4, 5). Unlike other MMP family members, MMP-2 production is largely refractory to stimulation by most biologic agents and is constitutively expressed by numerous cell types. Thus, the activity of MMP-2 is stringently regulated predominantly on the posttranslational level and many studies have focused on zymogen activation and enzyme-inhibitor binding as primary mechanisms for control of MMP-2-mediated proteolysis (reviewed in 1–3, 6). Activation of secreted proMMP-2 occurs at the cell surface via formation of a ternary complex between proMMP-2, tissue inhibitor of metalloproteinase-2 (TIMP-2) and a transmembrane MMP designated membrane type 1-MMP (MT1-MMP) (7–10). Pericellular TIMP-2 plays a dual role, as it is critical to promote ternary complex formation for zymogen activation, but can also function to inhibit either MMP-2 or MT1-MMP catalytic activity via formation of a 1:1 noncovalent inactive enzyme-inhibitor complex (7–10).

Active MMP-2 undergoes concentration-dependent autolysis at Pro<sup>394</sup>–Ile<sup>395</sup>, resulting in cleavage of the hemopexin-like domain from the catalytic domain (11). This observation suggests that the active state of MMP-2 is unstable in the absence of substrate and indicates that autolytic inactivation may function as an alternative mechanism for posttranslational control of MMP-2 activity (11). This hypothesis is supported by the observation that a hemopexin-like domain fragment of MMP-2 can be recovered from tumor tissues (12). Moreover, intermolecular autolytic cleavage of MMP-2 also occurs on the cell surface (13), indicating that a functional consequence of zymogen activation

<sup>1</sup> To whom correspondence should be addressed at Northwestern University Medical School, Department of Cell & Molecular Biology, 303 E. Chicago Avenue, Tarry 8-715, Chicago, IL 60611. Fax: (312) 503-7912. E-mail: mss130@northwestern.edu.

<sup>2</sup> Abbreviations used: MMP-2, matrix metalloproteinase-2; FNII, fibronectin type II; TIMP-2, tissue inhibitor of metalloproteinase-2; MT1-MMP, membrane type 1-MMP; APMA, amino-phenylmercuric acid; MMPI, MMP inhibitor; BSA, bovine serum albumin; DMSO, dimethylsulfoxide.

may be the generation and sequestration of sufficient MMP-2 to support autolytic processing.

In addition to TIMP-2-mediated regulation of zymogen activation and substrate cleavage, exosite interactions between MMP-2 and pericellular macromolecules may also influence enzyme activity. Previous studies have demonstrated that the FNII-like modules inserted within the MMP-2 catalytic domain promote protein-protein interaction between MMP-2 and type I collagen fibrils, gelatins, and insoluble elastin (14–17). While binding to gelatins may be predicted to promote enzyme activity, the significance of type I collagen binding is unclear, as only avian MMP-2 has been shown to function as an interstitial collagenase (18), while MMP-2 from other species is inactive against type I collagen (19–22). However, processing of MMP-2 by neutrophil elastase into inactive products is dramatically slowed in the presence of type I collagen or gelatin, suggesting that exosite interactions between the FNII-like domains of MMP-2 and pericellular matrix proteins such as type I collagen may protect the enzyme from proteolytic degradation (23). This hypothesis is supported by studies showing that addition of soluble type I collagen or gelatin to purified MMP-2 decreased the rate of autolysis (10). Furthermore, cellular MT1-MMP-mediated proMMP-2 activation is enhanced in the presence of exogenous recombinant FNII-like domain, suggesting that disruption of the proMMP-2/pericellular collagen interaction may promote filtration of proMMP-2 into the MT1-MMP activation pathway (5). Together, these data suggest that MMP-2 binding to type I collagen functions as a positive regulator of MMP-2 proteolytic potential. To advance this hypothesis, the effect of type I collagen on MMP-2 activity, inhibition by TIMP-2, and enzyme stability was examined. These data indicate that collagen binding does not alter net MMP-2 enzymatic activity, but functions to significantly reduce the rate of autolysis.

## MATERIALS AND METHODS

**Materials.** Purified human MMP-1, MMP-2 (TIMP-2-free), and TIMP-2 were generous gifts of Dr. Hideaki Nagase (Kennedy Institute of Rheumatology, Imperial College School of Medicine, United Kingdom). Bovine serum albumin and type I gelatin, amino-phenylmercuric acetate (APMA), dimethyl sulfoxide, and human type I collagen, fibrinogen, elastin, laminin-1, and pepsin were purchased from Sigma (St. Louis, MO). The quenched fluorescent peptide substrate, Mca-Pro-Leu-Gly-Leu-Dpa-Ala-Arg-NH<sub>2</sub>, and peptide standard, Mca-Pro-Leu-OH were acquired from BACHEM BioSciences, Inc. (King of Prussia, PA). The serine protease inhibitor aprotinin was purchased from Alexis Biochemicals (San Diego, CA). The broad spectrum hydroxamic acid-based MMP inhibitor designated MMP INH-3850-PI (MMPI) was purchased from Peptides International (Louisville, KY).

**Collagenase assays.** Cleavage of native or denatured type I collagen was evaluated by incubating type I collagen or gelatin (10  $\mu$ g) with the indicated concentrations of MMPs in Tris-glucose buffer (50 mM Tris, 200 mM glucose, 200 mM NaCl, pH 7.4) for 18 h (25°C), followed by electrophoretic resolution on 8–15% SDS-polyacryl-

amide gels (24). Collagen degradation was visualized by staining gels with Coomassie blue. Prior to incubation with collagen or gelatin, MMPs were diluted to a concentration of 1  $\mu$ M and incubated for 30 min (37°C) with 2 mM APMA to promote enzyme auto-activation. Type I gelatin was prepared by thermal denaturation of human type I collagen (60°C, 20 min).

**Collagen binding.** Microtiter plates (high binding; Greiner, Lake Mary, FL) were coated overnight by passive adsorption at 4°C in assay buffer (100 mM Tris-HCl, pH 7.5, 100 mM NaCl, 10 mM CaCl<sub>2</sub>, 0.05% Brij-35) containing 100  $\mu$ g of the indicated matrix protein. Nonspecific binding sites on coated wells were blocked by incubation with a 200- $\mu$ l volume of 3% BSA in assay buffer for 2 h (37°C). To evaluate the structural integrity of immobilized collagen or gelatin, wells were incubated with MMP-2 (~1 nM, 35°C, 18 h) or pepsin (1 unit in 0.1% acetic acid, pH 2.6, 37°C, 15 min) prior to solubilization in reducing Laemmli sample dilution buffer (24) and electrophoresis on 8% SDS-polyacrylamide gels. Protein degradation was visualized by staining gels with Coomassie blue. To evaluate the activity of collagen-bound MMP-2, purified MMP-2 was activated with APMA as described above, diluted to 50 nM in assay buffer, and incubated overnight (4°C) in protein-coated wells in a 50- $\mu$ l volume. Aliquots (5  $\mu$ l) were removed and analyzed by gelatin substrate zymography (designated "solution phase") (25). Wells were then washed five times with 50  $\mu$ l of assay buffer and bound MMP eluted by incubation with 50  $\mu$ l of nonreducing Laemmli sample dilution buffer (24) for 1 h at 25°C (designated "bound") prior to evaluation by gelatin zymography. The presence of bound MMP-2 was confirmed by incubating wells overnight at 4°C with 10% DMSO to disrupt MMP-2-type I collagen interactions (16). In control experiments, wells were incubated with 50  $\mu$ l of assay buffer in place of Laemmli buffer.

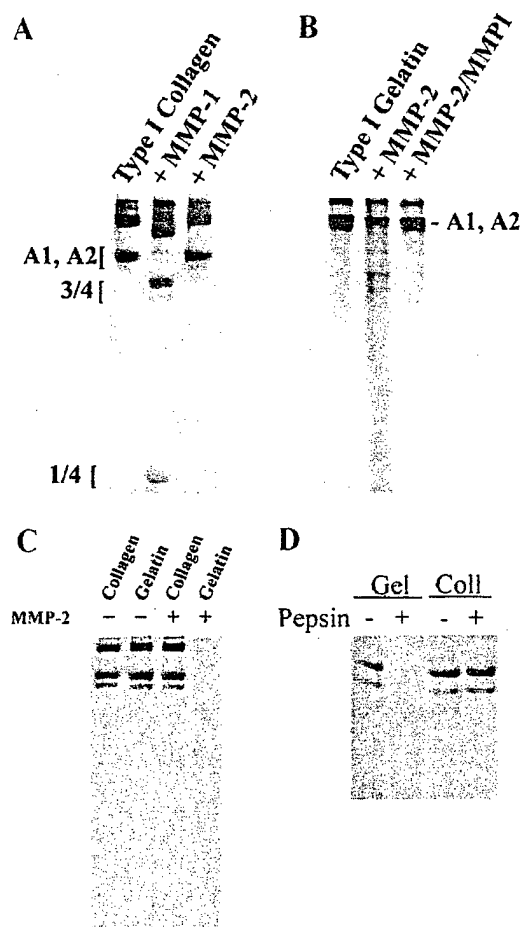
**MMP activity assays.** To quantify the activity of bound MMP-2, wells were coated with collagen (100  $\mu$ g) as described above and incubated overnight (4°C) with a 100- $\mu$ l volume of APMA-activated MMP-2 (10 nM) containing 1% DMSO. Unbound enzyme was removed and wells washed twice with 100  $\mu$ l of assay buffer before adding 100  $\mu$ l of fresh assay buffer. The plate was then switched to 37°C, the quenched fluorescent peptide substrate Mca-Pro-Leu-Gly-Leu-Dpa-Ala-Arg-NH<sub>2</sub> (26) was added to wells (10  $\mu$ M), and substrate cleavage was evaluated using an excitation wavelength of 326 nm and monitoring emission at 396 nm with a fluorescent plate reader (Molecular Devices, SpectraMAX Gemini). A 1% concentration of DMSO was used to ensure the solubility of the synthetic substrate without affecting the ability of MMP-2 to bind collagen (data not shown; Ref. (16)). Steady-state initial velocities of substrate cleavage were established for solution phase and bound MMP-2 over a period of 15 min. Standard curves were generated by measuring the relative fluorescence emission of the cleavage product Mca-Pro-Leu-OH in solution containing 1% DMSO. Plots were constructed of velocity (fmol/s) vs substrate ( $\mu$ M) using SigmaPlot software, and regression values calculated to produce kinetic constants ( $V_{max}$ ,  $k_{cat}$ , and  $K_m$ ). Inhibition of MMP-2 was evaluated by adding increasing amounts of TIMP-2 and monitoring initial velocity as described above. Analyses were carried out in triplicate.

**Enzyme stability.** The stability of bound MMP-2 was determined by incubating APMA-activated MMP-2 in protein-coated microtiter wells overnight (4°C) in the presence of 1  $\mu$ g/ml aprotinin (although no contaminating serine proteases were detected in the enzyme or matrix protein preparations). The temperature was raised to 37°C for 18 h to induce MMP-2 autolysis. Following incubation, MMP-2 activity in aliquots was analyzed using the quenched fluorescent peptide substrate and by gelatin zymography as described above.

## RESULTS AND DISCUSSION

### Interaction of MMP-2 with Type I Collagen

To evaluate the role of type I collagen binding in regulation of MMP-2 proteolytic potential, the func-

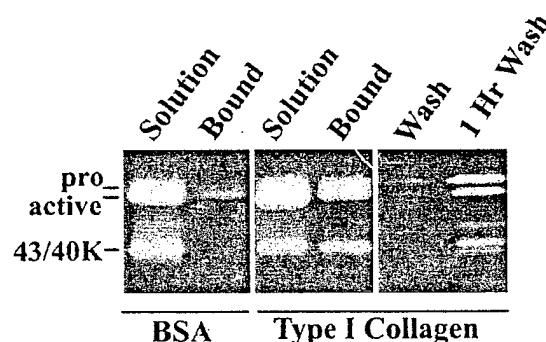


**FIG. 1.** MMP-2 does not cleave soluble or immobilized type I collagen. (A) Soluble human placental type I collagen (10  $\mu$ g) was incubated at 25°C for 18 h in the presence of MMP-2 or MMP-1 (50 nM) as indicated. Reaction products were analyzed by electrophoresis on 8–15% gradient SDS–polyacrylamide gels followed by Coomassie blue staining. The migration positions of the  $\frac{3}{4}$  and  $\frac{1}{4}$  collagenase cleavage products are indicated. (B) Type I gelatin (10  $\mu$ g) was incubated in the presence or absence of MMP-2 (50 nM) as indicated under conditions as described in (A). Control reactions contained the broad spectrum hydroxamic acid-based inhibitor MMPI (10  $\mu$ M). (C) Collagen- or gelatin-coated microtiter wells were incubated with MMP-2 (~1 nM) for 18 h at 35°C followed by solubilization and analysis of bound protein by electrophoresis on 8% SDS–polyacrylamide gels and Coomassie blue staining. (D) Collagen- or gelatin-coated microtiter wells were incubated with pepsin (1 unit) for 15 min at 37°C followed by solubilization and analysis of bound protein by electrophoresis on 8% SDS–polyacrylamide gels and Coomassie blue staining.

tional consequences of the MMP-2–collagen interaction were evaluated. Although the gelatinolytic activity of MMP-2 is well established, evidence that MMP-2 can cleave soluble type I collagen is limited to a single report (18). To determine whether MMP-2 functions as an interstitial collagenase, type I collagen was incubated with catalytic amounts of TIMP-2-free MMP-2 or MMP-1 (collagenase-1). While MMP-1 cleaves native type I collagen into 3/4 and 1/4 alpha chain fragments, no collagen cleavage is catalyzed by MMP-2 (Fig. 1A).

Equivalent concentrations of MMP-2 efficiently cleave type I gelatin (Fig. 1B), confirming that the purified enzyme is catalytically active. These results support previous conclusions that native type I collagen does not function as substrate for human MMP-2 (19–22). Thus, the interstitial collagenase activity previously attributed to MMP-2 (18) may reflect enzymatic properties unique to the avian enzyme.

As interaction of MMP-2 with type I collagen may function as a mechanism for posttranslational regulation of MMP-2 activity, association of MMP-2 with collagen immobilized on microtiter plates by passive adsorption was evaluated. To first assess the structural integrity of immobilized collagen, microtiter plates coated with collagen or gelatin were incubated with either MMP-2 (Fig. 1C) or pepsin (Fig. 1D). Whereas gelatin was susceptible to cleavage by both MMP-2 and pepsin (Fig. 1C, lane 4; Fig. 1D, lane 2), immobilized collagen was resistant to these gelatinolytic proteinases, indicating that immobilization does not result in collagen denaturation. Microtiter plates coated with type I collagen or BSA by passive adsorption were then incubated with MMP-2 overnight, and a qualitative analysis of collagen-bound MMP-2 obtained by gelatin zymography of solubilized proteins. Bound MMP-2 was detectable only in type I collagen-coated wells, but not in BSA-coated control samples (Fig. 2, lanes 2 and 4). Major autolytic fragments of MMP-2 (43/40K) lacking the hemopexin domain but retaining the FNII repeats (11) were also collagen-associated (Fig. 2). To evaluate the reversibility of binding, collagen-coated wells containing bound MMP-2 were



**FIG. 2.** MMP-2 binds to type I collagen. MMP-2 (50 nM) was preactivated with APMA as described under Materials and Methods and incubated overnight (4°C) in wells coated with type I collagen or BSA (150  $\mu$ g) as indicated. Soluble enzyme was removed (designated "solution," lanes 1 and 3). After washing wells five times with assay buffer (100 mM Tris–HCl, pH 7.15, 100 mM NaCl, 10 mM CaCl<sub>2</sub>, 0.05% Brij-35), bound enzyme was eluted using nonreducing Laemmli sample dilution buffer (50  $\mu$ l, designated "bound," lanes 2 and 4). To assess the reversibility of binding, collagen-coated wells containing bound MMP-2 were washed with assay buffer as described above (lane 5), incubated for 1 h in assay buffer, and the solubilized enzyme analyzed (designated "1 h wash," lane 6). All samples were evaluated by gelatin zymography on 9% SDS–polyacrylamide gels containing copolymerized gelatin as described under Materials and Methods.

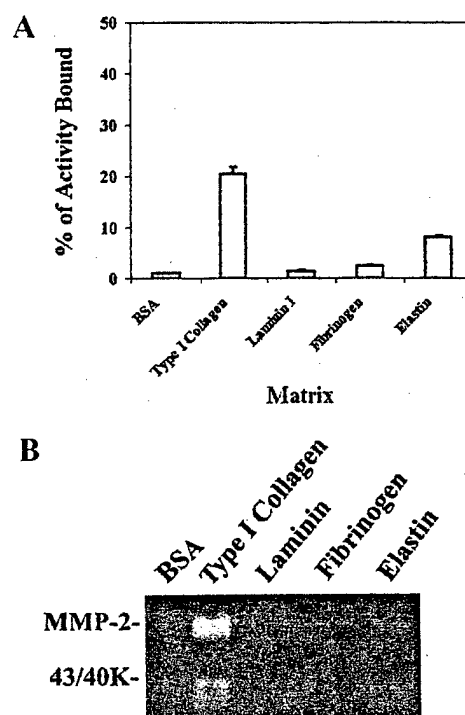
washed free of detectable enzyme, followed by incubation in assay buffer. Within 1 h significant MMP-2 is dissociated from collagen into the solution phase (Fig. 2, lane 6), indicating that MMP-2 interaction with immobilized type I collagen is reversible. These data are in good agreement with previous reports that have estimated that the dissociation constant for MMP-2 binding to type I collagen is in the low micromolar range (16, 17).

To quantify the catalytic activity of bound MMP-2, wells were coated with various matrix proteins and incubated with MMP-2 as described above. Laminin-1 and the fibrous proteins fibrinogen and elastin (27) were utilized to control for matrix specificity and non-specific enzyme trapping within fibrous matrices. Following incubation, soluble enzyme was removed (solution phase), and the activity of bound MMP-2 evaluated by the addition of a quenched fluorescent peptide substrate (26). Type I collagen- and elastin-coated wells reproducibly retained ~20 and ~8% of total MMP-2 activity, respectively, relative to other control matrix protein surfaces upon which little enzymatic activity was detected (Fig. 3A). Gelatin zymography following solubilization of proteins confirmed the presence of collagen-bound MMP-2 activity (Fig. 3B). These data support previously published results (17) which demonstrate binding of both pro- and active MMP-2 to type I collagen and suggest that collagen binding does not negatively influence enzymatic activity.

#### *MMP-2 Kinetic Activity in the Presence of Type I Collagen*

As the FNII-like modules reside within the catalytic domain of MMP-2, enzymatic activity may be influenced by collagen binding. To test this hypothesis, the kinetics of substrate cleavage by MMP-2 were measured in the absence or presence of type I collagen using a quenched fluorescent peptide substrate. Although steady-state velocity was reproducibly higher in the presence of collagen, no significant difference in catalytic efficiency ( $k_{cat}/K_m$ ) was observed (Fig. 4), indicating that overall enzyme activity is not altered by collagen binding. As MMP-2-collagen binding is of relatively low affinity (16, 17) and likely involves continual exchange of enzyme between the insoluble (bound) and solution phase (Fig. 2), these data demonstrate that transient collagen interactions do not decrease MMP-2 proteolytic potential. It should be noted, however, that minor variations in the activity of bound MMP-2 (relative to solution phase) may not be detected in this system, which evaluates the equilibrium effects of collagen binding on catalytic activity.

In addition to substrate cleavage, interaction of MMP-2 with its primary inhibitor TIMP-2 may also be influenced by collagen binding (28, 29). To address this



**FIG. 3.** Quantification of MMP-2 catalytic activity. (A) To quantify the activity of MMP-2 bound to collagen, MMP-2 (10 nM) was incubated overnight (4°C) in wells coated with type I collagen, Laminin-1, fibrinogen, elastin, or BSA as indicated. Unbound enzyme was removed, wells washed five times, and the activity of MMP-2 quantified using the quenched fluorescent peptide substrate Mca-Pro-Leu-Gly-Leu-Dpa-Ala-Arg-NH<sub>2</sub> (10  $\mu$ M) and monitoring emission at 396 nm using an excitation wavelength of 326 nm. Steady-state velocities were established and compared with the activity of 10 nM soluble MMP-2 (designated 100%) ( $n = 3$ ). (B) Following quantitative analysis, MMP-2 was eluted from wells (coated with specific proteins, as indicated) using nonreducing Laemmli sample buffer and analyzed by gelatin zymography.

possibility, MMP-2 was incubated with increasing molar amounts of TIMP-2 in the presence or absence of collagen, and the remaining enzymatic activity evaluated (Fig. 5). TIMP-2 effectively inhibited MMP-2 activity at a MMP-2:TIMP-2 molar ratio of approximately 1.2:1 and this ratio was unaltered by collagen. Further, no differences were observed in the rate of inhibition (not shown), indicating that collagen binding does not restrict access of the inhibitor to the enzyme active site. However, as indicated above, the dissociation of MMP-2 from collagen fibers during the time course of the assay may mask subtle differences in inhibition kinetics. In this regard, it is interesting to note that inhibition of MMP-2 by membrane-localized TIMP-2 is slowed in the presence of soluble type I collagen or gelatin (10). These differences may reflect collagen-induced changes in enzyme stability during the time course of the assay, as stabilization against autolysis would contribute to overall higher levels of catalytic activity.

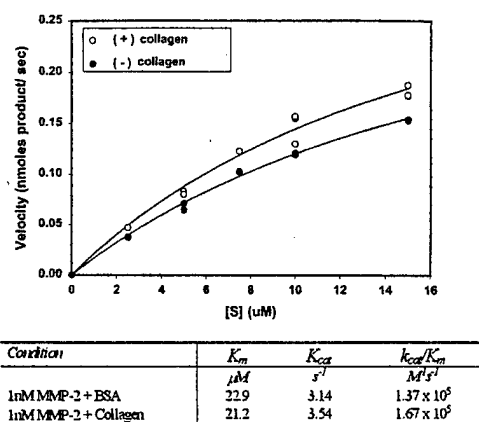


FIG. 4. MMP-2 kinetic activity is not altered by type I collagen. Microtiter plates were coated with type I collagen or BSA (100  $\mu g$ ) as indicated. Wells were loaded with increasing concentrations of quenched fluorescent substrate (0–15  $\mu M$ , as indicated) and substrate cleavage initiated by the addition of APMA-activated MMP-2 (10 nM). Substrate cleavage was monitored as described in Fig. 3, and kinetic parameters analyzed by nonlinear regression of the velocity data. Kinetic constants of substrate cleavage in type I collagen- or BSA-coated wells are summarized in the inset.

#### Type I Collagen Stabilizes MMP-2 against Autolysis

Previous studies have demonstrated that MMP-2 undergoes autolytic processing in solution phase, resulting in a truncated enzyme with reduced or abrogated catalytic activity (10, 11). To evaluate the effect of collagen binding on enzyme stability, MMP-2 autolysis was examined in the presence of collagen or control matrix proteins. Binding of activated MMP-2 to immobilized proteins was carried out at 4°C, followed by incubation at 37°C to promote enzyme autolysis. In solution phase, a significant decrease in activity is

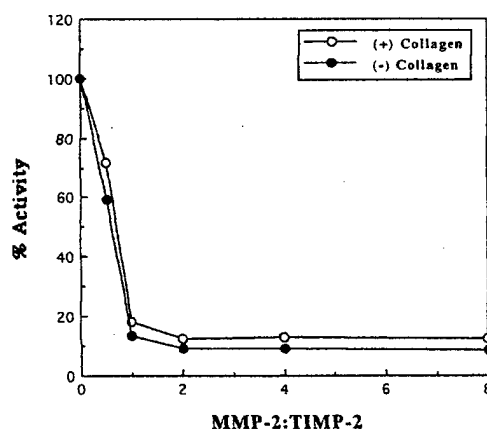


FIG. 5. Effect of type I collagen on MMP-2 inhibition by TIMP-2. MMP-2 (10 nM) was allowed to bind to collagen-coated wells overnight (4°C) before addition of the quenched fluorescent peptide substrate (10  $\mu M$ ) and the indicated molar ratio of TIMP-2. Steady-state velocity was calculated as described under Materials and Methods. Data are plotted as percentage activity, with MMP-2 activity in the absence of TIMP-2 designated as 100%.

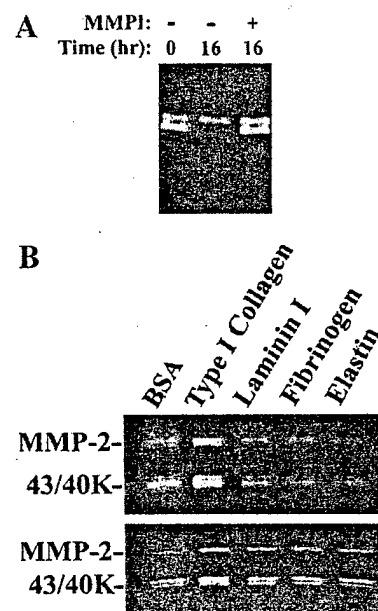


FIG. 6. Collagen stabilizes MMP-2 against autolysis. (A) APMA-activated MMP-2 (10 nM) was incubated for 16 h at 37°C in the absence or presence of the MMP inhibitor MMPI (10  $\mu M$ ) as indicated to prevent autolysis. (B) Microtiter wells were coated with the indicated matrix proteins (100  $\mu g$ ), incubated with MMP-2 (10 nM) overnight (4°C), and shifted to 37°C for 18 h to promote enzyme autolysis. Dimethyl sulfoxide (10% final concentration) was added to wells to elute bound MMP-2 and duplicate samples were analyzed by gelatin zymography (top and bottom).

observed following incubation for 16 h at 37°C (Fig. 6A). However, in the presence of type I collagen, MMP-2 activity is stabilized (Fig. 6B). This effect is specific to type I collagen, as neither laminin-1, fibrinogen, nor elastin enhanced MMP-2 stability (Fig. 6B). This result was confirmed using the quenched fluorescent peptide substrate, demonstrating a statistically significant retention of MMP-2 catalytic activity (Table I). Together these data indicate that although collagen binding has no effect on MMP-2 catalytic activity or TIMP-2 inhibition, proteolytic potential may be en-

TABLE I  
Type I Collagen Stabilizes MMP-2 Activity<sup>a</sup>

Condition	Velocity (fmol/s)	Product generated (pmol $\pm$ SD)
Bovine serum albumin	66.9 $\pm$ 1.1	206.9 $\pm$ 9.0
Type I collagen	118.5 $\pm$ 2.1	340.9 $\pm$ 4.3
Laminin I	86.7 $\pm$ 3.6	242.8 $\pm$ 5.1
Fibrinogen	80.6 $\pm$ 2.9	224.1 $\pm$ 9.6
Elastin	90.4 $\pm$ 3.9	241.5 $\pm$ 7.4

<sup>a</sup> Microtiter wells were coated with the indicated matrix proteins (100  $\mu g$ ), incubated with MMP-2 (10 nM) overnight (4°C), and shifted to 37°C for 18 h to promote enzyme autolysis. Substrate (7.5  $\mu M$ ) was added and steady-state reaction velocities and product generation were evaluated for 45 min ( $N = 3$ ).

hanced in the presence of collagen due to protection from autolytic inactivation.

It has previously been reported that high concentrations (0.5 mg/ml) of soluble type I collagen stabilize MMP-2 activity (10). Our data support these findings and demonstrate that immobilized collagen, which may mimic more closely the insoluble collagen structures found *in vivo*, can also potentiate MMP-2 activity. We hypothesize that as MMP-2 binds to immobilized type I collagen, the concentration of solution-phase enzyme is decreased, subsequently reducing the extent of soluble enzyme autolytic turnover. Further, these data demonstrate that type I collagen may play a dual role in regulation of MMP-2-mediated pericellular proteolysis. Initially, cellular binding to collagen or experimental engagement of collagen binding integrins using immobilized antibodies induces MT1-MMP-mediated activation of proMMP-2 in a variety of cell types (5, 30–35), thus increasing the concentration of active pericellular MMP-2. Subsequently, binding of the active proteinase to this integrin-associated collagen can further potentiate substrate cleavage by stabilizing active MMP-2 against autolytic inactivation. Based on these data, it is interesting to speculate that binding to type I collagen may function as an additional post-translational mechanism for regulation of MMP-2 activity by enhancing enzyme stability as well as increasing the proximity of active proteinase to potential extracellular matrix substrates.

#### ACKNOWLEDGMENTS

The authors thank Dr. Carl Waltenbaugh, Northwestern University, for the use of the Molecular Devices SpectraMAX Gemini fluorescent microtiter plate reader. This work is supported by training Grant 5T32 GM08061 (S.M.E.) from the National Institute of Health, training grant DAMD170010386 (Y.I.W.) from the U.S. Army MRMC and research grant RO1 CA86984 (M.S.S.) from the National Cancer Institute, National Institutes of Health.

#### REFERENCES

- Birkedal-Hansen, H., Moore, W. G. I., Bodden, M. K., Windson, L. J., Birkedal-Hansen, B., Decarlo, A., and Engler, J. A. (1993) *Crit. Rev. Oral Biol. Med.* **4**, 197–250.
- Murphy, G., and Knauper, V. (1997) *Matrix Biol.* **15**, 511–518.
- Nagase, H., and Woessner, J. F., Jr. (1997) *J. Biol. Chem.* **274**, 21491–21494.
- Murphy, G., Allan, J. A., Willenbrock, F., Cockett, M. I., O'Connell, J. P., and Docherty, A. J. P. (1992) *J. Biol. Chem.* **267**, 9612–9618.
- Steffensen, B., Bigg, H. F., and Overall, C. M. (1998) *J. Biol. Chem.* **273**, 20622–20628.
- Ellerbroek, S. M., and Stack, M. S. (1999) *Bioessays* **21**, 940–949.
- Zucker, S., Drews, M., Conner, C., Foda, H. D., DeClerck, Y. A., Langley, K. E., Bahou, W. F., Docherty, A., and Cao, J. (1998) *J. Biol. Chem.* **273**, 12116–1222.
- Butler, G. S., Butler, M. J., Atkinson, S. J., Will, H., Tamura, T., van Westrum, S. S., Crabbe, T., Clements, J., d'rtho, M. P., and Murphy, G. (1998) *J. Biol. Chem.* **273**, 871–880.
- Imai, K., Ohuchi, E., Aoki, T., Nomura, H., Fujii, Y., Sato, H., Seiki, M., and Okada, Y. (1996) *Cancer Res.* **56**, 2707–2710.
- Itoh, Y., Ito, A., Iwata, K., Tanzawa, K., Mori, Y., and Nagase, H. (1998) *J. Biol. Chem.* **273**, 24360–24367.
- Bergmann, U., Tuuttila, A., Stetler-Stevenson, W. G., and Trygvsen, K. (1995) *Biochemistry* **34**, 2819–2825.
- Brooks, P. C., Silletti, S., von Schalscha, T. L., Friedlander, M., and Cheresch, D. A. (1998) *Cell* **92**, 391–400.
- Atkinson, S. J., Crabbe, T., Cowell, S., Ward, R. V., Butler, M. J., Sato, H., Seiki, M., Reynolds, J. J., and Murphy, G. (1995) *J. Biol. Chem.* **270**, 30479–30485.
- Banyai, L., and Patthy, L. (1991) *FEBS Lett.* **282**, 23–25.
- Banyai, L., Tordai, H., and Patthy, L. (1994) *Biochem. J.* **298**, 403–407.
- Steffensen, B., Wallon, U. M., and Overall, C. M. (1995) *J. Biol. Chem.* **270**, 11555–11566.
- Allan, J. A., Docherty, A. J., Barker, P. J., Huskisson, N. S., Reynolds, J. J., and Murphy, G. (1995) *Biochem. J.* **309**, 299–306.
- Aimes R. T., and Quigley, J. P. (1995) *J. Biol. Chem.* **270**, 5872–5876.
- Seltzer, J. L., Adams, S. A., Grant, G. A., and Eisen, A. Z. (1981) *J. Biol. Chem.* **256**, 4662–4668.
- Collier, I. E., Wilhelm, S. M., Eisen, A. Z., Marmer, B. L., Grant, G. A., Seltzer, J. L., Kronberger, A., He, C. S., Bauer, E. A., and Goldberg, G. I. (1988) *J. Biol. Chem.* **263**, 6579–6587.
- Ohuchi, E., Imai, K., Fujii, Y., Sato, H., Seiki, M., and Okada, Y. (1997) *J. Biol. Chem.* **272**, 2446–2451.
- Seltzer, J. L., and Eisen, A. (1999) *J. Invest. Dermatol.* **112**, 993–994.
- Rice, A., and Banda, M. J. (1995) *Biochemistry* **34**, 9249–9256.
- Laemmli, U. K. (1970) *Nature* **227**, 680–685.
- Heussen, C., and Dowdle, E. B. (1980) *Anal. Biochem.* **102**, 196–202.
- Knight, C. G., Willenbrock, F., and Murphy, G. (1992) *FEBS Lett.* **296**, 263–266.
- Hay, E. D. (1991) in *Cell Biology of Extracellular Matrix* (Hay, E. D., Ed.), 2nd ed., pp. 449–452, Plenum Press, New York, NY.
- Goldberg, G. I., Marmer, B. L., Grant, G. A., Eisen, A. Z., Wilhelm, S., and Chengshi, H. (1989) *Proc. Natl. Acad. Sci. USA* **86**, 8207–8211.
- Howard, E. W., Bullen, E. C., and Banda, M. J. (1991) *J. Biol. Chem.* **266**, 13064–13069.
- Azzam, H. S., and Thompson, E. W. (1992) *Cancer Res.* **52**, 4540–4544.
- Tomesek, J. J., Halliday, N. L., Updike, D. L., Ahern-Moore, J. S., Vu, T. K., Liu, R. W., and Howard, E. W. (1997) *J. Biol. Chem.* **272**, 7482–7787.
- Haas, T. L., Davis, S. J., and Madri, J. A. (1998) *J. Biol. Chem.* **273**, 3604–3610.
- Lehti K., Lohi, J., Valtanen, H., and Keski-Oja, J. (1998) *Biochem. J.* **334**, 345–353.
- Ellerbroek, S. M., Fishman, D. A., Kearns, A. S., Bafetti, L. M., and Stack, M. S. (1999) *Cancer Res.* **59**, 1635–1641.
- Hernandez-Barrantes, S., Toth, M., Bernardo, M. M., Yurkova, M., Gervasi, D. C., Raz, Y., Sang, Q. A., and Fridman, R. (2000) *J. Biol. Chem.* **275**, 12080–12089.

**PROTEINASE SUPPRESSION BY E-CADHERIN MEDIATED CELL-CELL ATTACHMENT  
IN PREMALIGNANT ORAL KERATINOCYTES.**

H.G. Munshi\*, S. Ghosh\*, S. Mukhopadhyay, Y.I. Wu, R. Sen, K.J. Green, and M.S. Stack

Division of Hematology/Oncology, Department of Medicine (H.G.M.); Departments of Cell & Molecular Biology (S.G., S.M., Y.I.W., R.S. and M.S.S.), Obstetrics & Gynecology (M.S.S.), Pathology (K.J.G.) and Dermatology (K.J.G.), Feinberg School of Medicine, Northwestern University; and the Robert H. Lurie Comprehensive Cancer Center of Northwestern University (H.G.M., K.J.G. and M.S.S.), Chicago, IL 60611.

\* These authors contributed equally to this work.

Running Title: MMP-9 and uPA regulation by E-cadherin

Key Words: E-cadherin, MMP-9, uPA, TIMP-1, PAI-1, phosphatidylinositol 3'-kinase, keratinocytes

Address for correspondence: M. Sharon Stack, Ph.D.  
Northwestern University Medical School  
Department of Cell and Molecular Biology  
303 E. Chicago Ave., Tarry 8-715  
Chicago IL 60611, USA  
Tel: (312)908-8216  
Fax: (312)503-7912  
e-mail: [mss130@northwestern.edu](mailto:mss130@northwestern.edu)

## ABSTRACT

The expression and activity of epithelial proteinases is under stringent control to prevent aberrant hydrolysis of structural proteins and disruption of tissue architecture. E-cadherin-dependent cell-cell adhesion is also important for maintenance of epithelial structural integrity and loss of E-cadherin expression has been correlated with enhanced invasive potential in multiple tumor models. To address the hypothesis that there is a functional link between E-cadherin and proteinase expression, we have examined the role of E-cadherin in proteinase regulation. Using a calcium switch protocol to manipulate junction assembly, our data demonstrate that initiation of *de novo* E-cadherin-mediated adhesive contacts suppresses expression of both relative matrix metalloproteinase-9 (MMP-9) levels and net urinary type plasminogen activator (uPA) activity. E-cadherin-mediated cell-cell adhesion increases both phosphatidylinositol 3'-kinase (PI3-kinase)-dependent AKT phosphorylation and epidermal growth factor receptor (EGFR)-dependent mitogen-activated protein kinase (MAPK)/extracellular signal regulated kinase (ERK) activation. Pharmacologic inhibition of the PI3-kinase pathway, but not the EGFR/MAPK pathway, prevents E-cadherin-mediated suppression of proteinases and delays junction assembly. Moreover, inhibition of junction assembly with a function blocking anti-E-cadherin antibody stimulates proteinase-dependent Matrigel invasion. As MMP-9 and uPA potentiate the invasive activity of oral squamous cell carcinoma, these data suggest E-cadherin-mediated signaling through PI3-kinase can regulate the invasive behavior of cells by modulating proteinase secretion.



## INTRODUCTION

Degradation of the extracellular matrix by proteolytic enzymes is necessary for a number of normal and pathological processes, including embryonic development, tissue resorption and remodeling, angiogenesis, and wound healing (1-3). Proteinases have also been implicated in the invasion and metastasis of malignant cells (4-6). Predominant among these enzymes are the matrix metalloproteinases (MMPs) and the plasminogen activator (PA) urinary-type PA (uPA) (7-10). MMPs are a large family of metallo-endopeptidases with activity directed against a variety of extracellular matrix substrates (11). MMP-9 (gelatinase B), a 92 kD gelatinase which efficiently degrades native type IV collagen, has been implicated in tumor dissemination, as evidenced by enhanced MMP-9 expression in tumor samples exhibiting matrix invasion and distant metastases (12). This is supported by studies using tumor-bearing MMP-9-deficient mice, which exhibit decreased propensity to develop metastatic foci, indicating that MMP-9 plays a critical role in tumor development (5). Post-translational regulation of MMP-9 activity is mediated by interaction with tissue inhibitor of metalloproteinases (TIMP)-1 which forms a 1:1 non-covalent inactive enzyme:inhibitor complex (12). Under many conditions, secretion of MMP-9 and TIMP-1 is coordinately regulated (12).

In addition to MMP-9, upregulation of uPA expression has also been correlated with malignant progression of a wide variety of neoplasms (9). uPA is a serine proteinase that functions in the conversion of the circulating zymogen plasminogen to the active enzyme plasmin (9). Plasmin is a broad-spectrum serine proteinase that can directly cleave a number of protein substrates (9), as well as activate many additional proteinase zymogens including proMMP-9 (13). uPA is localized to the cell surface via interaction with a glycosyl phosphatidylinositol-anchored receptor, designated uPA receptor or uPAR (9). Proteolytic activity is also regulated by the serpin plasminogen activator inhibitor 1 (PAI-1) which forms a covalent enzyme:inhibitor complex with both free and receptor-localized uPA (9). In a number of tumor models, downregulation of either uPA or its receptor decreases invasion and reduces metastatic potential (14,15).

Like proteolytic enzymes, dysregulation of adhesion molecules is often observed in malignant

cells. Cadherins are a family of cell surface adhesion molecules that participate in  $\text{Ca}^{2+}$ -dependent cell-cell adhesion (16) and thus are essential for maintenance of tissue integrity. E-cadherin is a widely distributed transmembrane intercellular adhesion molecule (17). In addition to functioning in cell-cell adhesion, the cytoplasmic tail of E-cadherin binds to  $\beta$  or  $\gamma$ -catenin/plakoglobin, thereby providing a mechanism for association with additional proteins, including signaling molecules such as phosphatidylinositol 3'-kinase (PI3-kinase) and epidermal growth factor receptor (18-21). Loss of E-cadherin expression is frequently observed in carcinomas (22,23) and transfection of ectopic E-cadherin into breast (24), colon (25), and prostate cancer cells (26) decreases cellular invasion.

In multiple tumor models, loss of E-cadherin expression and increased proteinase activity correlate with more invasive and metastatic tumors (9, 12, 14, 15, 22, 23, 27). To address the hypothesis that there is a functional link between E-cadherin and proteinase expression, in the current study we have examined the role of E-cadherin in the regulation of proteinase expression in premalignant oral keratinocytes. Our data demonstrate that initiation of *de novo* E-cadherin-mediated cell-cell adhesion suppresses both relative MMP-9 levels and net uPA activity in premalignant oral keratinocytes. Concomitant with decreased proteinase expression, secretion of TIMP-1 and PAI-1 is also downregulated. E-cadherin mediated cell-cell adhesion increases PI3-kinase-dependent AKT activation and epidermal growth factor receptor (EGFR)-dependent mitogen-activated protein kinase (MAPK)/extracellular signal regulated kinase (ERK) activation. Inhibition of the PI3-kinase pathway, but not EGFR-MAPK pathway, interferes with formation of adherens junctions and prevents E-cadherin mediated suppression of proteinases. Furthermore, prevention of junction assembly with a function blocking E-cadherin antibody stimulates proteinase-dependent Matrigel invasion. Together these data support the hypothesis that E-cadherin-mediated signaling via PI3-kinase can regulate the invasive behavior of cells by modulating proteinase expression.

## EXPERIMENTAL PROCEDURES

*Materials* – Gelatin, cell culture reagents, D-Val-Leu-Lys-*p*-nitroanilide (VLKpNA), rat anti-E-cadherin (DECMA clone) and peroxidase conjugated secondary antibodies were purchased from Sigma (St Louis, MO). Keratinocyte-SFM was obtained from Gibco-BRL (Grand Island, NY). Plasminogen was purified by affinity chromatography from outdated human plasma as described previously (28). Anti-mouse E-cadherin (HECD-1 clone) and isotype specific IgG1 antibodies were obtained from Calbiochem (San Diego, CA); anti-phosphorylated p42/p44 (MAPK/ERK) was obtained from Promega (Madison, WI); anti-ERK1/2 (anti-p42/p44) antibody anti AKT antibody were purchased from Santa Cruz Biotechnology (Santa Cruz, CA); anti-phosphorylated AKT (Thr 308) was obtained from Upstate Biotechnology (Waltham, MA); anti-uPAR antibody (399R) and function blocking anti-uPA antibody (394) were obtained from American Diagnostica (Greenwich, CT); and Alexa Fluor 594 goat anti-mouse and anti-rat antibodies were from Molecular Probes (Eugene, OR). TIMP-1 and MMP-9 ELISA kits were from Oncogene Research Products (Boston, MA) and PAI-1 ELISA kit was purchased from American Diagnostica. The mitogen-activated protein kinase/extracellular signal-regulated kinase kinase (MEK) inhibitor PD98059, PI3-kinase inhibitor LY294002, and EGFR specific inhibitor AG1478 were obtained from Calbiochem. The MMP inhibitor GM6001 was purchased from Chemicon (Temecula, CA). Polyvinylidene difluoride membrane was from Amersham (Arlington Heights, IL). Supersignal enhanced chemiluminescence (ECL) reagent, EZ-Link Sulfo-NHS-Biotin and UltraLink Immobilized Streptavidin Gel were obtained from Pierce (Rockford, IL). Microcon 10 microconcentrators were purchased from Millipore (Bedford, MA).

*Cell cultures* – Premalignant oral keratinocytes (pp126 cells) were the gift of Dr. D. Oda (University of Washington, Seattle, WA) (29,30). Early passage (between 3 and 8) pp126 cells were maintained at 37 °C in a humidified atmosphere of 5% CO<sub>2</sub> in Keratinocyte-SFM containing 0.09 mM calcium and supplemented with 100 units/ml penicillin, 100 ng/ml EGF, and 50 µg/ml bovine pituitary extract.

*E-cadherin activation* - The calcium switch method was utilized to assess the consequences of *de novo* E-cadherin activation (19-21,31,32). Briefly, pp126 cells were seeded at a constant density ( $1.5 \times 10^5$  cells/well) in 12-well tissue culture plates. After 24 hours, the cells were starved for 6-8h and calcium was removed by incubation with Keratinocyte-SFM containing 4 mM EGTA and 1 mM  $MgCl_2$  at 37 °C. After 30 min the calcium-free medium was removed, and Keratinocyte-SFM containing 0.09 mM calcium was immediately added to induce E-cadherin mediated cell-cell interactions (designated "E-cadherin activation +"). In control experiments, cells received fresh media in the absence of EGTA such that original junctions are maintained, but *de novo* activation of E-cadherin is not induced (designated "E-cadherin activation -"). In selected experiments, either anti-E-cadherin antibody (HECD-1 clone) or isotype specific control antibody was added to the calcium-containing medium at 10 µg/ml. In additional studies, the PI3-kinase inhibitor LY294002 (10 µM), the MEK inhibitor PD98059 (5 µM), the EGFR inhibitor AG1478 (250 nM), or the appropriate vehicle was added to the medium. Conditioned medium was collected for proteinase analysis after 24-36 h.

*Immunofluorescence microscopy* - pp126 cells were grown on glass coverslips at 37 °C in Keratinocyte-SFM. Following a 30 min-incubation with serum-free medium containing 4 mM EGTA and 1 mM  $MgCl_2$ , cells were incubated with Keratinocyte-SFM containing 0.09 mM  $Ca^{2+}$  in the presence of either control IgG antibody or anti-E-cadherin antibody (HECD-1, 10 µg/ml). In additional studies, the PI3-kinase inhibitor LY294002 (10 µM), the MEK inhibitor PD98059 (5 µM), the EGFR inhibitor AG1478 (250 nM), or the appropriate vehicle was added to the medium. For immunofluorescence staining, cells were washed with PBS and fixed with ice-cold methanol for 2 min or with 3.7% formaldehyde for 5 min followed by 0.5% Triton X-100 for 7 min. After washing with PBS, cells were blocked with 1 % bovine serum albumin in PBS and incubated with mouse anti-E-cadherin antibody (HECD-1) or rat anti-E-cadherin antibody (DECMA) for 1 h at 37 °C. After three washes with PBS, cells were incubated for 1 h at room temperature with Alexa Fluor 594-labeled goat anti-mouse or anti-rat antibody. Glass coverslips

were washed with PBS three times, mounted and examined under a UV microscope (Nikon) using the appropriate filter.

*Analysis of MMP-9 and TIMP-1 expression* – Gelatinase activities in the conditioned media at 36h were determined using SDS-PAGE gelatin zymography as previously described (33). Briefly, SDS-PAGE gels (9% acrylamide) were co-polymerized with 0.1% gelatin and samples were electrophoresed without reduction or boiling using 5X Laemmli sample buffer (34). SDS was removed through a 30 min incubation in 2.5% Triton X-100 and gels were incubated in 20 mM Glycine (pH 8.3), 10 mM  $\text{CaCl}_2$ , 1  $\mu\text{M}$   $\text{ZnCl}_2$  at 37 °C for 24-36 h. The gels were stained with Coomassie Blue to visualize zones of gelatinolytic activity. MMP-9 levels in the conditioned media were also quantified by ELISA (Oncogene Research Products) following concentration of the conditioned media 25-30 fold with Microcon 10. Levels of TIMP-1 protein in the conditioned media were quantified by ELISA (Oncogene Research Products) according to the manufacturer's specifications.

*Analysis of uPA activity and PAI-1 protein levels* – Net uPA activity in the conditioned media at 24 h was quantified using a coupled assay to monitor plasminogen activation and resulting hydrolysis of a colorimetric substrate (VLKpNA) as described previously (28). Levels of PAI-1 protein in the conditioned media were quantified by ELISA (American Diagnostica) according to the manufacturer's specifications.

*Cell surface biotinylation* – pp126 cells were grown in a 6-well plate, washed with ice-cold PBS, and incubated at 4 °C with gentle shaking for 30 min with 0.5 mg/ml cell-impermeable Sulfo-NHS-Biotin in ice cold PBS, followed by washing with 100 mM Glycine to quench free biotin. Cells were then detached by scraping, lysed in modified RIPA buffer (50 mM tris, pH 7.4, 150 mM NaCl, 5 mM EDTA, 1% Triton X-100 and 0.1% SDS) with proteinase inhibitors, and clarified by centrifugation. To isolate biotinylated cell-surface proteins, equal amounts of protein from each of the samples were incubated with streptavidin

beads at 4 °C for 14 hours, followed by centrifugation. After boiling in Laemmli sample dilution buffer (34) to dissociate streptavidin bead-biotin complexes, the samples were analyzed by SDS-PAGE (9% gels), and immunoblotted for uPAR (1:1000, American Diagnostica, clone 399R).

*MAPK and AKT activation* – E-cadherin was activated by the calcium switch method as described above and at the indicated time points cells were lysed in modified RIPA buffer containing 20 mM sodium fluoride, 10 mM sodium pyrophosphate, 1 mM sodium orthovanadate, 1 µg/ml aprotinin, 1 µM pepstatin, and 10 µM leupeptin. The samples were analyzed by SDS-PAGE (9% gels) and the blots were probed with anti-ERK1/2 antibody (1:1000) or with anti-AKT antibody (1:1000) to detect total ERK1/2 or AKT expression or with anti-phosphorylated ERK1/2 antibody (1:1000) or anti-phosphorylated AKT antibody (1:1000) to detect active (phosphorylated) forms of ERK or AKT.

*Analysis of Invasion* – Invasive activity was quantified using a Boyden Chamber (8 µm pore size) coated with Matrigel (10 µg). Cells ( $2 \times 10^5$ ) were added to the chamber in 500 µl of serum-free medium with 25 µg/ml of E-cadherin function-blocking antibody (HECD-1 clone) or isotype-specific control antibody, followed by incubation for 40 h. Nonmigrating cells were removed from the upper chamber with a cotton swab, filters were fixed and stained with Diff-Quik Stain, and migrating cells adherent to the underside of the filter were enumerated using an ocular micrometer and counting a minimum of 10 high-powered fields. Data are expressed as relative migration (number of cells/field). In selected experiments, the proteinase-dependence of invasion was determined by quantifying invasion in the presence of the MMP inhibitor GM6001 (2.5 µM) (Chemicon) or function blocking anti-uPA antibody (15 µg/ml) (American Diagnostica, clone 394).

## RESULTS

### *Calcium dependent cell-cell adhesion modulates proteinase and inhibitor expression.*

E-cadherin dependent cell-cell adhesion is important for the maintenance of epithelial structural integrity and the loss of E-cadherin expression has been shown to correlate with increased invasive potential of both carcinoma cell lines and human tumor samples (21,22,27,35). Recent data demonstrate that specific proteinases, including tumor-associated MMPs, can modulate cell-cell adhesion by cleaving E-cadherin (36-38). As E-cadherin itself couples to signal transduction pathways (18-21), the hypothesis that E-cadherin may participate in proteinase regulation was tested in premalignant gingival keratinocytes (pp126 cells). The calcium-switch method, in which E-cadherin mediated cell-cell adhesion was disrupted with EGTA treatment and restored by replacing  $\text{Ca}^{2+}$ , was utilized to initiate *de novo* adherens junction assembly (19-21,31,32). Control cells present a typical pattern of E-cadherin staining at the level of cell-cell contacts (Fig. 1A); however, in cells treated with EGTA, E-cadherin is absent from cell junctions (Fig. 1B). After addition of calcium, adherens junctions are again formed (Fig. 1C), with complete restoration by 1 h of treatment (Fig. 1D). To evaluate the effect of E-cadherin activation on proteinase expression, after 24-36h conditioned media were collected and analyzed. Gelatin zymography demonstrated that calcium mediated cell-cell adhesion (designated E-cad Actn +) decreased relative MMP-9 levels (Fig. 1E). This was confirmed using an ELISA kit which recognizes both free and TIMP-1-complexed MMP-9, demonstrating a 6.5-fold decrease in MMP-9 levels in concentrated conditioned media following calcium mediated cell-cell adhesion (Fig. 1E). Concomitant with MMP-9 downregulation, *net* uPA activity was also decreased by 2-3 fold (Fig. 1F). Evaluation of proteinase inhibitor expression by ELISA indicated a coordinate decrease in both TIMP-1 and PAI-1 levels (TABLE 1). Disruption of cell-cell junctions using the calcium switch method did not affect cell proliferation (data not shown).

### *Proteinase suppression following cell-cell adhesion requires engagement of E-cadherin.*

To confirm that proteinase suppression is due to E-cadherin engagement and is not an unrelated

consequence of calcium modulation, a function blocking anti-E-cadherin antibody (HECD-1 clone) was utilized. To verify that the HECD-1 antibody blocked cell-cell attachment following the calcium switch protocol, cells were treated with EGTA to dissociate cell-cell junctions, then incubated for 40 min in calcium-containing medium in the presence of either function-blocking E-cadherin antibody (HECD-1, 10  $\mu$ g/ml) or isotype-matched control IgG. Cells were then processed for immunofluorescence microscopy using rat anti-E-cadherin antibody (DECMA clone). Similar to the control experiment shown in Fig. 1B, no E-cadherin staining is visible at cell-cell junctions following EGTA treatment (Fig. 2A). Following calcium restoration, junctional E-cadherin is prevalent in IgG treated cells (Fig. 2B), but not in anti-E-cadherin-treated cells (Fig. 2C), demonstrating that the antibody indeed blocks cell-cell attachment. To assess the effect of E-cadherin function blocking antibodies on proteinase suppression, cell-cell junctions were disrupted by calcium chelation and junction assembly was initiated by the addition of calcium in the presence of blocking antibody (10  $\mu$ g/ml) to prevent formation of adherens junctions. Control samples contained an equal concentration of isotype specific IgG. In additional controls, antibodies were added without prior disruption of cell-cell junctions by calcium chelation (designated E-cad Actn -). Blocking E-cadherin engagement prevented the adhesion-mediated suppression of both the relative MMP-9 levels (Fig. 2D, lane 4) and the net uPA activity (Fig. 2E). Addition of the function-blocking HECD-1 antibody at 10  $\mu$ g/ml without prior junction disruption (designated E-cad Actn -) was ineffective (Fig. 2D, lane 2; Fig. 2E). Moreover, in IgG-treated control samples, in which junction reformation was not prevented, proteinase expression was suppressed (Fig. 2D, lane 3; Fig. 2E). Similar results were obtained for TIMP-1 and PAI-1, in which suppression of expression by E-cadherin engagement was also blocked by anti-E-cadherin antibody (TABLE 2). In control experiments, treatment of cells with EGTA in the presence or absence of blocking antibody did not alter proliferation (data not shown). Together these data demonstrate that *de novo* E-cadherin engagement suppresses proteinase expression.

Since uPA activity can also be modulated by cell surface association (9), the effect of E-cadherin mediated cell-cell adhesion on uPAR expression was evaluated. Cell-cell junctions were disrupted by calcium chelation and the samples treated with either HECD-1 blocking antibody or control IgG as



described above. Cells were then incubated with cell impermeable NHS-biotin to label surface proteins and lysed in modified RIPA buffer. Following precipitation of surface-labeled proteins with streptavidin beads, samples were electrophoresed and probed for uPAR by immunoblotting. There was no change in uPAR surface expression induced by E-cadherin mediated cell-cell adhesion (Fig. 3). In addition, there was no change in total cellular uPAR protein levels (surface and cytoplasmic) as measured by Western blot (data not shown). These data suggest that, although the net uPA activity is suppressed, the receptor remains available.

#### *Inhibition of MAPK does not block E-cadherin-mediated suppression of proteinases*

Because we have previously reported that MAPK activation regulates proteinase expression in pp126 cells (30), levels of phosphorylated (active) ERK1/2 were assessed in pp126 cells following the calcium-switch. Cells were lysed at various time points after calcium-induced initiation of junction assembly, and samples analyzed by western blotting using antibodies directed against total ERK1/2 or the phosphorylated (active) species of ERK 1/2. A time-dependent phosphorylation of ERK1/2 following *de novo* engagement of E-cadherin was observed in pp126 cells (Fig. 4A), with maximal MAPK activation at approximately 15 min. There was no change in the total amount of ERK 1/2 protein (Fig. 4A). To confirm that MAPK phosphorylation was a specific consequence of E-cadherin engagement, junction assembly was initiated in the presence of the function blocking anti-E-cadherin antibody or control IgG as described above. Inhibition of E-cadherin engagement decreased ERK1/2 phosphorylation, indicating that engagement of E-cadherin leads to MAPK activation (Fig. 4B). Moreover, E-cadherin mediated MAPK activation was blocked with the MEK inhibitor PD98059, demonstrating the involvement of the MEK-ERK pathway (Fig. 4C). Interestingly, the epidermal growth factor receptor (EGFR)-specific tyrosine kinase inhibitor AG1478 also completely abrogated E-cadherin mediated MAPK activation (Fig. 4C), supporting the observation that E-cadherin mediated activation of MAPK is dependent on EGFR (20).

Using the MEK inhibitor PD98059, the role of MAPK in the E-cadherin mediated suppression of proteinases was evaluated. Cells were incubated with EGTA and 5  $\mu$ M PD98059 or an equal amount of

DMSO vehicle for 30 min before the addition of calcium-replete medium containing either 5  $\mu$ M PD98059 or DMSO. Under basal conditions (designated E-cad Actn -), PD98059 did not affect the relative MMP-9 levels or the net uPA activity (Fig. 5A, lane 2; Fig. 5C). However following E-cadherin activation by EGTA treatment and calcium restoration, inhibition of MEK activity did not prevent the suppression of proteinase expression (Fig. 5A, lane 4; Fig. 5C). Similar results were obtained with TIMP-1 and PAI-1 (data not shown).

To further evaluate the role of MAPK in the control of E-cadherin-regulated proteinase expression, the EGFR-kinase specific inhibitor tyrphostin AG1478 was employed. Cells were treated with EGTA followed by calcium restoration in the presence of AG1478 (250 nM). Under basal conditions (designated E-cad Actn -) AG1478 (250 nM) did not affect MMP-9 or uPA expression (Fig. 5B, lane 2; Fig. 5D). Similar to the results obtained with PD98059, specific inhibition of the EGFR-kinase also failed to abrogate the suppressive effect of E-cadherin engagement on the relative MMP-9 levels or the net uPA activity (Fig. 5B, lane 4; Fig. 5D). Together these data demonstrate that, although E-cadherin engagement can activate MAPK in pp126 cells via a mechanism involving the EGFR kinase, this signaling pathway does not modulate E-cadherin regulation of proteinase expression.

#### *Inhibition of PI3-kinase blocks E-cadherin-mediated suppression of proteinases.*

Formation of *de novo* E-cadherin-mediated cell-cell contact activates PI3-kinase (19-21,31,32,39-41) and induces physical association of PI3-kinase with E-cadherin (19,21, data not shown). To determine whether PI3-kinase activation may play a role in the E-cadherin regulation of proteinase expression, activation of PI3-kinase was assessed in pp126 cells following calcium-induced adherens junction assembly by evaluating activation (phosphorylation) of the downstream substrate AKT. Cells were lysed at various time points and samples analyzed by western blotting using antibodies directed against total AKT or the phosphorylated (active) species. A time-dependent phosphorylation of AKT following E-cadherin activation was observed in pp126 cells (Fig. 6A, upper panel) with no change in total AKT protein (Fig. 6A, lower panel). AKT activation was blocked with the PI3-kinase inhibitor LY294002,

demonstrating the involvement of the PI3-kinase-AKT pathway (Fig. 6B). To confirm that AKT activation resulted from E-cadherin engagement, junction assembly was initiated in the presence of the function blocking anti-E-cadherin antibody or control IgG as described above. Inhibition of E-cadherin engagement decreased AKT activation (Fig. 6C), indicating that engagement of E-cadherin leads to PI3-kinase activation.

Using the inhibitor LY294002, the role of PI3-kinase in E-cadherin-mediated suppression of MMP-9 and uPA expression was evaluated. Cells were pre-incubated with EGTA and LY294002 (10  $\mu$ M) or an equal amount of ethanol vehicle for 30 min before the addition of calcium-replete medium containing LY294002 or ethanol. Under control conditions when the adherens junctions were not disrupted with EGTA treatment (designated E-cad Actn -), LY294002 did not alter the relative MMP-9 levels or the net uPA activity (Fig. 7A, lane 2; Fig. 7B). In EGTA-treated cells, calcium-induced engagement of E-cadherin decreased the relative MMP-9 levels and the net uPA activity, as previously demonstrated (Fig. 7A, lane 3; Fig. 7B). However, concomitant treatment with LY294002 abrogated the E-cadherin-mediated proteinase suppression, and restored the relative MMP-9 levels and the net uPA activity (Fig. 7A, lane 4; Fig. 7B), implicating PI3-kinase in E-cadherin-mediated proteinase regulation. Similar results were obtained with TIMP-1 and PAI-1 (data not shown).

#### *PI3-kinase controls integrity of adherens junctions in pp126 cells.*

Recent data indicate that PI3-kinase can regulate either the assembly or maintenance of adherens junctions (21,32). As both PI3-kinase inhibition (using LY294002) and prevention of E-cadherin junction formation (with blocking antibodies) restored proteinase expression, these data suggest that PI3-kinase may participate in regulation of E-cadherin junctions in pp126 cells. To test this hypothesis, the effect of PI3-kinase inhibition (10  $\mu$ M LY294002) on junction formation was evaluated. Control experiments included inhibitors of EGFR tyrosine kinase (250 nM AG1478) or MEK (5  $\mu$ M PD98059). Cells were pre-incubated with EGTA in the presence of inhibitor or DMSO vehicle for 30 min before the addition of calcium-replete medium containing the specific inhibitor or DMSO. After 45 min, cells were processed

for immunofluorescence microscopy using anti-E-cadherin antibody. Control cells present a typical pattern of E-cadherin staining at the level of cell-cell contacts (Fig. 8A). After 30 min of treatment with EGTA, E-cadherin was absent from sites of cell-cell contact (Fig. 8B). Following calcium addition, E-cadherin mediated adherens junctions were again formed at 45 min (Fig. 8C). Similar results were observed in cells treated with PD98059 or AG1478 (Figs. 8D and 8E). In contrast, cells treated with LY294002 showed significantly reduced E-cadherin staining at sites of cell-cell contact (Fig. 8F), indicating that PI3-kinase participates in the formation of *de novo* E-cadherin-mediated adherens junctions in pp126 cells.

*Prevention of cell-cell adhesion enhances pp126 cell invasion.*

To assess the functional consequences of E-cadherin-regulated proteinase expression, the impact of preventing cell-cell adhesion on cellular invasive activity was evaluated. pp126 cells were seeded into Boyden chambers overlaid with Matrigel to provide a three-dimensional, protein-rich barrier to invasion in the presence of E-cadherin blocking antibody (HECD-1) or control IgG. Prevention of *de novo* E-cadherin cell-cell contacts resulted in an increase in the relative MMP-9 levels and the net uPA activity (Figs. 9A and 9B). Concomitant with enhanced proteinase expression, inhibition of junction formation significantly increased Matrigel invasion (Fig. 9C). The enhanced invasive activity was partially blocked with either a broad-spectrum MMP inhibitor (2.5  $\mu$ M GM6001) or by a function blocking anti-uPA antibody (15  $\mu$ g/ml), and was completely abrogated by a mixture of the two inhibitors (Fig. 9C), implicating both MMP-9 and uPA in Matrigel invasion by pp126 cells. These data demonstrate that the proteinase upregulation resulting from inhibition of E-cadherin engagement can promote cellular invasive behavior.

## DISCUSSION

Studies using multiple cancer models have demonstrated that loss of E-cadherin-mediated adherens junctions leads to increased invasion and metastases (22,23,27,35,42). Additional data suggest a correlation between E-cadherin status and proteinase levels. For example, downregulation of E-cadherin increased MMP-9 secretion in murine skin carcinoma cell lines (43), while overexpression of E-cadherin decreased MMP-2 activity in prostate cancer cells (26) and MT1-MMP in squamous cancer cells (44). However a mechanistic examination of the potential functional link between cell-cell adhesion and proteolysis has not been reported. Our current data demonstrate that E-cadherin plays a direct role in proteinase regulation in premalignant oral keratinocytes. Initiation of *de novo* E-cadherin-mediated cell-cell junctions resulted in suppression of MMP-9 and uPA expression. Conversely, prevention of junction formation enhanced proteinase expression and consequent cellular invasive behavior, suggesting a biochemical mechanism by which down-regulation of E-cadherin may promote metastasis.

The detailed signal transduction pathway through which E-cadherin regulates proteinase gene expression is unknown. However, our data support a role for PI3-kinase activity in the E-cadherin mediated suppression of MMP-9 and uPA expression. Formation of *de novo* E-cadherin junctions activates PI3-kinase (Fig. 6, and ref [19-21,31,32,39-41]) and leads to the physical association of PI3-kinase with E-cadherin (19,21, and data not shown). Activation of PI3-kinase recruits the GTP exchange factor Tiam-1 to the adherens junctions, resulting in activation of Rac-GTPase (45). In keratinocytes, Rac-GTPases play an important role in forming and stabilizing adherens junctions by recruiting F-actin to these junctions (46,47). Supporting this model, inhibition of PI3-kinase blocks the recruitment of F-actin to sites of cell-cell contact in intestinal epithelial cells (21) and destabilizes adherens junctions in mammary epithelial cells (48). Moreover, additional data indicate that PI3-kinase may participate in maturation and maintenance of cadherin-based adhesions (32, 40), in part via regulation of productive adhesive contact formation following initial homophilic ligation (32). Our current data support the hypothesis that PI3-kinase activity also functions to regulate formation of adherens junctions in pp126 cells. Thus, inhibition of PI3-kinase activity with LY294002 destabilizes junctions, thereby abrogating the

suppressive effect of E-cadherin engagement on proteinase expression.

In addition to activation of PI3-kinase, E-cadherin engagement has also been shown to enhance MAPK activity through the recruitment and activation of EGFR (20). A similar effect was observed in the current study, wherein junction formation induced maximal MAPK activation in pp126 cells at 15 min. MAPK activation was completely abrogated with the EGFR-kinase inhibitor AG1478, implicating EGFR signaling in MAPK activation. However, inhibition of MEK (with PD98059) or EGFR-kinase (with AG1478) was insufficient to restore proteinase expression, suggesting that E-cadherin-mediated proteinase regulation does not involve EGFR-initiated MAPK signaling. Furthermore, inhibition of MEK and EGFR kinase activity at the time of calcium switch did not prevent adherens junction re-formation in pp126 cells. It should be noted, however, that the MAPK pathway is important in both growth factor induced secretion of MMP-9 in carcinoma cells (49) and in integrin-mediated upregulation of uPA in pp126 cells (30). These data support the hypothesis that the signaling pathways that regulate formation of adherens junctions (PI3-kinase) may also regulate cadherin-mediated suppression of proteinases. This effect may be, in part, due to sequestration of  $\beta$ -catenin at cell-cell junctions as part of E-cadherin-catenin complex (50,51).  $\beta$ -catenin can translocate to the nucleus and form a complex with proteins of the T cell-factor (Tcf)/lymphoid-enhancer-factor (Lef) family (52). Tcf/Lef proteins act as transcription factors and have been shown to activate genes that are important in cancer progression including MMP-7, MMP-26, and uPAR. (50,51,53-58). A number of other MMP promoters, including MMP-9, have Tcf4 binding sites, and may consequently be regulated by  $\beta$ -catenin (54,57). Although we have not formally addressed the potential contribution of  $\beta$ -catenin signaling, no change in uPAR expression was observed following E-cadherin activation in our system, suggesting that additional mechanisms of proteinase regulation are engaged. Thus, it is interesting to speculate that net extracellular proteinase activity may result from a balance between signaling pathways differentially activated by engagement of cell-cell versus cell-matrix adhesion molecules.

In addition to enhanced proteinase expression (uPA, PAI-1) induced by E-cadherin disruption, a coordinate increase in the corresponding inhibitors (PAI-1, TIMP-1) was also observed. Although a

coordinate regulation of uPA and PAI-1 is apparent, a *net* increase in uPA activity is obtained following E-cadherin disruption and this functionally contributes to the increased Matrigel invasion. Similarly, the Matrigel invasion data also suggest that a net increase in MMP-9 activity is also likely. It has previously been shown in T47D and MCF-7 breast cancer cells that disruption of cell junctions with anti-E-cadherin antibodies increases uPA expression and collagen invasion (24). The enhanced collagen invasion was partially blocked using anti-catalytic uPA antibodies; however, the effect of MMP inhibitors was not evaluated (24). The current data demonstrate that Matrigel invasion by pp126 cells is dependent on both uPA and MMP9, as inhibiting both proteinases simultaneously completely abrogated the increase in Matrigel invasion by pp126 cells.

Recent studies have shown that proteinase expression may regulate cell-cell junction integrity by cleaving E-cadherin (36-38). Conversely, our data demonstrate that E-cadherin participates in proteinase regulation via a PI3-kinase-dependent mechanism, providing novel evidence for a bi-directional communication between proteinases and cadherins. As proteinases play a central role in a number of important cellular processes, these findings may provide a framework for a more detailed understanding of the mechanism by which E-cadherin-mediated cell-cell contacts regulate both normal epithelial cell behavior and the invasiveness of carcinoma cells.

#### ACKNOWLEDGEMENTS

This research was supported in part by research grant PO1 DE12328 (M.S.S. and K.J.G.) from the National Institute for Dental and Craniofacial Research and RO1 CA 85870 (M.S.S.) from the National Institutes of Health. H.G.M. was funded by Clinical Oncology Research Training Program grant from the National Cancer Institute (T32 CA79447).

## FOOTNOTES

The abbreviations used are: MMP-9, matrix metalloproteinase 9; TIMP-1, tissue of inhibitor of metalloproteinases 1; uPA, urinary-type plasminogen activator; uPAR, uPA receptor; PAI-1, plasminogen activator inhibitor 1; MEK, mitogen-activated protein kinase/extracellular signal-regulated kinase kinase; MAPK, mitogen-activated protein kinase; ERK, extracellular signal-regulated kinase; PI3-kinase, phosphatidylinositol 3'-kinase; ELISA, enzyme-linked immunosorbent assay; EGFR, epidermal growth factor receptor.



## REFERENCES

1. Werb, Z. (1997) *Cell* **91**(4), 439-42.
2. Sternlicht, M. D., and Werb, Z. (2001) *Annu Rev Cell Dev Biol* **17**, 463-516
3. Ellis, V., and Murphy, G. (2001) *FEBS Lett* **506**(1), 1-5.
4. Westermarck, J., and Kahari, V. M. (1999) *Faseb J* **13**(8), 781-92.
5. Itoh, T., Tanioka, M., Matsuda, H., Nishimoto, H., Yoshioka, T., Suzuki, R., and Uehira, M. (1999) *Clin Exp Metastasis* **17**(2), 177-81.
6. Murphy, G., and Gavrilovic, J. (1999) *Curr Opin Cell Biol* **11**(5), 614-21.
7. Nagase, H., and Woessner, J. F., Jr. (1999) *J Biol Chem* **274**(31), 21491-4.
8. Vu, T. H., and Werb, Z. (2000) *Genes Dev* **14**(17), 2123-33.
9. Andreasen, P. A., Kjoller, L., Christensen, L., and Duffy, M. J. (1997) *Int J Cancer* **72**(1), 1-22.
10. Ghosh, S., Ellerbroek, S.M., Wu, Y., and Stack, M.S. (2000) *Fibrinolysis and Proteolysis* **14** (2/3), 87-97.
11. Parks, W.C., and Mecham, R.P. (1998) *Matrix Metalloproteinases*, Academic Press, San Diego.
12. Vu, T.H., and Werb Z. (1998) in *Matrix Metalloproteinases* (Parks, W.C., and Mecham, R.P., eds), pp. 115-48, Academic Press, San Diego.
13. Mignatti, P., and Rifkin, D. B. (2000) *Adv Cancer Res* **78**, 103-57
14. Yu, H. R., and Schultz, R. M. (1990) *Cancer Res* **50**(23), 7623-33.
15. Kook, Y. H., Adamski, J., Zelent, A., and Ossowski, L. (1994) *Embo J* **13**(17), 3983-91.
16. Angst, B. D., Marozzi, C., and Magee, A. I. (2001) *J Cell Sci* **114**(Pt 4), 629-41.
17. Takeichi, M. (1991) *Science* **251**(5000), 1451-5.
18. Provost, E., and Rimm, D. L. (1999) *Curr Opin Cell Biol* **11**(5), 567-72.
19. Pece, S., Chiariello, M., Murga, C., and Gutkind, J. S. (1999) *J Biol Chem* **274**(27), 19347-51.
20. Pece, S., and Gutkind, J. S. (2000) *J Biol Chem* **275**(52), 41227-33.
21. Laprise, P., Chailier, P., Houde, M., Beaulieu, J. F., Boucher, M. J., and Rivard, N. (2001) *J Biol Chem* **276**(52), 52

22. Noe, V., Chastre, E., Bruyneel, E., Gespach, C., and Mareel, M. (1999) *Biochem Soc Symp* **65**, 43-62
23. Van Aken, E., De Wever, O., Correia da Rocha, A. S., and Mareel, M. (2001) *Virchows Arch* **439**(6), 725-51.
24. Frixen, U. H., and Nagamine, Y. (1993) *Cancer Res* **53**(15), 3618-23.
25. Miyaki, M., Tanaka, K., Kikuchi-Yanoshita, R., Muraoka, M., Konishi, M., and Takeichi, M. (1995) *Oncogene* **11**(12), 2547-52.
26. Luo, J., Lubaroff, D. M., and Hendrix, M. J. (1999) *Cancer Res* **59**(15), 3552-6.
27. Wijnhoven, B. P., Dinjens, W. N., and Pignatelli, M. (2000) *Br J Surg* **87**(8), 992-1005.
28. Stack, S., Gonzalez-Gronow, M., and Pizzo, S. V. (1990) *Biochemistry* **29**(20), 4966-70.
29. Oda, D., Bigler, L., Lee, P., and Blanton, R. (1996) *Exp Cell Res* **226**(1), 164-9.
30. Ghosh, S., Brown, R., Jones, J. C., Ellerbroek, S. M., and Stack, M. S. (2000) *J Biol Chem* **275**(31), 23869-76.
31. Kim, S. H., Li, Z., and Sacks, D. B. (2000) *J Biol Chem* **275**(47), 36999-7005.
32. Nakagawa, M., Fukata, M., Yamaga, M., Itoh, N., and Kaibuchi, K. (2001) *J Cell Sci* **114**(Pt 10), 1829-38.
33. Munshi, H. G., and Stack, M. S. (2002) *Methods Cell Biol* **69**, 195-205.
34. Laemmli, U. K. (1970) *Nature* **227**(259), 680-5.
35. Frixen, U. H., Behrens, J., Sachs, M., Eberle, G., Voss, B., Warda, A., Lochner, D., and Birchmeier, W. (1991) *J Cell Biol* **113**(1), 173-85.
36. Noe, V., Fingleton, B., Jacobs, K., Crawford, H. C., Vermeulen, S., Steelant, W., Bruyneel, E., Matrisian, L. M., and Mareel, M. (2001) *J Cell Sci* **114**(Pt 1), 111-118.
37. Steinhusen, U., Weiske, J., Badock, V., Tauber, R., Bommert, K., and Huber, O. (2001) *J Biol Chem* **276**(7), 4972-80.
38. Ryniers, F., Stove, C., Goethals, M., Brackenier, L., Noe, V., Bracke, M., Vandekerckhove, J., Mareel, M., and Bruyneel, E. (2002) *Biol Chem* **383**(1), 159-65.

39. Li, G., Satyamoorthy, K., and Herlyn, M. (2001) *Cancer Res* **61**(9), 3819-25.
40. Kovacs, E. M., Ali, R. G., McCormack, A. J., and Yap, A. S. (2001) *J Biol Chem* **276**, 13
41. Shinohara, M., Kodama, A., Matozaki, T., Fukuhara, A., Tachibana, K., Nakanishi, H., and Takai, Y. (2001) *J Biol Chem* **276**(22), 18941-6.
42. Schipper, J. H., Frixen, U. H., Behrens, J., Unger, A., Jahnke, K., and Birchmeier, W. (1991) *Cancer Res* **51**(23 Pt 1), 6328-37.
43. Llorens, A., Rodrigo, I., Lopez-Barcons, L., Gonzalez-Garrigues, M., Lozano, E., Vinyals, A., Quintanilla, M., Cano, A., and Fabra, A. (1998) *Lab Invest* **78**(9), 1131-42.
44. Ara, T., Deyama, Y., Yoshimura, Y., Higashino, F., Shindoh, M., Matsumoto, A., and Fukuda, H. (2000) *Cancer Lett* **157**(2), 115-21.
45. Sander, E. E., van Delft, S., ten Klooster, J. P., Reid, T., van der Kammen, R. A., Michiels, F., and Collard, J. G. (1998) *J Cell Biol* **143**(5), 1385-98.
46. Braga, V. M., Machesky, L. M., Hall, A., and Hotchin, N. A. (1997) *J Cell Biol* **137**(6), 1421-31.
47. Braga, V. M., Del Maschio, A., Machesky, L., and Dejana, E. (1999) *Mol Biol Cell* **10**(1), 9-22.
48. Somasiri, A., Wu, C., Ellchuk, T., Turley, S., and Roskelley, C. D. (2000) *Differentiation* **66**(2-3), 116-25.
49. McCawley, L. J., Li, S., Wattenberg, E. V., and Hudson, L. G. (1999) *J Biol Chem* **274**(7), 4347-53.
50. Barker, N., and Clevers, H. (2000) *Bioessays* **22**(11), 961-5.
51. Huber, A. H., and Weis, W. I. (2001) *Cell* **105**(3), 391-402.
52. Love, J. J., Li, X., Case, D. A., Giese, K., Grosschedl, R., and Wright, P. E. (1995) *Nature* **376**(6543), 791-5.
53. Wong, N. A., and Pignatelli, M. (2002) *Am J Pathol* **160**(2), 389-401.
54. Brabletz, T., Jung, A., Dag, S., Hlubek, F., and Kirchner, T. (1999) *Am J Pathol* **155**(4), 1033-8.
55. Crawford, H. C., Fingleton, B., Gustavson, M. D., Kurpios, N., Wagenaar, R. A., Hassell, J. A., and Matrisian, L. M. (2001) *Mol Cell Biol* **21**(4), 1370-83.

56. Crawford, H. C., Fingleton, B. M., Rudolph-Owen, L. A., Goss, K. J., Rubinfeld, B., Polakis, P., and Matrisian, L. M. (1999) *Oncogene* **18**(18), 2883-91.
57. Marchenko, G. N., Marchenko, N. D., Leng, J., and Strongin, A. Y. (2002) *Biochem J* **363**(Pt 2), 253-62.
58. Mann, B., Gelos, M., Siedow, A., Hanski, M. L., Gratchev, A., Ilyas, M., Bodmer, W. F., Moyer, M. P., Riecken, E. O., Buhr, H. J., and Hanski, C. (1999) *Proc Natl Acad Sci U S A* **96**(4), 1603-8.

## FIGURE LEGENDS

**Fig. 1. Calcium-mediated cell-cell adhesion decreases proteinase expression.** (A-D). pp126 cells were left untreated (A) or treated with 4 mM EGTA for 30 min (B-D). To induce E-cadherin activation, the EGTA containing medium was then replaced with calcium-containing Keratinocyte-SFM (0.09 mM) for 30 min (C) or 1 h (D). Cells were fixed, incubated with anti-E-cadherin antibody (HECD-1), and detected with Alexa Fluor 594-conjugated anti-mouse antibody. (E) E-cadherin was activated (designated E-cad Actn. +) in pp126 cells using the calcium-switch method as described in Experimental Procedures. Control cells (designated E-cad Actn. -) were left untreated. Conditioned media were collected at 36h and analyzed for MMP-9 expression by gelatin zymography and by ELISA as described in Experimental Procedures. (F) uPA activity was analyzed in the conditioned media at 24 h using a coupled colorimetric plasminogen activation assay as described in Experimental Procedures. The results represent the mean  $\pm$  SE of five different experiments. \*, significantly different from control with  $p < 0.001$ .

**Fig. 2. Proteinase suppression following cell adhesion requires engagement of E-cadherin.** (A-C) pp126 cells were treated with 4 mM EGTA for 30 min (A-C). The EGTA-containing medium was replaced with Keratinocyte-SFM containing 0.09 mM calcium for 45 min in the presence of control IgG (10  $\mu$ g/ml) (B) or function-blocking anti-E-cadherin antibody (HECD-1, 10  $\mu$ g/ml) (C). Cells were fixed, incubated with anti-E-cadherin antibody (DECMA), and detected with Alexa Fluor 594-conjugated anti-rat antibody. (D,E) Cells were either left untreated or underwent activation of E-cadherin using the calcium-switch method in the presence of function-blocking anti-E-cadherin antibody (HECD-1, 10  $\mu$ g/ml) or isotype-matched IgG (10  $\mu$ g/ml) as described in Experimental Procedures. (D) Conditioned media were collected at 36 h and analyzed for MMP-9 activity by gelatin zymography. (E) uPA activity was analyzed in the conditioned media at 24 h using a coupled colorimetric plasminogen activation assay as described in Experimental Procedures. The results represent the mean  $\pm$  SE of three different experiments. \*, significantly different from control with  $p < 0.01$ .

**Fig. 3. E-cadherin mediated cell-cell adhesion does not affect surface uPAR expression.** Cells were either left untreated (designated E-cad Actn. -) or underwent activation of E-cadherin (designated E-cad Actn. +) using the calcium-switch method in the presence of function-blocking anti-E-cadherin antibody (HECD-1, 10  $\mu$ g/ml) or isotype-matched IgG (10  $\mu$ g/ml) as described in Experimental Procedures. After 24 h the cells were surface-biotinylated and lysed. Samples were immunoprecipitated with streptavidin beads to isolate cell-surface proteins, and electrophoresed on a 9% SDS-polyacrylamide gel. The membranes were immunoblotted with anti-uPAR antibody followed by peroxidase-conjugated secondary antibody and enhanced chemiluminescence detection.

**Fig. 4. E-cadherin-mediated adhesion enhances EGFR-mediated MAPK activity.** (A) Using the calcium-switch method, E-cadherin was activated in pp126 cells. The cells were lysed at the indicated times following E-cadherin activation. The lysates were separated by SDS-PAGE (9% gels), transferred to PVDF membrane, and probed with anti-phospho ERK1/2 antibody to detect the phosphorylated, active form of ERK (upper panel) or with anti-ERK 1/2 antibody to detect total ERK 1/2 expression (lower panel). (B) pp126 cells underwent activation of E-cadherin using the calcium-switch method in the presence of function-blocking anti-E-cadherin antibody (HECD-1, 10  $\mu$ g/ml) or isotype-matched IgG (10  $\mu$ g/ml) as described in Experimental Procedures. The cells were lysed at 15 min after calcium restoration. The lysates were analyzed for phospho-ERK (upper panel) or for total ERK expression (lower panel). (C) pp126 cells were treated with the MEK inhibitor, PD98059 (PD, 5  $\mu$ M), EGFR inhibitor, AG1478 (AG, 250 nM) or with an equal amount of DMSO vehicle as control at the time of disruption of cell-cell junctions as described above. The cells were lysed at 15 min after calcium restoration. The lysates were analyzed for phospho-ERK (upper panel) or for total ERK expression (lower panel). The results are representative of three independent experiments.

**Fig. 5. EGFR-MAPK pathway is not involved in E-cadherin-mediated suppression of proteinases.**

Serum-starved pp126 cells were either left untreated (designated E-cad Actn. -) or underwent activation of E-cadherin (designated E-cad Actn. +) using the calcium-switch method in the presence of 5  $\mu$ M PD98059 (PD), 250 nM AG1478 (AG) or an equal volume of DMSO as described in Experimental Procedures. (A, B) Conditioned media were collected at 36 h and analyzed for MMP-9 activity by gelatin zymography. (C, D) uPA activity was analyzed in the conditioned media at 24 h using a coupled colorimetric plasminogen activation assay. The results represent the mean  $\pm$  SE of three different experiments. \*, significantly different from control with  $p < 0.005$ .

**Fig. 6. E-cadherin-mediated adhesion induces PI3-kinase mediated AKT activity.** (A) Using the calcium-switch method, E-cadherin was activated in pp126 cells. The cells were lysed at the indicated times following E-cadherin activation. The lysates were separated by SDS-PAGE (9% gels), transferred to PVDF membrane, and probed with an antibody that specifically recognizes phosphorylation on Thr 308 (phospho-AKT). The membrane was then reprobed with an antibody against total AKT. (B) pp126 cells were treated with the PI3-kinase inhibitor, LY294002 (LY, 10  $\mu$ M), or an equal volume of ethanol for 30 min at the time of disruption of cell-cell junctions as described above. The cells were lysed at 30 min after calcium restoration and analyzed for phospho-AKT (upper panel) and total AKT (lower panel) as described above. (C) pp126 cells were either left untreated or underwent activation of E-cadherin using the calcium-switch method in the presence of function-blocking anti-E-cadherin antibody (HECD-1, 10  $\mu$ g/ml) or isotype-matched IgG (10  $\mu$ g/ml) as described in Experimental Procedures. The cells were lysed at 30 min after calcium restoration and analyzed for phospho-AKT or for total AKT expression as described above. The results are representative of three independent experiments.

**Fig. 7. Inhibition of PI3-kinase blocks E-cadherin-mediated suppression of proteinases.** Serum-starved pp126 cells were either left untreated (designated E-cad Actn. -) or underwent activation of E-

cadherin (designated E-cad Actn. +) using the calcium-switch method in the presence of 10  $\mu$ M LY 294002 (LY) or an equal volume of ethanol for 30 min as described in Experimental Procedures. (A) Conditioned media were collected at 36 h and analyzed for MMP-9 activity by gelatin zymography. (B) uPA activity was analyzed in the conditioned media at 24 h using a coupled colorimetric plasminogen activation assay. The results represent the mean  $\pm$  SE of three different experiments. \* significantly different from control with  $p < 0.05$ .

**Fig. 8. PI3-kinase controls the integrity of adherens junctions in pp126 cells.** Serum-starved pp126 cells were either left untreated (A) or treated with 4 mM EGTA for 30 min (B-F) containing either DMSO as control (A-C), 5  $\mu$ M PD98059 (D), 250 nM AG1478 (E), or 10  $\mu$ M LY294008 (F). The EGTA containing medium was then replaced with Keratinocyte-SFM (0.09 mM  $\text{Ca}^{2+}$ ) containing DMSO or the corresponding inhibitor for 45 min. Cells were fixed, incubated with anti-E-cadherin antibody (HECD-1), and detected with Alexa Fluor 594-conjugated anti-mouse antibody.

**Fig. 9. Disruption of cell-cell adhesion enhances pp126 cell invasion.** pp126 cells were plated with either control antibody (IgG) or anti-E-cadherin antibody (HECD-1, designated E-cad). (A) Conditioned media were collected at 36 h and analyzed for MMP-9 activity by gelatin zymography. (B) uPA activity was analyzed in the conditioned media at 24 h using a coupled colorimetric plasminogen activation assay. \*, significantly different from control with  $p < 0.001$ . (C) Cells ( $2 \times 10^5/500 \mu\text{l}$ ) were added to porous polycarbonate filters (8  $\mu\text{m}$  pore) coated with Matrigel (10  $\mu\text{g}$ ) in the presence 25  $\mu\text{g/ml}$  of control antibody (IgG) or anti-E-cadherin antibody (HECD-1, designated E-cad) for 40 h. In wells containing E-cadherin antibody, either MMP inhibitor, GM6001 (2.5  $\mu\text{M}$ ), function blocking uPA antibody (American Diagnostica #394, 15  $\mu\text{g/ml}$ ) or both were added. Nonmigrating cells were removed from the upper chamber, filters were fixed and stained, and invading cells were enumerated using an ocular micrometer. The results represent the mean  $\pm$  SEM of three different experiments. \*, significantly different from IgG



treated cells with  $p < 0.001$ . †, significantly different from E-cadherin antibody treated cells with  $p < 0.05$ .

#, significantly different from E-cadherin antibody treated cells with  $p < 0.01$ .

*Table 1.* Calcium-mediated cell-cell attachment suppresses TIMP-1 and PAI-1.

E-cad Activation	TIMP-1 (ng/ml)	PAI-1 (ng/ml)
-	72 ± 3	40 ± 2
+	45 ± 3*	16 ± 1**

E-cadherin-mediated cell-cell adhesion was disrupted by incubating pp 126 cells with 4 mM EGTA for 30 min (designated + EGTA) and then re-initiated by replacing the medium with calcium-containing Keratinocyte-SFM (0.09 mM). Conditioned media were collected after 24-36 h and TIMP-1 and PAI-1 levels were analyzed by ELISA according to the manufacturer's specifications. The results represent the mean ± SE of three individual experiments. \*, significantly different from control with  $p < 0.005$ ; \*\*, significantly different from control with  $p < 0.001$ .

Table 2. Suppression of TIMP-1 and PAI-1 following cell adhesion requires E-cadherin.

Antibody	E-cad Activation	TIMP-1 (ng/ml)	PAI-1 (ng/ml)
IgG	-	94 ± 6	25 ± 2
E-cad	-	83 ± 5	23 ± 2
IgG	+	46 ± 3*	13 ± 1**
E-cad	+	70 ± 5	21 ± 1

E-cadherin-mediated cell-cell adhesion was disrupted by incubating pp 126 cells with 4 mM EGTA for 30 min (designated + EGTA) and then re-initiated by replacing the medium with calcium-containing Keratinocyte-SFM (0.09 mM) in the presence of anti-E-cadherin antibody (HECD-1, 10 µg/ml) or isotype-matched IgG (10 µg/ml). Conditioned media were collected after 24-36h and TIMP-1 and PAI-1 levels in the conditioned media were analyzed by ELISA according to the manufacturer's specifications.

\*, significantly different from control with  $p < 0.001$ ; \*\*, significantly different from control with  $p < 0.01$ .

Fig 1

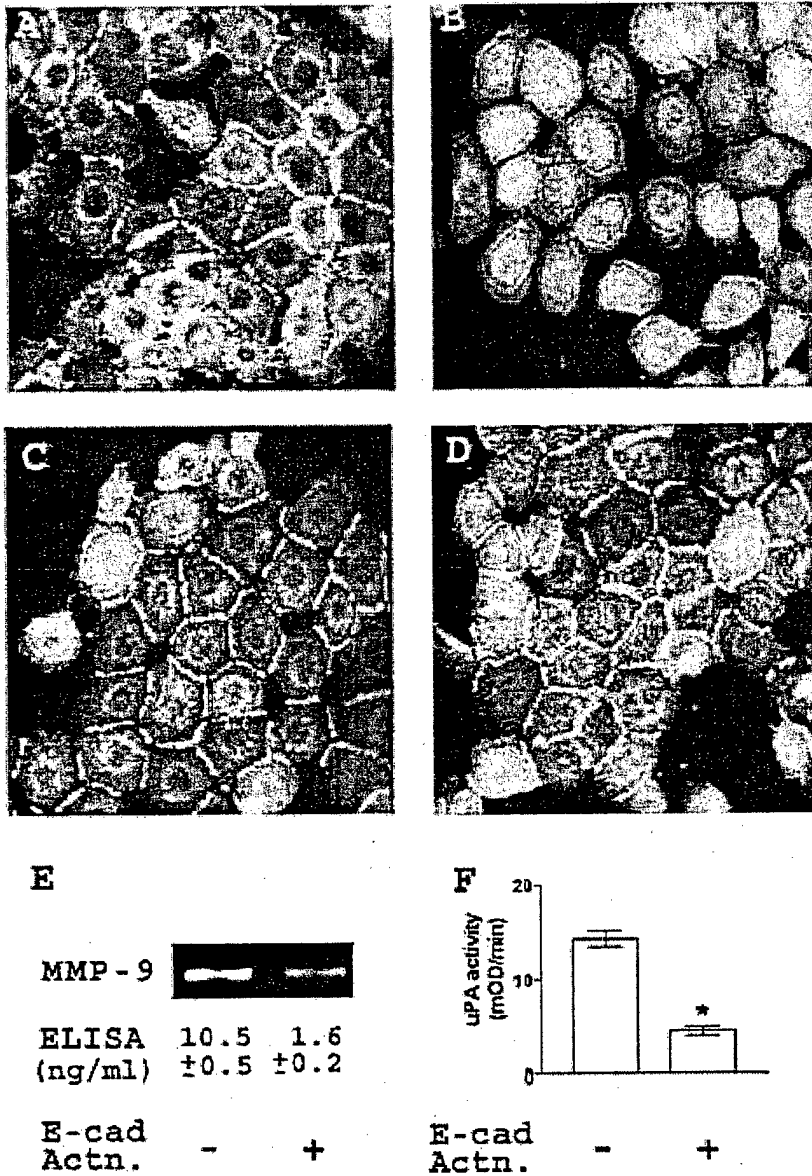
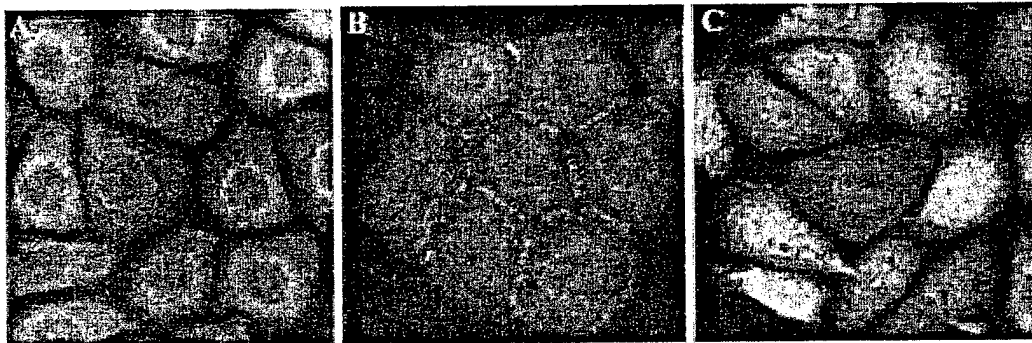
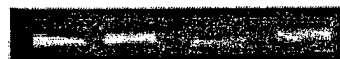


Fig 2

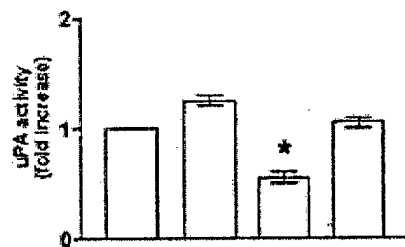


D



E-cad	-	-	+	+
Actn.				
Ab	IgG	E-cad	IgG	E-cad

E



E-cad	-	-	+	+
Actn.				
Ab	IgG	E-cad	IgG	E-cad

Fig 3


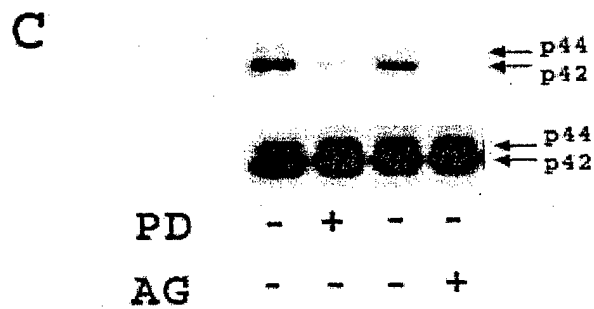
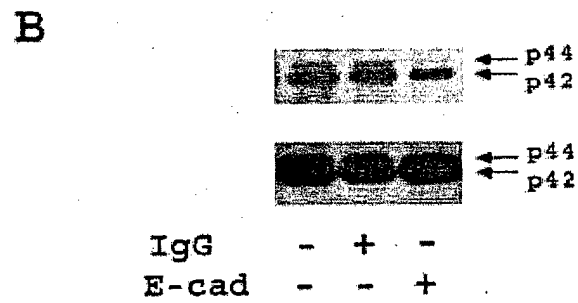
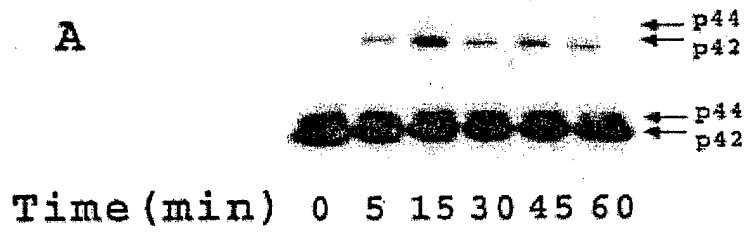
uPAR				
E-cad Actn.	-	-	+	+
Ab	IgG	E-cad	IgG	E-cad

Fig 4



# Fig 5

A



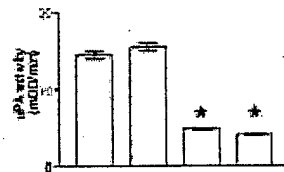
E-cad	-	-	+	+
Actn.	-	-	+	+
PD	-	+	-	+

B



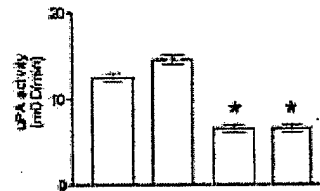
E-cad	-	-	+	+
Actn.	-	-	+	+
AG	-	+	-	+

C



E-cad	-	-	+	+
Actn.	-	-	+	+
PD	-	+	-	+

D



E-cad	-	-	+	+
Actn.	-	-	+	+
AG	-	+	-	+



# Fig 6

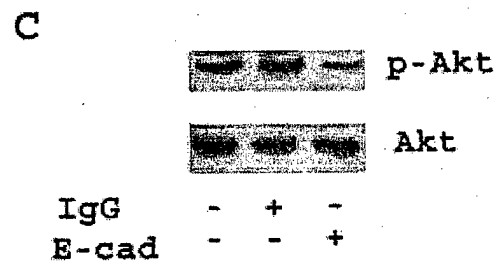
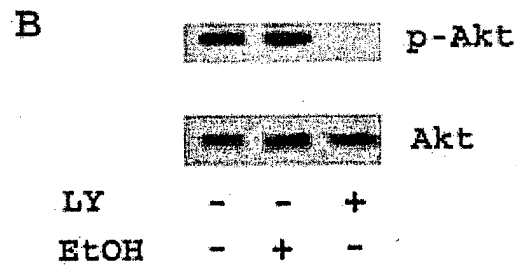
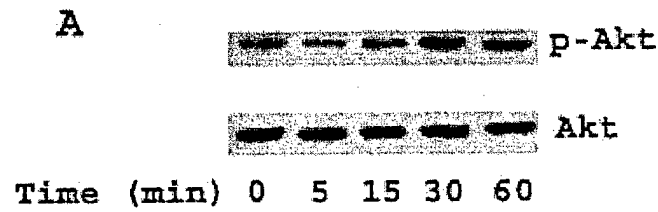


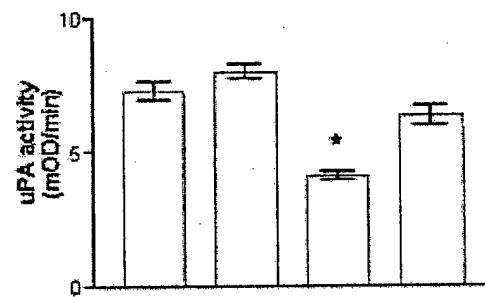
Fig 7

A



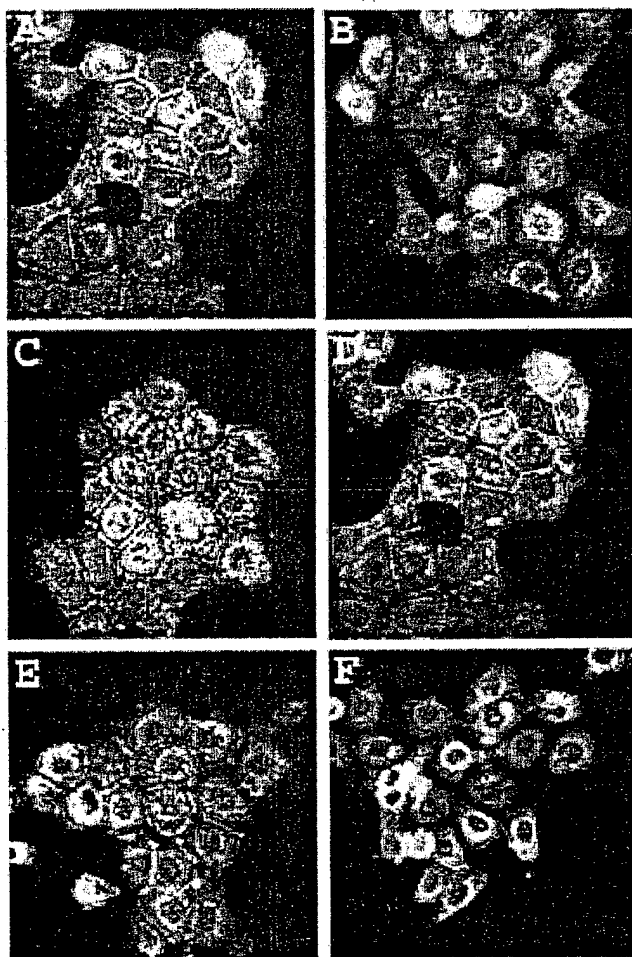
E-cad Actn.	-	-	+	+
LY	-	+	-	+

B



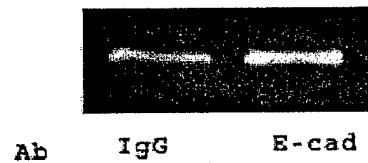
E-cad Actn.	-	-	+	+
LY	-	+	-	+

Fig 8

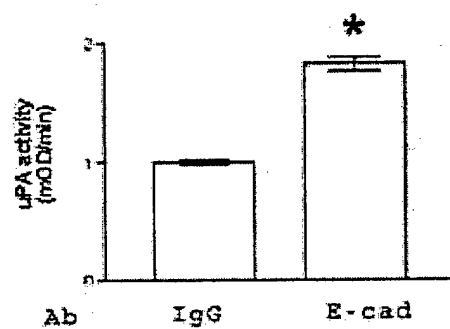


# Fig 9

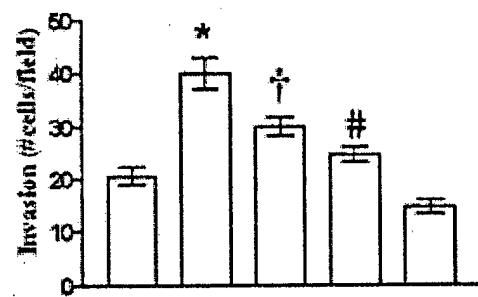
A



B



C



Ab	IgG	E-cad	E-cad	E-cad	E-cad
MMPI	-	-	+	-	+
uPA-Ab	-	-	-	+	+

## Functional Interplay between Type I Collagen and Cell Surface Matrix Metalloproteinase Activity\*

Received for publication, June 27, 2000, and in revised form, April 4, 2001  
Published, JBC Papers in Press, April 30, 2001, DOI 10.1074/jbc.M005631200

Shawn M. Ellerbroek‡, Yi I. Wu‡, Christopher M. Overall§, and M. Sharon Stack‡¶

From the ‡Departments of Cell and Molecular Biology and Obstetrics and Gynecology, Northwestern University Medical School, Chicago, Illinois 60611 and the §Faculty of Dentistry and Department of Biochemistry and Molecular Biology, Faculty of Medicine, University of British Columbia, Vancouver, British Columbia V6T 1Z3, Canada

Type I collagen stimulation of pro-matrix metalloproteinase (pro-MMP)-2 activation by ovarian cancer cells involves  $\beta_1$  integrin receptor clustering; however, the specific cellular and biochemical events that accompany MMP processing are not well characterized. Collagenolysis is not required for stimulation of pro-MMP-2 activation, and denatured collagen does not elicit an MMP-2 activation response. Similarly, DOV13 cells bind to intact collagen utilizing both  $\alpha_2\beta_1$  and  $\alpha_3\beta_1$  integrins but interact poorly with collagenase-treated or thermally denatured collagen. Antibody-induced clustering of  $\alpha_3\beta_1$  strongly promotes activation of pro-MMP-2, whereas  $\alpha_2\beta_1$  integrin clustering has only marginal effects. Membrane-type 1 (MT1)-MMP is present on the DOV13 cell surface as both an active 55-kDa TIMP-2-binding species and a stable catalytically inactive 43-kDa form. Integrin clustering stimulates cell surface expression of MT1-MMP and co-localization of the proteinase to aggregated integrin complexes. Furthermore, cell surface proteolysis of the 55-kDa MT1-MMP species occurs in the absence of active MMP-2, suggesting MT1-MMP autolysis. Cellular invasion of type I collagen matrices requires collagenase activity, is blocked by tissue inhibitor of metalloproteinases-2 (TIMP-2) and collagenase-resistant collagen, is unaffected by TIMP-1, and is accompanied by pro-MMP-2 activation. Together, these data indicate that integrin stimulation of MT1-MMP activity is a rate-limiting step for type I collagen invasion and provide a mechanism by which this activity can be down-regulated following collagen clearance.

The MMP family is composed of at least 25 zinc-dependent extracellular endopeptidases whose activities are regulated predominantly by expression as inactive precursors, or zymogens (1–3). Although precise physiological activators of MMPs<sup>1</sup> are unknown, a variety of serine proteinases and other

MMPs in the extracellular milieu execute the initial propeptide cleavage events *in vitro* (2). An exception to serine protease activation is pro-MMP-2 (72-kDa gelatinase A), which lacks the necessary basic amino acid cleavage sites in its pro-domain (4). A primary mechanism of pro-MMP-2 activation involves zymogen association with the cell surface via formation of a ternary complex containing tissue inhibitor of metalloproteinase (TIMP)-2 and membrane type 1-MMP (MT1-MMP, MMP-14) (3–6). Following trimeric complex formation, it is hypothesized that a neighboring MT1-MMP molecule that is not associated with TIMP-2 cleaves pro-MMP-2 at the Asn<sup>37</sup>–Leu<sup>38</sup> peptide bond within the pro-domain (7). Intermediately processed MMP-2 (Leu<sup>38</sup>–MMP-2) undergoes further concentration-dependent autolytic cleavage(s) to generate mature enzymes that can be released into the soluble phase or remain surface-associated (8). Although biological mechanisms of active MMP-2 release from the cell surface are not well characterized and dissociation kinetics provide little insight, cellular binding affinities may shift following pro-MMP-2 cleavage.

Culturing a variety of cell types within a three-dimensional gel of type I collagen stimulates cellular activation of pro-MMP-2 (9–12). Although MT1-MMP is implicated in MMP processing, regulation of cellular events that promote MMP processing are poorly understood. As cellular interaction with type I collagen is mediated largely through integrin receptors, it has been postulated that collagen stimulation occurs either directly or indirectly through integrin signaling (12–16). In support, we have previously demonstrated that culturing DOV13 ovarian cancer cells in a three-dimensional collagen gel elicits a strong pro-MMP-2 activation response that can be mimicked by clustering of  $\beta_1$  integrin receptors (12). Furthermore, pro-MMP-2 activation coincides with the processing of MT1-MMP into truncated 55- and 43-kDa forms on the cell surface. In this study, we utilize a variety of approaches to elucidate the biochemical requirements of type I collagen stimulation of MMP zymogen activation, characterize processed forms of MT1-MMP that are generated in this response, and examine the proteinase requirements for cellular invasion of type I collagen gels. Our findings illustrate a general mechanism by which cells may regulate cell surface-associated MMP activity via interactions with pericellular collagen matrix.

### EXPERIMENTAL PROCEDURES

**Materials**—Bovine serum albumin, gelatin, cell culture reagents, human placental type I collagen, aminophenylmercuric acetate, anti-(rabbit IgG)-peroxidase conjugates, purified mouse immunoglobulins, 2.97- $\mu$ m diameter latex beads, concanavalin A (ConA), and *ortho*-phenanthroline were all purchased from Sigma. Anti-human  $\beta_1$  integrin

\* This work was supported by National Institutes of Health Training Grant 5T32 GM08061 (to S. M. E.), United States Army MRC Training Grant DAMD170010386 (to Y. I. W.), and NCI Research Grant RO1 CA86984 (to M. S. S.) from the National Institutes of Health. The costs of publication of this article were defrayed in part by the payment of page charges. This article must therefore be hereby marked "advertisement" in accordance with 18 U.S.C. Section 1734 solely to indicate this fact.

¶ To whom correspondence should be addressed: Dept. of Cell and Molecular Biology, Northwestern University Medical School, 303 E. Chicago Ave., Tarry 8-715, Chicago, IL 60611. Tel.: 312-908-8216; Fax: 312-503-7912; E-mail: mss130@northwestern.edu.

<sup>1</sup> The abbreviations used are: MMP, matrix metalloproteinase; MT1-MMP, membrane type-1 matrix metalloproteinase; TIMP, tissue inhibitor of matrix metalloproteinase; ConA, concanavalin A; rCBD123, recombinant collagen binding domain; rCD, recombinant carboxyl hemopexin domain; PBS, phosphate-buffered saline; TBS, Tris-buffered

saline; BSA, bovine serum albumin; mAb, monoclonal antibody; CR, collagenase-resistant; MES, 4-morpholineethanesulfonic acid; MMPI, MMP inhibitor; CHO, Chinese hamster ovary.

mAb clones 21C8 and P5D2, anti-human  $\alpha_2$  mAb clones P1E6 and AK7, anti-human  $\alpha_3$  integrin mAb clones P1B5 and ASC-6, anti-human  $\alpha_3\beta_1$  heterodimer integrin mAb clone M-KD102, anti-human (carboxyl domain) TIMP-2 mAb clone 67-4H11, and anti-human MT1-MMP polyclonal antibody (AB815, hinge domain) were all obtained from Chemicon (Temecula, CA). Hydrobond-P:polyvinylidene difluoride membrane was obtained from Amersham Pharmacia Biotech. Super-Signal-enhanced chemiluminescence reagents were purchased from Pierce. The general hydroxamic acid MMP inhibitor INH-3850-PI (MMPI) was purchased from Peptides International (Louisville, KY). Purified TIMP-2 and TIMP-1 and anti-MT1-MMP (raised against amino acids 160–173/catalytic domain) polyclonal antibody MTK3 were generous gifts of Dr. Hideaki Nagase (Kennedy Institute of Rheumatology, Imperial College School of Medicine, UK). Recombinant MMP-2 type II fibronectin domain repeats (rCBD123) and hemopexin carboxyl domain (Gly<sup>417</sup>-Cys<sup>631</sup>) were generated as described previously (17, 18). Collagenase-resistant (CR) murine type I collagen ( $\alpha_1(I)$  chain mutations, Gln<sup>774</sup> → Pro<sup>774</sup>, Ala<sup>777</sup> → Pro<sup>777</sup>, and Ile<sup>778</sup> → Met<sup>778</sup>) and wild type murine type I collagen were the generous gifts of Dr. Stephen Krane (Harvard University) (19).

**Cell Culture**—The ovarian carcinoma cell line DOV13 was provided by Dr. Robert Bast, Jr. (M.D. Anderson Cancer Center, Houston, TX). Cell culture was maintained under standard conditions in 75-cm<sup>2</sup> cell culture flasks (20).

**Quantification of Cell Adhesion**—96-well cluster plate chambers were coated with 50  $\mu$ l of 10  $\mu$ g/ml type I collagen,  $\frac{3}{4}$ ,  $\frac{1}{4}$  collagen fragments (prepared as described below), or type I gelatin (1.6  $\mu$ g/cm<sup>2</sup>) in sterile phosphate-buffered saline (PBS) for 4 h at 25 or 37 °C, blocked with 3% BSA in minimal essential medium for 1 h at 37 °C, washed with PBS, and air-dried. Cells ( $1 \times 10^6$  cells/ml in serum-free medium) were incubated for 20 min at 37 °C with specific integrin function-blocking antibodies or nonspecific control antibodies, plated at a density of  $2 \times 10^4$  cells/well, and allowed to adhere for 75 min. Unbound cells were removed by washing with PBS, and adherent cells were fixed in ethanol (10 min), stained with 0.5% crystal violet (20 min), washed extensively with water, and solubilized with 100  $\mu$ l 1% SDS. Relative adhesion was quantified by monitoring the absorbance of released dye at 540 nm ( $n = 5$ ).

**Isolation of Collagen Fragments and Preparation of Collagen-containing Surfaces**—Human placental collagen (7 mg) was cleaved into  $\frac{3}{4}$  and  $\frac{1}{4}$  fragments by incubating with 2  $\mu$ g of MMP-1 for 16 h at 25 °C in Tris-buffered saline (TBS) (pH 7.4) containing 60 mM CaCl<sub>2</sub>. Cleaved collagen was isolated using a modified ammonium sulfate precipitation protocol (21). Ammonium sulfate (12%) was added to collagen suspension on ice at 4 °C under constant stirring for 1 h and then centrifuged (15,000  $\times g$ , 1 h, 4 °C). The 12% pellet containing intact collagen was washed with ice-cold TBS containing 12% ammonium sulfate, re-centrifuged (15,000  $\times g$ , 1 h, 4 °C), solubilized with 0.2 M acetic acid, and dialyzed against PBS. To isolate the  $\frac{3}{4}$  and  $\frac{1}{4}$  fragments, ammonium sulfate was added to the 12% supernatant to a final concentration of 25%, incubated for 1 h, and centrifuged (15,000  $\times g$ , 1 h, 4 °C). The 25% pellet containing  $\frac{3}{4}$  and  $\frac{1}{4}$  collagen fragments was washed with ice-cold TBS containing 25% ammonium sulfate, re-centrifuged (15,000  $\times g$ , 1 h, 4 °C), solubilized, and dialyzed as described above. Type I gelatin was produced by thermal denaturation of type I collagen for 20 min at 60 °C. Protein concentrations were determined using the Bio-Rad D<sub>C</sub> kit and bovine albumin as a standard.

Assays using thin deposits of type I collagen were performed by dialyzing acid-solubilized collagen against PBS, diluting to 10  $\mu$ g/ml in 100 mM sodium carbonate (pH 9.6), and coating 24-well cluster plate chambers with 200  $\mu$ l (10  $\mu$ g/ml, 1.1  $\mu$ g/cm<sup>2</sup>) of collagen. Chambers were incubated for 1 h at 37 °C, washed with sterile PBS, and air-dried. For three-dimensional collagen gel experiments, dialyzed type I collagen was diluted to 1.5 mg/ml with cold minimum essential medium containing 20 mM Hepes (pH 7.4). Diluted collagen (200  $\mu$ l, 158  $\mu$ g/cm<sup>2</sup>) was added to 24-well plates and allowed to gel at 37 °C for 30 min before the addition of cells ( $2.5 \times 10^6$ ) to wells. Cells were incubated for 48–72 h in serum-free medium at 37 °C before collection of conditioned media.

**Integrin Clustering**—Anti-integrin subunit-specific antibodies or control IgG were passively adsorbed onto 2.97- $\mu$ m diameter latex beads as described previously using the following modifications (12, 24). Latex beads were incubated at a final suspension of 0.1% in 100 mM MES buffer pH 6.1, with 25  $\mu$ g/ml appropriate antibody in 1-ml volumes overnight at 4 °C under agitation, and then blocked with 10 mg/ml BSA for 2 h at room temperature. Blocked beads were pelleted (3,000  $\times g$ , 3 min, 25 °C), washed twice with 1 ml of serum-free media, and resuspended to 1% by volume. Protein concentration assays using a BCA detection kit (Sigma) indicated 60–70% adsorption of immunoglobulins.

Cells were plated at a density of  $2.5 \times 10^6$  cells/well in 24-well cluster plates (Becton Dickinson) overnight in serum-containing medium, incubated for 2 h in serum-free medium prior to the addition of fresh medium containing soluble antibodies (10  $\mu$ g/ml), concanavalin A (20  $\mu$ g/ml), (25) or antibody-adsorbed latex beads (3–4  $\mu$ g/ml; 0.02% beads by final volume) for 18–20 h. All final volumes were 500  $\mu$ l/well.

**Gelatin Zymography**—Gelatinase activities in conditioned media were determined using SDS-polyacrylamide gel electrophoresis zymography. Conditioned media (20  $\mu$ l) from an equivalent number of cells were electrophoresed without reduction on SDS-polyacrylamide gel electrophoresis gels prepared with 9% acrylamide containing 0.1% gelatin (23). SDS was removed through a 1-h incubation in 2.5% Triton X-100, and gels were incubated in 20 mM glycine, 10 mM CaCl<sub>2</sub>, 1  $\mu$ M ZnCl<sub>2</sub> (pH 8.3), at 37 °C for 24 h prior to staining for gelatin with Coomassie Blue. Enzyme activity was visualized as zones of gelatin clearance within the gels.

**MMP-2 Competition Experiments**—Cells were grown to confluency in 24-well chamber plates and incubated for 2 h in serum-free medium. Fresh medium containing various concentrations of rCBD123 (17) or recombinant hemopexin carboxyl domain (18) were added to cells in a 500- $\mu$ l volume. After 2 h, ConA was added to a final concentration of 20  $\mu$ g/ml, and cells were incubated for an additional 18 h. Conditioned media and cell lysates were collected and processed as described above.

**MT1-MMP Immunoblots**—Cells were incubated under various conditions, collected with lysis buffer, and protein concentration of lysates was analyzed using the Bio-Rad D<sub>C</sub> detection kit and bovine albumin standards. Cell lysates (5–15  $\mu$ g) were electrophoresed on 9% SDS-polyacrylamide gels, transferred to polyvinylidene difluoride membrane, and blocked with 3% BSA in 50 mM Trizma (Tris base) (pH 7.5), 300 mM NaCl, 0.2% Tween 20 (TBST). Membranes were incubated for 1 h at room temperature with a 1:4000 dilution of anti-human MT1-MMP polyclonal antibody in 3% BSA/TBST. Immunoreactive bands were visualized with a peroxidase-conjugated anti-rabbit-IgG (1:5000 in 3% BSA/TBST) and enhanced chemiluminescence.

**Isolation of Biotin-labeled Cell Surface Proteins**—Cells were grown to confluency in 6-well cluster dishes, washed with PBS, and incubated for 2 h in serum-free medium. Fresh serum-free medium (1 ml) containing a 0.06% antibody-coated bead suspension or 20  $\mu$ g/ml concanavalin A was added, and cells were incubated for 20 h. Conditioned medium was removed; cells were washed with  $2 \times 2$  ml of PBS, and surface proteins were labeled with a non-cell-permeable sulfo-NHS biotin analog (500  $\mu$ l at 500  $\mu$ g/ml PBS, Pierce) under gentle shaking at 4 °C for 30 min. After washing, cells were incubated with 1 ml of 100 mM glycine/PBS for an additional 20 min under gentle shaking at 4 °C. Washed cells were lysed with 500  $\mu$ l of lysis buffer (50 mM sodium phosphate buffer (pH 8.0), 150 mM NaCl, 1% Nonidet P-40, 0.5% Triton X-100, 1  $\mu$ g/ml aprotinin, 1  $\mu$ M pepstatin, 10  $\mu$ M leupeptin, and 10  $\mu$ M E64), collected with a cell scraper, and clarified by centrifugation (10,000  $\times g$ , 10 min, 4 °C). Protein concentrations were calculated as described. To precipitate biotin-labeled cell surface proteins, lysate (1 ml, 750  $\mu$ g/ml) was added to either ImmunoPure immobilized monomeric avidin or multimeric streptavidin gel (40  $\mu$ l) (Pierce) and incubated overnight at 4 °C on a rotator. Gels were washed 5 $\times$  with lysis buffer. In some experiments, 10 mM free D-Biotin/PBS (Pierce) was added to aliquots of monomeric avidin gel-immobilized protein to compete off bound protein at 4 °C overnight. Eluates (30  $\mu$ l) were analyzed by gelatin substrate zymography or immunoblotting. Control conditions utilized non-biotinylated cell lysates.

**Isolation of Plasma Membranes**—DOV13 cells were grown to confluency in 15-cm culture dishes, washed with PBS, switched to serum-free medium for 2 h, and incubated in 5 ml of fresh serum-free medium containing 20  $\mu$ g/ml ConA for 20 h. Cells were washed twice with 5 ml of PBS, collected with a cell scraper, and pelleted by centrifugation (1500  $\times g$ , 10 min, 4 °C). Cells were resuspended in ice-cold 5 mM Tris/HCl (pH 7.8) and incubated for 10 min prior to homogenization by 30 passages through a 26 $\frac{1}{4}$ -gauge needle (8). Crude membrane preparations were isolated by centrifuging whole cell lysates (10,000  $\times g$ , 10 min, 4 °C), retaining the supernatant, and centrifuging the supernatant (100,000  $\times g$ , 1 h, 4 °C). The recovered pellet was washed in 20 mM Tris/HCl (pH 7.8), 10 mM CaCl<sub>2</sub>, 0.05% Brij 35 and recentrifuged (100,000  $\times g$ , 45 min, 4 °C). The plasma membrane-containing pellet was resuspended in washing buffer, and protein concentration was assessed as described above.

**Cross-linking and Immunoprecipitation**—To isolate TIMP-2-binding MT1-MMP species, cell surface proteins were cross-linked, and TIMP-2 complexes were isolated through immunoprecipitation. Confluent cells were incubated for 16 h in 5 ml of serum-free medium containing 20  $\mu$ g/ml ConA and 125 ng/ml TIMP-2. After washing ( $2 \times 5$  ml of PBS),

cell surface proteins were cross-linked with 2 mM 3,3'-dithiobis(sulfosuccinimidylpropionate) (Pierce) in PBS at 4 °C for 25 min under gentle shaking. Cells were washed (2 × 10 ml of PBS), and lysates were collected in cold lysis buffer. Clarified cell lysates (700 µg/ml) were incubated with 5 µg of anti-TIMP-2 (carboxyl-terminal) mAb clone 67-4H11 or murine IgG (κ) for 2.5 h at 4 °C on a rotator prior to the addition of a 50% slurry of protein A-agarose (20 µl) for 90 min. Immunoprecipitates were centrifuged (10,000 × g, 3 min, 4 °C), washed with lysis buffer (5 × 1 ml), and protein solubilized with 50 µl of 5× Laemmli buffer and processed for MT1-MMP immunoblotting as described above. To evaluate MT1-MMP activity, immunoprecipitations using anti-MT1-MMP hinge antibodies were performed using lysates from cells that were not exposed to cross-linking agent. Lysates were evaluated by gelatin zymography as described above.

**Stable Transfection of MT1-MMP**—The eukaryotic plasmid vector pCR3.1-Uni (Invitrogen, Carlsbad, CA) containing the MT1-MMP gene under a cytomegalovirus promoter was the generous gift of Dr. Duanqing Pei (University of Minnesota). A 6 histidine repeat was incorporated 3' of the carboxyl terminus using a polymerase chain reaction based approach with a 5' primer of ATgggCAGCgATgAAGTC and 3' primer of CgTCTAgATCAgTgATgATggTggTgATggACCTTgTCCAgCAGggA. The amplified polymerase chain reaction product was cloned back into the vector using a unique *FseI* restriction site and the *XbaI* restriction site in the 3' polylinker region of the vector. Plasmid DNA was sequenced and then isolated for transfection experiments using a Qiafilter maxi-kit (Qiagen, Valencia, CA). The vector control used in experiments is the pCR3.1-Uni vector driving the chloramphenicol transferase gene (pCR3.1/CAT, Invitrogen). pCR3.1/MT1-His<sub>6</sub> and control pCR3.1/CAT were transfected with LipofectAMINE (Pierce) as a delivery vehicle and isolated transformants screened for neomycin resistance selection (450 µg/ml G418). Soluble recombinant MT1-MMP lacking the linker from the carboxyl-terminal hemopexin domain through the cytoplasmic tail was expressed in CHO cells using the pW1HG vector. Soluble MT1-MMP purified from CHO serum-free conditioned medium was examined by electrophoresis on SDS-polyacrylamide gels and silver staining to visualize proteins.

**Immunocytochemistry**—Cells were cultured on glass coverslips overnight prior to addition of a 1-ml volume of serum-free medium containing 0.005% β<sub>1</sub> integrin mAb-coated beads. Cells were fixed with 3.7% formaldehyde without permeabilization and incubated with anti-MT1-MMP polyclonal antibody (MTK3) or normal rabbit serum in PBS. Immunoreactivity was visualized with a fluorescein-conjugated anti-rabbit secondary antibody previously purified against cross-reactivity to mouse immunoglobulins (Chemicon). Phase contrast and indirect fluorescent images were collected using a Zeiss fluorescence microscope (model II) and Adobe PhotoShop Software (version 4.0).

**Cellular Migration and Invasion**—Type I collagen was dissolved in 0.5 M acetic acid at a concentration of 2 mg/ml. For invasion experiments, the collagen stock was neutralized with 100 mM Na<sub>2</sub>CO<sub>3</sub> (pH 9.6) to a final concentration of 0.4 mg/ml. Transwell inserts (0.8 µm, Becton Dickinson, Bedford, MA) were coated on the underside with 500 µl of collagen diluted to a concentration of 100 µg/ml at 37 °C for 1 h. Collagen gels were prepared in the inner well by adding 50 µl of collagen (20 µg) at room temperature and allowing gels to air-dry overnight. Collagen-coated inserts were then washed with minimum essential medium three times to remove salts and used immediately. In some experiments, transwell inserts were coated with collagenase-resistant (19), rather than wild type, collagen. Cells were trypsinized, washed with serum-free medium, and 1 × 10<sup>5</sup> cells were added to the inner invasion chamber in a volume of 200 µl. The outer wells contained 400 µl of culture medium (serum-free, except in experiments using murine collagen). To evaluate the MMP dependence of invasion, after a 2-h incubation, the MMP inhibitors TIMP-1 (10 nM), TIMP-2 (10 nM), or MMPI (10 µM) were added to the inner and outer chambers as indicated. Control wells for MMPI contained the solvent Me<sub>2</sub>SO. Cells were allowed to invade for 24–48 h as indicated; non-invading cells were removed from inner wells using a cotton swab, and invading cells adherent to the bottom of membrane were fixed and stained using a Diff-Quick staining kit (DADE AG, Miami, FL). Invading cells were enumerated by dividing membranes into 4 quadrants and counting the number of cells in 3 distinct areas for each quadrant under a 10× objective using an ocular micrometer. Assays were performed in triplicate. To evaluate the integrin dependence of invasion, after a 2-h incubation anti-integrin antibodies (15 µg/ml) or control IgG (15 µg/ml) were added to the inner and outer chambers, as indicated. To evaluate the collagen structural requirements of invasion, wells were coated with thermally denatured collagen (gelatin, 50 µg/well in a 50-µl volume) and allowed to invade for 24 h in the presence of TIMP-1 (10 nM),

TABLE I

Rapid attachment of DOV13 cells requires α<sub>2</sub>β<sub>1</sub> and α<sub>3</sub>β<sub>1</sub> integrins

DOV13 cells (2 × 10<sup>4</sup>/well) were preincubated with the indicated concentration of antibodies for 20 min under standard cell culture conditions prior to addition to collagen-coated wells. Cell attachment was measured as described under "Experimental Procedures." DOV13 cells utilize both α<sub>2</sub>β<sub>1</sub> and α<sub>3</sub>β<sub>1</sub> integrins to bind native type I collagen. Values were corrected for control binding to BSA-coated wells.

Matrix + condition	Absorbance at 540 nm
Type I collagen	226 ± 41
+ 15 µg/ml mouse IgG	196 ± 51
+ 15 µg/ml anti-β <sub>1</sub> integrin (P5D2)	48 ± 4 <sup>a</sup>
+ 5 µg/ml anti-α <sub>2</sub> integrin (P1E6)	167 ± 40
+ 15 µg/ml anti-α <sub>2</sub> integrin	126 ± 24 <sup>b</sup>
+ 5 µg/ml anti-α <sub>3</sub> integrin (P1B5)	149 ± 10 <sup>b</sup>
+ 15 µg/ml anti-α <sub>3</sub> integrin	117 ± 23 <sup>b</sup>
+ 7.5 µg/ml anti-α <sub>2</sub> integrin/µg/ml anti-α <sub>3</sub> integrin	83 ± 12 <sup>a</sup>

<sup>a</sup> *p* < 0.05.

<sup>b</sup> *p* < 0.005 relative to IgG controls.

TIMP-2 (10 nM), or aprotinin (20 µg/ml), as indicated. Invasion of native and denatured collagen was also evaluated in the presence of the MMP-2 carboxyl hemopexin-like domain (rCD, 100 nM) (18) or the fibronectin type II-like domain (rCBD, 100 nM) (17) under the conditions described above.

To assess cell motility, migration through transwell membranes coated with a thin layer of collagen (100 µg/ml, 37 °C, 1 h) on both the upper and lower surfaces was evaluated as described above using an incubation time of 5.0 h. Haptotactic motility was assessed as described previously by plating cells on coverslips coated with colloidal gold overlaid with type I collagen (100 µg/ml) (22). Cells were allowed to migrate for 18 h, and phagokinetic tracks were monitored by visual examination using a Zeiss microscope with dark-field illumination. Semi-quantitative analysis of phagokinetic tracks was performed by measuring track area using computer-assisted image analysis and NIH Image.

## RESULTS

**Collagen Structure Regulates Cell Adhesion**—To evaluate the relative contribution of α<sub>2</sub>β<sub>1</sub> and α<sub>3</sub>β<sub>1</sub> integrins to collagen binding, attachment of DOV13 cells to type I collagen in the presence of integrin function-blocking antibodies was evaluated. DOV13 cells adhere rapidly to type I collagen-coated microtiter wells in an integrin-dependent fashion (Table I). Addition of anti-β<sub>1</sub> integrin function-blocking monoclonal antibodies (15 µg/ml, clone P5D2) significantly reduced binding to collagen relative to a nonspecific IgG control (75%), whereas equivalent amounts of either α<sub>2</sub> (P1E6) or α<sub>3</sub> (P1B5) integrin-blocking antibodies inhibited adhesion by 35–40% (Table I). Combination of α integrin blocking antibodies (7.5 µg/ml each) together reduced adhesion nearly 60%, supporting the conclusion that both α<sub>2</sub>β<sub>1</sub> and α<sub>3</sub>β<sub>1</sub> integrin heterodimers contribute to DOV13 cell attachment to type I collagen.

To assess the collagen structural requirements for integrin-mediated binding, adhesion to both collagenase-cleaved and thermally denatured collagen was analyzed. Native type-I collagen was incubated with collagenase-1 (MMP-1) and the ¼ and ¼ digestion products isolated through ammonium sulfate precipitation (21). Intact collagen heterofibrils, also isolated through this approach, were gelatinized by thermal denaturation. Intact collagen, ¼ and ¼ collagen fragments, or gelatin were coated onto microtiter wells at either 25 or 37 °C, and adhesion was evaluated as described above. Both intact collagen and ¼ and ¼ fragments support adhesion of DOV13 cells when matrices are coated at 25 °C; however, adhesion to ¼ and ¼ fragments was significantly reduced when matrices were coated at physiologic temperature (Table II). Although cells will slowly adhere to thermally denatured collagen (3–4 h), little adhesion to this matrix was observed under any coating condition over the course of the assay (75 min) (Table II). These results indicate that ¼ and ¼ collagen fragments coated at

TABLE II

Intact collagen is required for DOV13 attachment

Type I collagen,  $\frac{1}{4}$  and  $\frac{1}{2}$  collagen fragments, and type I gelatin were coated at the indicated temperature ( $1.6 \mu\text{g}/\text{cm}^2$ ), blocked with BSA, and cell attachment ( $2 \times 10^4/\text{well}$ ) measured as described under "Experimental Procedures." Values are reported as the percent absorbance at 540 nm in comparison to intact type I collagen, coated at the specified temperature.

10 $\mu\text{g}/\text{ml}$ matrix	% Bound relative to collagen
	%
Coating at 25 °C	
Type I collagen	100
Type I gelatin	$28.1 \pm 10.7^a$
$\frac{1}{4}$ and $\frac{1}{2}$ type I collagen	$94.3 \pm 11.7$
Coating at 37 °C	
Type I collagen	100
Type I gelatin	$9.7 \pm 9.2^a$
$\frac{1}{4}$ and $\frac{1}{2}$ type I collagen	$9 \pm 6.3^a$

<sup>a</sup>  $p < 0.005$  relative to intact type I collagen coated at the specified temperature.

25 °C retain a triple helical conformation that is required for recognition by  $\alpha_2\beta_1$  and  $\alpha_3\beta_1$  integrins, whereas coating at 37 °C results in destabilization of fragment helices (21). Together, these data suggest that collagenase activity at the cell/matrix interface can reduce the efficiency of integrin-mediated adhesion on the surface of DOV13 cells, thereby potentially affecting matrix-induced signaling events that are involved in cellular invasion.

**Integrin Clustering Promotes Cell Surface MMP-2 Processing**—To evaluate the matrix structural requirements for collagen induction of pro-MMP-2 activation, cells were cultured in the presence of native or thermally denatured collagen. Processing of pro-MMP-2 was not observed by cells cultured on type I gelatin (Fig. 1, lanes 4 and 5). However, culturing cells with collagenase-resistant collagen (19) stimulated pro-MMP-2 processing as efficiently as wild type collagen (Fig. 1, lanes 6 and 7), indicating that collagen processing is not necessary to promote a cellular gelatinase activation response. Similar to the wild type protein, gelation of collagenase-resistant collagen abrogated the ability to elicit pro-MMP-2 activation (Fig. 1, lane 5). In conjunction with cell adhesion studies, these data indicate that integrin interaction with intact triple-helical collagen is necessary to stimulate pro-MMP-2 activation and that destabilization of the collagen matrix following collagenase activity will reduce the ability of pericellular collagen to elicit an MMP response.

We have demonstrated previously that  $\beta_1$  integrin clustering stimulates a pro-MMP-2 processing event that correlates with enhanced gelatinolytic activity in conditioned media, indicating that integrin signaling is sufficient to elicit pro-MMP-2 activation (12). As adhesion of DOV13 cells to type I collagen is supported by both  $\alpha_2\beta_1$  and  $\alpha_3\beta_1$  integrins (Table I), integrin clustering was induced through the  $\alpha$ -subunit to evaluate the effects of clustering each specific integrin heterodimer on pro-MMP-2 activation. Consistent with adhesion blocking assays,  $\alpha_2$ ,  $\alpha_3$ , and  $\beta_1$  integrin antibody-coated beads attached with similar efficacy (data not shown); however, analysis of conditioned media by zymography demonstrates that clustering  $\alpha_3$  or  $\beta_1$  integrins elicits a stronger pro-MMP-2 activation response than  $\alpha_2$  integrins (Fig. 2A, lower panel). The observed difference in  $\alpha$  integrin subunit specificity was independent of the antibody clone used to promote clustering, and utilization of antibodies recognizing an  $\alpha_3\beta_1$  heterodimer-specific epitope also resulted in a pro-MMP-2 activation response (Fig. 2A, lower panel, lane 8). Soluble integrin antibodies did not influence pro-MMP-2 expression or activation (Fig. 2A, upper panel), supporting the hypothesis that multivalent integrin

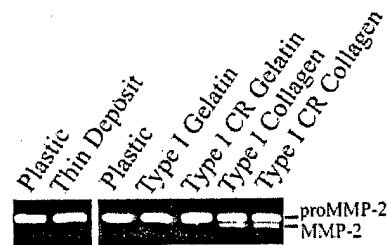
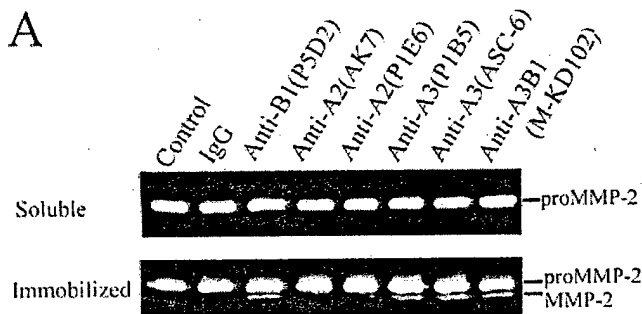


Fig. 1. Collagen stimulation of pro-MMP-2 activation. DOV13 cells ( $2.5 \times 10^5$  cells/well) were incubated on plastic or a thin deposit of type I collagen ( $1.1 \mu\text{g}/\text{cm}^2$ ), in the presence of thermally denatured wild type or collagenase-resistant (CR) collagen (Gelatin or CR Gelatin, respectively,  $158 \mu\text{g}/\text{cm}^2$ ), or within wild type or CR type I collagen gels (Collagen or CR Collagen, respectively,  $158 \mu\text{g}/\text{cm}^2$ ), as indicated, in serum-free medium for 48 h. Conditioned media were analyzed by gelatin zymography. The relative migration positions of pro- and active MMP-2 are indicated.

A



B

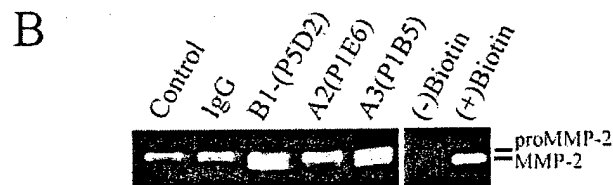


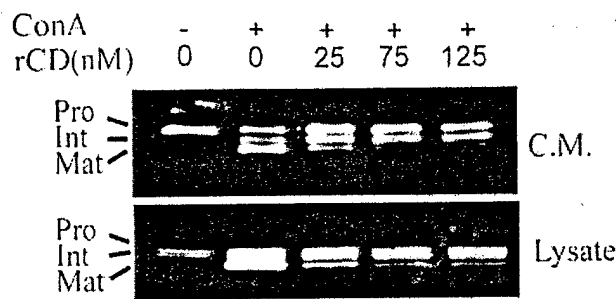
Fig. 2.  $\alpha_3\beta_1$  integrin clustering promotes MMP-2 processing and surface association. A, DOV13 cells were treated with the indicated soluble ( $10 \mu\text{g}/\text{ml}$ ) (upper panel) or bead-immobilized ( $4 \mu\text{g}/\text{ml}$ ) (lower panel) antibodies for 20 h, and conditioned media were analyzed by gelatin zymography. Antibody clone numbers are given in parentheses. The relative migration positions of pro- and active MMP-2 are indicated. B, cells were untreated (Control) or treated with the indicated bead-immobilized antibodies ( $12 \mu\text{g}/\text{ml}$ ) for 20 h prior to biotinylation of surface proteins using a non-cell-permeable biotin and cell lysis. Labeled protein ( $750 \mu\text{g}$ ) was captured with monomeric avidin gels, eluted with D-biotin, and eluates analyzed by gelatin zymography. The lack of activity eluted from non-biotinylated ConA-treated ( $20 \mu\text{g}/\text{ml}$ ) cell lysates (-Biotin) demonstrates the specificity of the system for cell surface proteins, as shown in the biotinylated, ConA-treated ( $20 \mu\text{g}/\text{ml}$ ) control (+Biotin).

aggregation is necessary for proteinase induction.

As the transmembrane proteinase MT1-MMP is predicted to catalyze cell surface integrin-mediated pro-MMP-2 activation, MMP-2 association with the plasma membrane was evaluated by surface labeling with cell-impermeable s-NHS-biotin and isolating biotinylated proteins with monomeric avidin-agarose gels. Proteins were eluted from avidin-agarose gels using  $10 \text{ mM}$  free D-biotin and analyzed by zymography for MMP activity. Clustering of both  $\alpha_3$  and  $\beta_1$  integrins promoted a significant association of MMP-2 to the cell surface (Fig. 2B, lanes 3 and 5) relative to cells subjected to  $\alpha_2$  integrin clustering (Fig. 2B, lane 4) or controls (Fig. 2B, lanes 1 and 2), confirming that  $\alpha_3\beta_1$  integrins elicit a more robust pro-MMP-2 processing response.

**Release of MMP-2 from the Cell Surface**—Secreted pro-MMP-2 binds to the cell surface through the carboxyl-terminal hemopexin domain, and an intermediately processed form is



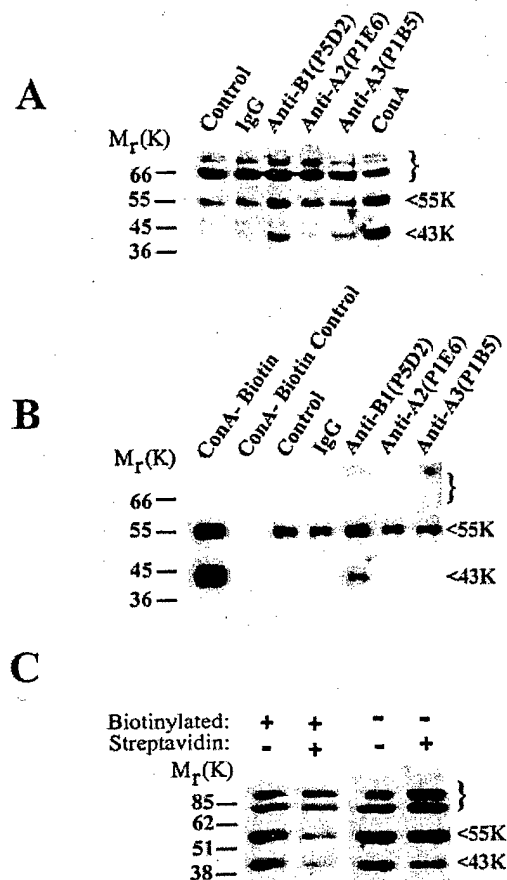


**FIG. 3. Competition of MMP-2 from the cell surface.** Cells were cultured for 20 h in the presence or absence of ConA (20  $\mu$ g/ml) and recombinant MMP-2 carboxyl hemopexin domain (rCD, 0–125 nM), as indicated. Conditioned media (C.M.) and cell lysates (5  $\mu$ g of total protein) were analyzed by gelatin zymography for processed forms of MMP-2. *Pro*, pro-MMP-2 (66 kDa); *Int*, intermediately processed MMP-2 (64 kDa); *Mat*, mature MMP-2 (62 kDa).

generated through MT1-MMP-mediated cleavage of the MMP-2 pro-domain at the Asn<sup>37</sup>–Leu<sup>38</sup> peptide bond (7). The MMP-2 intermediate is then predicted to undergo maturation to an active enzyme through concentration-dependent autolysis at the cell surface (8). Although formation of the trimeric MT1-MMP-TIMP-2-MMP-2 activation complex at the cell surface is well established (reviewed in Ref. 3), the mechanism by which active MMP-2 is released from the plasma membrane is presently unclear. Saturation binding studies are not technically feasible due to the instability of the intermediate and mature forms of the activated enzyme in concentrated solution. Thus, the ability of the MMP-2 hemopexin domain to dissociate surface-bound MMP-2 was evaluated. In the presence of increasing concentrations of recombinant hemopexin domain, active MMP-2 is not associated with the cell surface (Fig. 3A). In control experiments, competition of MMP-2 from the cell surface was not observed with rCBD123 at the same molar concentrations (data not shown).

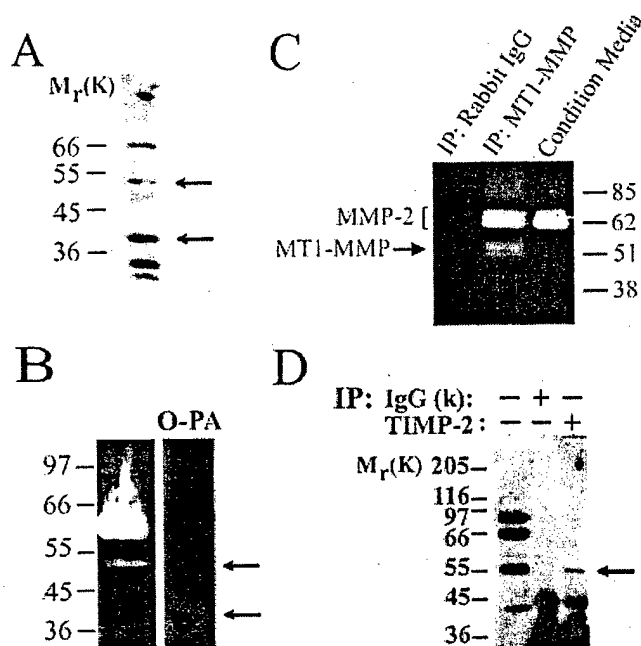
**Integrin Clustering Promotes Cell Surface MT1-MMP Processing**—The appearance of active MMP-2 on the cell surface implicates the involvement of MT1-MMP in integrin stimulation of pro-MMP-2 processing. To evaluate the effect of  $\alpha$  integrin clustering on events further upstream in the zymogen activation pathway, cells were treated with integrin antibody-coated beads, and cell lysates were immunoblotted with an antibody reactive against the hinge domain of MT1-MMP. Consistent with previous observations (12), stimulation of DOV13 cells with ConA promotes accumulation of 55- and 43-kDa forms of MT1-MMP in cell lysates (Fig. 4A, lane 6). Clustering of  $\beta_1$  integrins, and to a lesser extent  $\alpha_3$  integrins, promoted processing of MT1-MMP to a 43-kDa form (Fig. 4A, lanes 3 and 5, respectively), whereas little or no change in MT1-MMP expression was observed following clustering of  $\alpha_2$  integrins (lane 4) or under control conditions with nonspecific IgG (lane 2). Furthermore,  $\beta_1$  integrin clustering results in a small, but reproducible, accumulation of 55-kDa MT1-MMP in cell lysates (lane 3).

To address whether integrin clustering stimulates MT1-MMP expression on the cell surface, biotin-labeled cell surface proteins were isolated and immunoblotted for MT1-MMP species. ConA treatment promoted a strong accumulation of 55- and 43-kDa MT1-MMP species on the cell surface (Fig. 4B, lane 1). Higher molecular weight species that were detected in immunoblots of cell lysates (brackets, Fig. 4A) were absent in cell surface preparations (brackets, Fig. 4B), indicating that these proteins are likely intracellular. Consistent with cell lysate results, clustering of  $\beta_1$  integrins promoted cell surface expression of 55- and 43-kDa forms of MT1-MMP (Fig. 4B, lane 5), whereas clustering of either  $\alpha$  integrin subunit was not suffi-



**FIG. 4. Integrin clustering promotes MT1-MMP cell surface expression and processing.** A, integrin-induced MT1-MMP processing. Cells were treated for 20 h with bead-immobilized antibodies (4  $\mu$ g/ml) as indicated, and lysates (10  $\mu$ g for all samples except ConA, 7  $\mu$ g) were electrophoresed on 8% polyacrylamide gels and Western-blotted using an antibody to the MT1-MMP hinge region. Blots were developed using enhanced chemiluminescence. The migration position of molecular weight standards is indicated in the left margin, and the migration positions of the 55- and 43-kDa species of MT1-MMP are indicated in the right margin. B, cells were treated with ConA (20  $\mu$ g/ml) or the indicated bead-immobilized antibodies (12  $\mu$ g/ml) for 20 h prior to biotinylation of surface proteins using a non-cell-permeable biotin and cell lysis. Labeled protein (750  $\mu$ g) was captured with monomeric avidin gels, eluted with D-biotin, and eluates analyzed by electrophoresis and Western blotting for MT1-MMP. The lack of protein eluted from non-biotinylated ConA-treated cell lysates (lane designated ConA-Biotin Control) demonstrates the specificity of the system. C, to evaluate what fraction of the total pool of 55- and 43-kDa MT1-MMP species resides on the cell surface, cells were stimulated with ConA (20  $\mu$ g/ml) for 20 h, surface-biotinylated, lysed, and the lysate (750  $\mu$ g, + Biotin) depleted of biotin-labeled proteins through precipitation using multimeric streptavidin-conjugated agarose gels (+ Streptavidin). Streptavidin-depleted or control lysates (7.5  $\mu$ g) were analyzed by electrophoresis and Western blotting for MT1-MMP.

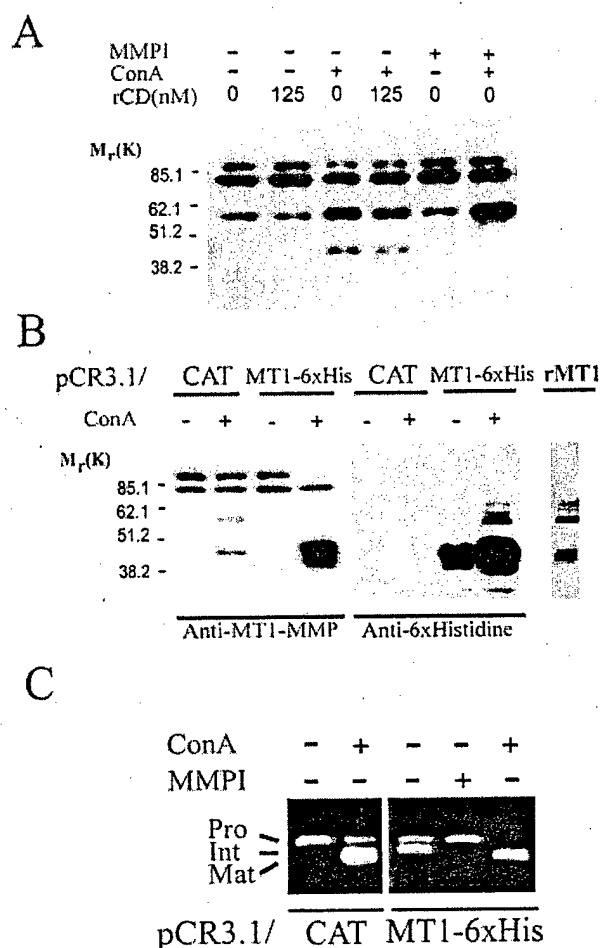
cient to promote detectable changes in the cell surface expression profile of MT1-MMP (Fig. 4B, lanes 6 and 7). Together, these data suggest that clustering of  $\beta_1$  integrins promotes these MMP-2 cell surface binding and activation through increased expression of cell surface-localized MT1-MMP. Furthermore, cell surface gelatinolytic profiles indicate that  $\alpha_3\beta_1$  integrins potentiate a stronger MMP response than  $\alpha_2\beta_1$  integrins (Fig. 2B). The ability to detect enhanced levels of cellular, but not cell surface, MT1-MMP following  $\alpha_3$  integrin clustering likely reflects the technical limitations of the assay, as  $\beta_1$  integrin clustering induces a more robust overall response. To evaluate further the pool of MT1-MMP species that reside on the cell surface, cells were stimulated with ConA, surface



**FIG. 5. Identification of active MT1-MMP species.** DOV13 cells were cultured in the presence of ConA (20  $\mu$ g/ml) for 20 h, lysed, and homogenized. Plasma membranes were isolated by centrifugation, and aliquots (20  $\mu$ g) were analyzed for MT1-MMP protein (A) and activity (B) by immunoblotting and gelatin zymography, respectively. A, Western blot of plasma membranes showing proteins cross-reactive with MT1-MMP antibody. The arrows indicate the migration positions of the 55- and 43-kDa MT1-MMP species. B, zymogram depicting MT1-MMP gelatinolytic activity associated with the 55-kDa species (upper arrow). (Note that the prevalent gelatinase activity in this sample is due to plasma membrane-bound MMP-2.) All gelatinase activity is inhibited by the zinc chelating agent *ortho*-phenanthroline (O-PA). C, immunoprecipitation (IP) of DOV13 cell lysates. Lysates (non-denatured) were immunoprecipitated with either IgG control or anti-MT1-MMP antibodies as indicated and analyzed by gelatin zymography. Although the immunoprecipitating antibody recognizes both the 43- and 55-kDa forms of MT1-MMP by immunoblotting (A), gelatinase activity corresponding to only the 55-kDa species is observed (arrow). MMP-2 co-precipitated as a component of the ternary complex, as evidenced by the co-migration with an MMP-2 standard (bracket). Lane designated *conditioned media*, DOV13 conditioned medium to designate migration position of MMP-2 (not subjected to immunoprecipitation). D, cross-linking and immunoprecipitation. Cells were treated with ConA (20  $\mu$ g/ml) and an excess of free TIMP-2 (125 ng/ml) for 18 h. After washing, cell surface proteins were cross-linked with a reducible cross-linking agent (2 mM 3,3'-dithiobis(sulfosuccinimidylpropionate), 25 min, 4  $^{\circ}$ C). Clarified cell lysates (700  $\mu$ g) were incubated with 5  $\mu$ g of anti-TIMP-2 (carboxyl-terminal) mAb clone 67-4H11 or murine IgG (κ) as indicated and precipitated using protein A-agarose. Immunoprecipitates were solubilized with Laemmli sample buffer, electrophoresed under reducing conditions on 8% polyacrylamide gels, and immunoblotted with the MT1-MMP hinge polyclonal antibody. The arrow designates the migration position of 55-kDa MT1-MMP, and the left margin indicates the migration position of molecular weight standards.

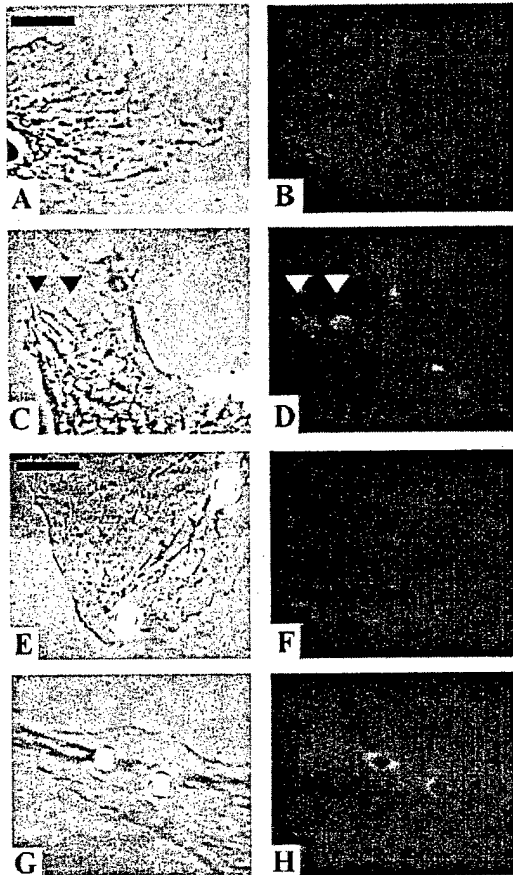
biotin-labeled, and lysates were depleted of biotinylated cell surface proteins using multimeric streptavidin-conjugated agarose. A selective depletion of only the 55- and 43-kDa forms of MT1-MMP was observed in streptavidin-treated samples compared with non-treated controls (Fig. 4C, lane 2), supporting the conclusion that these species, but not the higher molecular weight immunoreactive material present in Fig. 4A, are stably expressed on the cell surface.

**Characterization of Cell Surface MT1-MMP**—As MT1-MMP has been reported to have weak gelatinase activity (30, 31), plasma membrane preparations of ConA-treated DOV13 cells were analyzed by gelatin zymography to determine whether either of the surface-associated MT1-MMP species are proteolytically active. In addition to surface-bound MMP-2, an ortho-



**FIG. 6. MT1-MMP processing in the absence of cell surface MMP-2.** A, cells were cultured in the presence or absence of MMP1 (10  $\mu$ M), ConA (20  $\mu$ g/ml), or rCD (125 nM) as indicated. Lysates (7.5  $\mu$ g) were electrophoresed on 8% polyacrylamide gels and immunoblotted for MT1-MMP. B, stable DOV13 transfectants expressing polyhistidine-tagged MT1-MMP (MT1-6xHis) or control vector (CAT) were isolated, cultured in the presence or absence of ConA (20  $\mu$ g/ml) as indicated, and 7.5  $\mu$ g of cell lysates analyzed by electrophoresis and immunoblotting for MT1-MMP (lanes 1–4) or polyhistidine (lanes 4–8). Lane 9 contains soluble recombinant MT1-MMP (rMT1) lacking the transmembrane and cytoplasmic domain purified from CHO cell-conditioned medium and visualized by silver staining. C, DOV13 stable transfectants expressing polyhistidine-tagged MT1-MMP (MT1-6xHis) or vector controls (CAT) were isolated, cultured in the presence or absence of ConA (20  $\mu$ g/ml) or MMP1 (10  $\mu$ M) as indicated, and conditioned media analyzed for pro-MMP-2 activation by gelatin zymography. The relative migration positions of the pro-, intermediate (Int), and activated mature (Mat) forms of MT1-MMP are indicated in the left margin.

phenanthroline-sensitive gelatinolytic band that co-migrated with the non-reduced 55-kDa form of MT1-MMP was observed (Fig. 5B), whereas no gelatinase activity was attributable to the 43-kDa species. Control immunoblots demonstrate that both the 55- and 43-kDa species were prevalent in the experimental sample (Fig. 5A). To confirm that the observed 55-kDa gelatinolytic activity is a property of MT1-MMP, cell lysates were immunoprecipitated with an anti-MT1-MMP-specific antibody and the immunoprecipitates were analyzed by gelatin zymography. A 55-kDa gelatinolytic activity was recovered together with MMP-2, suggesting that both proteinases co-precipitate as components of the ternary complex (Fig. 5C). The relative ratio of MT1-MMP to MMP-2 gelatinase activity is enhanced by the immunoprecipitation approach (Fig. 5, C versus B). Similar to results obtained in whole plasma membrane preparations, there was no observable gelatinolytic activity attributable to

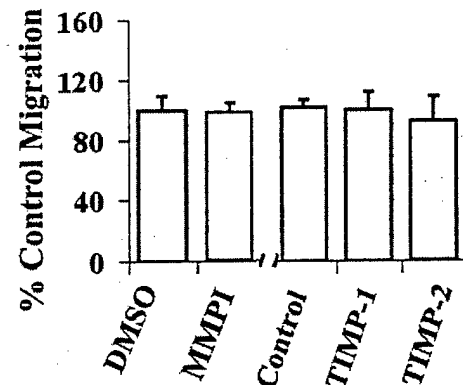


**FIG. 7. MT1-MMP localizes to cellular processes and redistributes to clustered  $\beta_1$  integrins.** Cells were cultured on glass coverslips in the absence (A–D) or presence (E–H) of anti- $\beta_1$  integrin (clone 21C8)-coated beads for 8 h and then processed for immunofluorescence as described under “Experimental Procedures.” Cells were incubated with normal rabbit serum (B and F) or anti-MT1-MMP antibody (D and H). Immunoreactivity was visualized with fluorescein-conjugated anti-rabbit secondary antibody previously purified against cross-reactivity to mouse immunoglobulins. Phase contrast images A, C, E, and G correspond with B, D, F, and H, respectively, and identify cellular processes and 2.97  $\mu$ m diameter latex beads. Arrowheads denote MT1-MMP immunoreactivity in cell surface projections. Magnification bar is 5  $\mu$ m (A–D) or 10  $\mu$ m (E–H), and images were collected with a 63 $\times$  objective using a Zeiss fluorescence microscope.

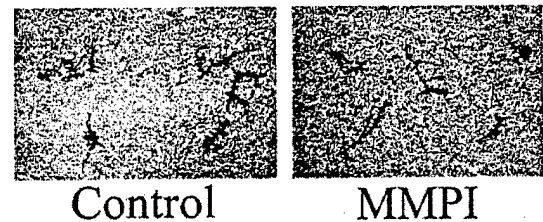
the 43-kDa form of MT1-MMP. As these results indicated that the 55-kDa form of MT1-MMP is an active species on the cell surface, the ability to bind TIMP-2 was assessed. Exogenous TIMP-2 was added directly to ConA-treated cells, followed by cross-linking with a reducible, cell-impermeable cross-linker. Cell lysates were then immunoprecipitated with an antibody specific to the carboxyl-terminal domain of TIMP-2, reduced, and analyzed by electrophoresis and immunoblotting for MT1-MMP. The 55-kDa species of MT1-MMP was specifically precipitated through TIMP-2 (Fig. 5D, lane 3), providing additional evidence that it is an active, TIMP-2-binding protein.

**MT1-MMP Processing in the Absence of Cell Surface MMP-2**—As reported previously (12), active 55-kDa MT1-MMP is converted to an inactive 43-kDa form through MMP-dependent proteolysis in DOV13 cells (Fig. 6A, compare lanes 3 and 6) (12). In a regulated cellular system generating an endogenous MMP-2/MT1-MMP cellular response, it is unclear whether this cleavage is mediated by activated MMP-2 or through concentration-dependent autolysis of MT1-MMP. As active MMP-2 is effectively removed from the cell system with 125 nm hemopexin domain (Fig. 3), cellular MT1-MMP processing in the absence of MMP-2 was assessed by immunoblotting. Conver-

A



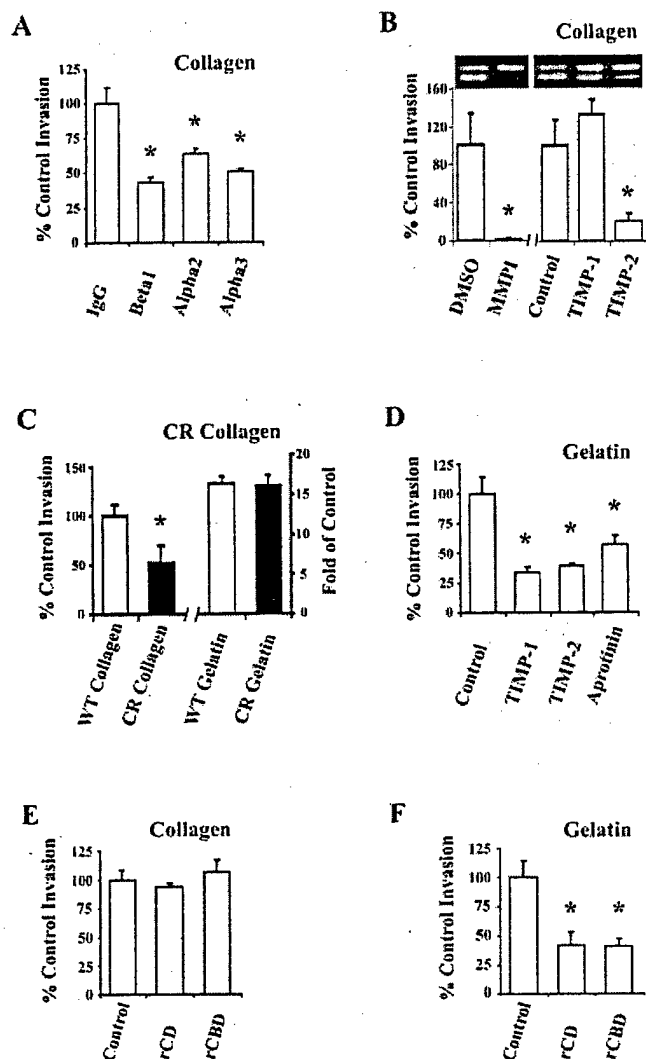
B



**FIG. 8. Migration of DOV13 cells is MMP-independent.** A, cells ( $2.5 \times 10^5$ ) were seeded on Transwell filters (8  $\mu$ m pore) coated with a thin layer of collagen (as described under “Experimental Procedures”) in the presence or absence of MMPI (10  $\mu$ M), Me<sub>2</sub>SO (DMSO, vehicle for MMPI), TIMP-1 (10 nM), or TIMP-2 (10 nM) as indicated and incubated for 5 h; filters were stained, and migrating cells adherent to the underside of the filter were enumerated using an ocular micrometer. Data are expressed as % of control migration (Me<sub>2</sub>SO for MMPI and PBS for TIMP-1 and -2). There is no significant difference in migration of inhibitor-treated samples relative to respective controls ( $p > 0.05$ ). B, haptotactic motility of DOV13 cells. Cells (1000) were plated onto coverslips coated with colloidal gold overlaid with type I collagen (100  $\mu$ g/ml) in the presence or absence of MMPI (10  $\mu$ M) as indicated, allowed to migrate for 24 h, and phagokinetic tracks visualized using dark field illumination.

sion of 55-kDa MT1-MMP to the 43-kDa form was not affected by the loss of active MMP-2 from the cell surface (Fig. 6A, lanes 3 and 4), indicating that MMP-2 is not required for proteolytic processing of endogenous 55-kDa MT1-MMP in DOV13 cells.

To determine whether MT1-MMP degradation proceeds through autolysis or through activity of an unidentified metalloprotease, DOV13 cells that stably overexpress full-length histidine-tagged MT1-MMP were generated. Overexpression of MT1-MMP resulted in accumulation of 40–45-kDa species of recombinant enzyme as detected by Western blotting with anti-MT1-MMP (Fig. 6B, lane 4) and confirmed using an antibody against the polyhistidine label (Fig. 6B, lanes 7 and 8). Similar results were obtained following expression of soluble recombinant MT1-MMP lacking the transmembrane and cytoplasmic domain, in which autolytic processing to 40–45-kDa species was also observed (Fig. 6B, lane 9, labeled rMT1), supporting the conclusion that the 55-kDa MT1-MMP-processing activity is directly attributable to the level of cell surface MT1-MMP activity (32). Together, these data indicate that active 55-kDa MT1-MMP undergoes concentration-dependent autolysis to an inactive 43-kDa form on the surface of DOV13 cells. Control experiments demonstrated MMP-dependent processing of pro-



**FIG. 9. Characterization of the proteinase requirements for invasion.** A–C and E, invasion of collagen. Cells ( $1.0 \times 10^6$ ) were added to collagen-coated Transwell chambers (20  $\mu$ g) in serum-free medium for 2 h prior to addition of reagents indicated below and allowed to invade for 48 h under the indicated conditions. Following invasion, cells were removed from the top chamber with a cotton swab; membranes were stained, and invading cells were enumerated using an ocular micrometer. C, D, and F, invasion of gelatin. Cells ( $1.0 \times 10^6$ ) were added to gelatin-coated Transwell chambers (50  $\mu$ g) in serum-free medium for 2 h prior to addition of reagents indicated and allowed to invade for 24 h under the indicated conditions. Invading cells were quantified as described. A, integrin subunit-specific antibodies block invasion of collagen. Integrin subunit-specific antibodies or control IgG (15  $\mu$ g/ml) were added as indicated. Results are expressed as % of control invasion (IgG), normalized to 100%. (\*,  $p < 0.05$  relative to control.) B, effect of MMP inhibitors on collagen invasion. Invasion was quantified in the presence or absence of MMPI (10  $\mu$ M), TIMP-1 (10 nM), or TIMP-2 (10 nM), as indicated. Results are expressed as % of control invasion. MMPI data are normalized to Me<sub>2</sub>SO controls (designated 100%), and TIMP-1 and -2 data are normalized to PBS controls (designated 100%). (\*,  $p < 0.05$  relative to control.) Inset, analysis of conditioned media from invasion chambers by gelatin zymography. C, invasion of wild type and CR collagen gels. Cells were allowed to invade gels composed of wild type or CR collagen or wild type and CR gelatin, as indicated. Invasion of CR collagen is expressed as % of control invasion (with wild type collagen designated 100%). Invasion of gelatin is designated as fold increase relative to wild type collagen control. (\*,  $p < 0.05$  relative to control.) D, effect of proteinase inhibitors on invasion of gelatin. Invasion was evaluated in the presence or absence of TIMP-1 (10 nM), TIMP-2 (10 nM), or aprotinin (20  $\mu$ g/well), as indicated. Invasion of gelatin is expressed as % of control invasion (designated 100%). (\*,  $p < 0.05$  relative to control.) E, effect of MMP-2 domains on collagen invasion. Invasion was quantified in the presence or absence of rCD (100 nM) or rCBD (100 nM), as indicated. Results are expressed as % of control invasion (designated 100%). (\*,  $p < 0.05$  relative to control.) F, effect of MMP-2 domains on gelatin invasion. Invasion was quantified in the presence or absence of rCD (100 nM) or rCBD (100 nM), as indicated. Results are expressed as % of control invasion (designated 100%). (\*,  $p < 0.05$  relative to control.)

MMP-2, confirming surface expression of the recombinant enzyme in DOV13 cells (Fig. 6C).

**Localization of Cell Surface MT1-MMP**—In previous studies, MT1-MMP has been localized to membrane protrusions, termed invadopodia, which are rich in matrix proteinases and integrins, including  $\alpha_3\beta_1$  integrins (27–29). Immunocytochemical analysis of MT1-MMP surface staining in non-permeabilized DOV13 cells demonstrates MT1-MMP localization to distinct cell surface projections (Fig. 7D), characteristic of integrin-rich sites of cell-matrix contact. Following  $\beta_1$  integrin clustering using antibody-coated beads, MT1-MMP immunoreactivity is substantially redistributed to the periphery of the aggregated integrins (Fig. 7H). These data indicate that MT1-MMP can be actively recruited to membrane sites containing clustered  $\beta_1$  integrins on the surface of DOV13 cells.

**MMP Dependence of Migration and Collagen Gel Invasion**—Three-dimensional collagen culture and clustering of collagen binding integrins up-regulate surface MMP activity in DOV13 cells. To assess the functional consequences of matrix-enhanced proteolytic potential, the ability of cells to migrate and to invade a three-dimensional collagen matrix was evaluated. MMP activity was not required for general cell motility, as cells migrated through uncoated transwell filters with equal efficiency in the presence or absence of a broad spectrum MMP inhibitor (MMPI) using computer-assisted image analysis gave relative migration areas of  $1.4 \pm 0.1$  and  $1.5 \pm 0.3$ , respectively, indicating that MMP activity does not contribute to collagen-driven migration of DOV13 cells.

DOV13 cells efficiently penetrate three-dimensional collagen gels via  $\alpha_2\beta_1$  and  $\alpha_3\beta_1$  integrin receptors, and obstructing collagen-induced integrin clustering using integrin function blocking antibodies inhibits invasion (Fig. 9A). Invasion correlates with collagen-induced pro-MMP-2 processing (Fig. 9B, inset), and in contrast to cellular migration, invasion of collagen is MMP-dependent, as both a broad spectrum MMPI and exogenous TIMP-2 abrogate invasion and reduce or eliminate pro-MMP-2 processing (Fig. 9B, lanes 2 and 5). TIMP-1, a poor inhibitor of MT1-MMP (26), failed to reduce either collagen invasion or MT1-MMP-mediated pro-MMP-2 processing (Fig. 9B), suggesting that MT1-MMP collagenolytic activity may potentiate invasion. The serine proteinase inhibitor aprotinin had no effect on invasion of intact collagen gels (not shown). Furthermore, although collagenase-resistant collagen is sufficient to stimulate pro-MMP-2 activation (Fig. 1), cellular penetration of this matrix is significantly inhibited relative to wild type collagen (Fig. 9C), providing further support for the hypothesis that collagenolysis is required for invasive activity. Disrupting the triple helical structure of collagen by thermal denaturation removes the requirement for collagenase activity, as no difference in invasion of cells through gelatin derived from either wild type or collagenase-resistant collagen is observed (Fig. 9C). This is supported by data using wild type gelatin, in which invasion is effectively blocked by both TIMP-1 and -2 as well as by the serine proteinase inhibitor aprotinin (Fig. 9D), indicating that additional (non-MMP) gelatinolytic proteinases potentiate invasion following destabilization of collagen triple helical structure. Collagen invasion is unaltered in

% of control invasion (designated 100%). F, effect of MMP-2 domains on gelatin invasion. Invasion was quantified in the presence or absence of rCD (100 nM) or rCBD (100 nM), as indicated. Results are expressed as % of control invasion (designated 100%). (\*,  $p < 0.05$  relative to control.)

the presence of either the rCD or rCBD of MMP-2 (Fig. 9E). However, both the rCD, which inhibits MMP-2 cell surface activation (Fig. 3) (6, 8), and rCBD, which prevents MMP-2 binding to native and denatured collagen (17), effectively inhibit the MMP-2-dependent component of gelatin invasion (Fig. 9F). Together these data suggest that the stimulation of MT1-MMP collagenolytic activity (31) through collagen-binding integrins is a rate-limiting step for invasion of native type I collagen-rich matrices.

#### DISCUSSION

MT1-MMP is a cell surface activator of pro-MMP-2 and has been implicated in collagen invasion and turnover (33–36). In this study, DOV13 ovarian cancer cells activate MT1-MMP as a consequence of culture in type I collagen gels and display MMP-dependent invasion of type I collagen, indicating that MMP activity is required for removal of collagen matrix constraints during invasion. However, migration over two-dimensional collagen is not impeded by MMP inhibitors. Although TIMP-1 does not interact with MT1-MMP, TIMP-2 specifically binds the proteinase, functioning in both inhibition and stabilization of the enzyme on the cell surface (26, 32). The ability of exogenous TIMP-2, in contrast to TIMP-1, to inhibit DOV13 collagen gel invasion implicates a cell surface proteolytic cascade initiated by MT1-MMP. This is further supported by data demonstrating that inhibition of MMP-2 cellular activation or collagen binding using rCD and rCBD (17, 18), respectively, has no effect on collagen invasion. As the cellular events that govern the collagen-induced MMP-2/MT1-MMP response are unclear and technically difficult to assess in three-dimensional collagen gel systems, a variety of biochemical approaches were employed in this study to dissect the interplay between collagen-cell interactions and regulation of cell surface MMP activity.

DOV13 cells bind type I collagen via  $\alpha_2\beta_1$  and  $\alpha_3\beta_1$  integrins. Recognition of collagen by these integrins depends on retention of the triple helical conformation, as thermal gelation of collagen abrogates cellular adhesion. Collagenase-cleaved type I collagen produces  $\frac{3}{4}$  and  $\frac{1}{4}$  fragments that display a lower  $T_m$  than intact fibrils (37). Adhesion data in the current study demonstrate that the triple helical conformation of the collagen fragments is stabilized at low coating temperatures but is lost under physiological coating conditions (21). Together, these data suggest that pericellular type I collagenolysis will reduce  $\alpha_2\beta_1$  and  $\alpha_3\beta_1$  integrin-mediated cell-matrix contacts. By using a similar approach, the appearance of cryptic  $\alpha_V\beta_3$  integrin-binding sites (RGD) in collagenase-generated collagen fragments was reported (21). However, DOV13 cells adhere weakly to type I gelatin or  $\frac{3}{4}$  and  $\frac{1}{4}$  fragments, and aggregation of  $\alpha_V\beta_3$  integrins on the surface of DOV13 cells does not elicit a cellular MMP processing response (12, 20). Nevertheless, the exposure of cryptic  $\alpha_V\beta_3$ - or  $\alpha_V\beta_5$ -binding sites in collagenase-cleaved collagen may further influence MMP expression in a cell type-specific manner. In support of this observation, we have previously demonstrated that vitronectin-induced aggregation of melanoma cell  $\alpha_V\beta_3$  integrins up-regulates MMP-2 expression (38). Relative to collagen gel penetration, DOV13 cells rapidly invade a gelatin matrix. Although pro-MMP-2 activation is not up-regulated over basal levels under these conditions, additional proteinases of other mechanistic classes can provide gelatinase activity (1, 39, 40). Together these data indicate that collagenase activity provided by MT1-MMP is critical to invasion of an intact collagen matrix. Subsequent clearance of resultant fragments can then proceed by activation of cell surface MMP-2 along with contributions from other cell surface proteinases including seprase (39) and the components of the plasminogen activator/plasmin system (40), which have

been implicated in DOV13 cellular invasion of Matrigel (22).

Stimulation of pro-MMP-2 activation does not require collagenolysis, as collagenase-resistant collagen is as efficacious as wild type type I collagen at inducing pro-MMP-2 processing. However, thermal denaturation of either collagen abolishes the ability to enhance MMP activation, suggesting that  $\alpha_2\beta_1$  and/or  $\alpha_3\beta_1$  integrin binding to intact triple-helical collagen mediates the MMP activation response in DOV13 cells. By using subunit-specific antibodies to dissect integrin requirements for MMP processing, our data demonstrate that clustering of  $\alpha_3$  integrins promotes a stronger cellular MMP processing response than  $\alpha_2$  integrin aggregation. A potential role for  $\alpha$  integrin-specific regulation has been demonstrated previously for type I collagen-induced cellular responses, including those involving MMP-1 expression (41, 42). Administration of function blocking antibodies against either  $\alpha$  integrin subunit reveals a role for both receptors during invasion. Although this study implicates the  $\alpha_3\beta_1$  heterodimer in mediating the MT1-MMP response, it is likely that both  $\alpha_2\beta_1$  and  $\alpha_3\beta_1$  integrins provide a mechanical advantage to the migration component of invasion. Furthermore, it is unclear at this level of investigation whether  $\alpha_3\beta_1$  integrins are required for effective dispersal of  $\alpha_3\beta_1$  into focal adhesions (43, 44). Interestingly,  $\alpha_3\beta_1$  integrins have recently been hypothesized to play a major organizational role in the formation of invadopodia in response to cellular engagement of type I collagen (45). As MT1-MMP also localizes to invadopodia (27–29), it is possible that  $\alpha_3\beta_1$  clustering in DOV13 cells selectively initiates cellular events that mimic formation of invadopodial projections, which in turn regulate MT1-MMP activity. Moreover, our data demonstrate localization of MT1-MMP immunoreactivity to the periphery of clustered  $\beta_1$  integrins, indicating that MT1-MMP redistribution occurs during integrin clustering events. This observation, together with previous reports of MT1-MMP localization to integrin-rich cellular protrusions, suggests a cellular regulatory mechanism for MT1-MMP aggregation, thereby promoting effective pro-MMP-2 processing and efficient matrix degradation. As MT1-MMP can function as a collagenase (31) and MT1-MMP null mice exhibit severe deficiencies in collagen remodeling (33), localization of the enzyme to cellular collagen receptors could clearly influence physiologic events such as collagen gel contraction, adhesion, and invasion. In addition, pro-MMP-2 bound to intact peri-cellular collagen may readily infiltrate the MT1-MMP activation pathway, resulting in a switch from a collagenase to a gelatinase environment as pro-MMP-2 activation and collagen triple helix denaturation ensues (17).

It has recently been demonstrated that exogenous MT1-MMP overexpressed in a MMP-2 null background undergoes autolysis to a 43-kDa form, the rate of which is regulated by TIMP-2 (32). Similarly, endogenously expressed MT1-MMP in DOV13 cells exists in two major forms of 55 and 43 kDa (12). The current data indicate that the 55-kDa form of MT1-MMP is the active TIMP-2-binding species, whereas the 43-kDa form is an inactive autolysis product. This result is consistent with the amino-terminal sequences of similar MT1-MMP species obtained from overexpression systems, which demonstrate a loss of essential amino acids in the zinc-binding consensus sequence (30, 32). Although catalytically inactive, the 43-kDa form of MT1-MMP is nevertheless retained on the cell surface. As this 43-kDa species contains the carboxyl-terminal domains necessary for invadopodial localization and enzyme aggregation, it is interesting to speculate that MT1-MMP-mediated proteolysis may be down-regulated through the dilution of active enzyme with truncated proteinase.

In summary, our data support the hypothesis that as DOV13

cells interact with type I collagen, integrin receptors cluster on the cell surface, resulting in up-regulation of MT1-MMP and pro-MMP-2 processing, recruitment of MT1-MMP to sites of cell-matrix contact, MMP-2 surface association, and MT1-MMP-dependent collagen gel invasion. As a consequence of MT1-MMP collagenolysis, the resulting collagen cleavage products thermally denature, providing a substrate for a number of proteinases. In addition, MMP-2 is released from the cell surface to further advance matrix clearance through directed gelatinase activity on denatured collagen fragments. As  $\alpha_2\beta_1$  or  $\alpha_3\beta_1$  integrin occupancy is reduced, collagen matrix stimulation of proteolysis is attenuated. Furthermore, MT1-MMP activity can be down-regulated by autolytic processing to a stable, inactive 43-kDa form that may functionally dilute productive enzyme-substrate interactions. Together, these data support an hypothesis wherein matrix status influences cell surface matrix-degrading potential to facilitate cellular functions including migration, invasion, and matrix remodeling.

**Acknowledgments**—We thank Dr. Jonathan Jones (Northwestern University) for the use of the Zeiss fluorescence photomicroscope and Yueying Liu for valuable help with computer-assisted image analysis.

#### REFERENCES

- Birkedal-Hansen, H., Moore, W. G., Bodden, M. K., Windsor, L. J., Birkedal-Hansen, B., DeCarlo, A., and Engler, J. A. (1993) *Crit. Rev. Oral Biol. Med.* **4**, 197-250
- Nagase, H. (1997) *Biol. Chem.* **378**, 151-160
- Ellerbroek, S. M., and Stack, M. S. (1999) *BioEssays* **11**, 940-949
- Corcoran, M. L., Hewitt, R. E., Kleiner, D. E., Jr., and Stetler-Stevenson, W. G. (1996) *Enzyme Protein* **49**, 7-19
- Sato, H., Takino, T., Okada, Y., Cao, J., Shinagawa, A., Yamamoto, E., and Seiki, M. (1994) *Nature* **370**, 61-65
- Strongin, A. Y., Collier, I., Bannikov, G., Marmer, B. L., Grant, G. A., and Goldberg, G. I. (1995) *J. Biol. Chem.* **270**, 5331-5338
- Strongin, A. Y., Marmer, B. L., Grant, G. A., and Goldberg, G. I. (1993) *J. Biol. Chem.* **268**, 14033-14039
- Atkinson, S. J., Crabbe, T., Cowell, S., Ward, R. V., Butler, M. J., Sato, H., Seiki, M., Reynolds, J. J., and Murphy, G. (1995) *J. Biol. Chem.* **270**, 30479-30485
- Azzam, H. S., and Thompson, E. W. (1992) *Cancer Res.* **52**, 4540-4544
- Tomesek, J. J., Halliday, N. L., Updike, D. L., Ahern-Moore, J. S., Vu, T. K., Liu, R. W., and Howard, E. W. (1997) *J. Biol. Chem.* **272**, 7482-7787
- Haas, T. L., Davis, S. J., and Madri, J. A. (1998) *J. Biol. Chem.* **273**, 3604-3610
- Ellerbroek, S. M., Fishman, D. A., Kearns, A. S., Bafetti, L. M., and Stack, M. S. (1999) *Cancer Res.* **59**, 1635-1641
- Seltzer, J. L., Lee, A. Y., Akers, K. T., Sudbeck, B., Southon, E. A., Wayner, E. A., and Eisen, A. Z. (1994) *Exp. Cell. Res.* **213**, 365-374
- Theret, N., Lehti, K., Musso, O., and Clement, B. (1999) *Hepatology* **30**, 462-468
- Nguyen, M., Arkell, J., and Jackson, C. J. (2000) *Int. J. Biochem. Cell Biol.* **32**, 621-631
- Boudreau, N., and Bissell, M. J. (1998) *Curr. Opin. Cell Biol.* **10**, 640-646
- Steffensen, B., Bigg, H. F., and Overall, C. M. (1998) *J. Biol. Chem.* **273**, 20622-20628
- Wallon, U. M., and Overall, C. M. (1997) *J. Biol. Chem.* **272**, 7473-7481
- Liu, X., Wu, H., Byrne, M., Jeffrey, J., Krane, S., and Jaenisch, R. (1995) *J. Cell Biol.* **130**, 227-237
- Moser, T. L., Pizzo, S. V., Bafetti, L. M., Fishman, D. A., and Stack, M. S. (1996) *Int. J. Cancer* **67**, 695-701
- Messent, A. J., Tuckwell, D. S., Knauper, V., Humphries, M. J., Murphy, G., and Gavrilovic, J. (1998) *J. Cell Sci.* **111**, 1127-1135
- Ellerbroek, S. M., Hudson, L. G., and Stack, M. S. (1998) *Int. J. Cancer* **78**, 331-337
- Laemmli, U. K. (1970) *Nature* **227**, 680-685
- Miyamoto, S., Akiyama, S. K., and Yamada, K. M. (1995) *Science* **267**, 883-885
- Overall, C. M., and Sodek, J. (1990) *J. Biol. Chem.* **265**, 21141-21151
- Will, H., Atkinson, S. J., Butler, G. S., Smith, B., and Murphy, G. (1996) *J. Biol. Chem.* **271**, 17119-17123
- Nakahara, H., Howard, L., Thompson, E. W., Sato, H., Seiki, M., Yeh, Y., and Chen, W. T. (1997) *Proc. Natl. Acad. Sci. U. S. A.* **94**, 7959-7964
- Urena, J. M., Merlos-Suarez, A., Baselga, J., and Arribas, J. (1999) *J. Cell Sci.* **112**, 773-784
- Lehti, K., Valtanen, H., Wickstrom, S., Lohi, J., and Keski-Oja, J. (2000) *J. Biol. Chem.* **275**, 15006-15013
- Lehti, K., Lohi, J., Valtanen, H., and Keski-Oja, J. (1998) *Biochem. J.* **334**, 345-353
- D'Ortho, M. P., Will, H., Atkinson, S., Butler, G., Messent, A., Gavrilovic, J., Smith, B., Timpl, R., Zardi, L., and Murphy, G. (1997) *Eur. J. Biochem.* **250**, 751-757
- Hernandez-Barrantes, S., Toth, M., Bernardo, M. M., Yurkova, M., Gervasi, D. C., Raz, Y., Sang, Q. A., and Fridman, R. (2000) *J. Biol. Chem.* **275**, 12080-12089
- Holmbeck, K., Bianco, P., Caterina, J., Yamada, S., Kromer, M., Kuznetsov, S. A., Mankani, M., Robey, P. G., Poole, A. R., Pidoux, I., Ward, J. M., and Birkedal-Hansen, H. (1999) *Cell* **99**, 81-92
- Cockett, M. I., Murphy, G., Birch, B. L., O'Connell, J. P., Crabbe, T., Millican, A. T., Hart, I. R., and Docherty, A. J. (1998) *Biochem. Soc. Symp.* **63**, 295-313
- Chambers, A. F., and Matrisian, L. M. (1997) *J. Natl. Cancer Inst.* **89**, 1260-1270
- Hotary, K., Allen, E., Punturieri, A., Yana, I., and Weiss, S. J. (2000) *J. Cell Biol.* **149**, 1309-1323
- Danielsen, C. C. (1987) *Biochem. J.* **247**, 725-729
- Bafetti, L. M., Young, T. N., Itoh, Y., and Stack, M. S. (1998) *J. Biol. Chem.* **273**, 143-149
- Pineiro-Sanchez, M. L., Goldstein, L. A., Dodt, J., Howard, L., Yeh, Y., and Chen, W. T. (1997) *J. Biol. Chem.* **272**, 7595-7601
- Andreasen, P. A., Egelund, R., and Petersen, H. H. (2000) *Cell. Mol. Life Sci.* **57**, 25-40
- Langholz, O., Rockel, D., Mauch, C., Kozlowska, E., Bank, I., Krieg, T., and Eckes, B. (1995) *J. Cell Biol.* **131**, 1903-1915
- Lichtner, R. B., Howlett, A. R., Lerch, M., Xuan, J. A., Brink, J., Langton-Webster, B., and Schneider, M. R. (1998) *Exp. Cell Res.* **240**, 368-376
- Grenz, H., Carbonetto, S., and Goodman, S. L. (1993) *J. Cell Sci.* **105**, 739-751
- DiPersio, C. M., Shah, S., and Hynes, R. O. (1995) *J. Cell Sci.* **108**, 2321-2336
- Mueller, S. C., Gherzi, G., Akiyama, S. K., Sang, Q. X., Howard, L., Pineiro-Sanchez, M., Nakahara, H., Yeh, Y., and Chen, W. T. (1999) *J. Biol. Chem.* **274**, 24947-24952

## Dendritic organization of actin comet tails

Lisa A. Cameron\*, Tatyana M. Svitkina†, Danijela Vignjevic‡, Julie A. Theriot\*\* and Gary G. Borisy\*

Polymerization of actin filaments is necessary for both protrusion of the leading edge of crawling cells and propulsion of certain intracellular pathogens [1], and it is sufficient for generating force for bacterial motility in vitro [2]. Motile intracellular pathogens are associated with actin-rich comet tails containing many of the same molecular components present in lamellipodia [3], and this suggests that these two systems use a similar mechanism for motility. However, available structural evidence suggests that the organization of comet tails differs from that of lamellipodia. Actin filaments in lamellipodia form branched arrays [4], which are thought to arise by dendritic nucleation mediated by the Arp2/3 complex [5, 6]. In contrast, comet tails have been variously described as consisting of short, randomly oriented filaments [7], with a higher degree of alignment at the periphery [8], or as containing long, straight axial filaments with a small number of oblique filaments [9]. Because the assembly of pathogen-associated comet tails has been used as a model system for lamellipodial protrusion, it is important to resolve this apparent discrepancy. Here, using a platinum replica approach, we show that actin filament arrays in comet tails in fact have a dendritic organization with the Arp2/3 complex localizing to Y-junctions as in lamellipodia [10]. Thus, comet tails and lamellipodia appear to share a common dendritic nucleation mechanism for protrusive motility. However, comet tails differ from lamellipodia in that their actin filaments are usually twisted and appear to be under significant torsional stress.

Addresses: \*Departments of Biochemistry and †Microbiology and Immunology, Beckman Center, Stanford University School of Medicine, Stanford, California 94305, USA. ‡Department of Cell and Molecular Biology, Northwestern University Medical School, Chicago, Illinois 60611, USA.

Correspondence: Tatyana M. Svitkina  
E-mail: t-svitkina@northwestern.edu

Received: 22 September 2000  
Revised: 29 November 2000  
Accepted: 29 November 2000

Published: 23 January 2001

Current Biology 2001, 11:130–135

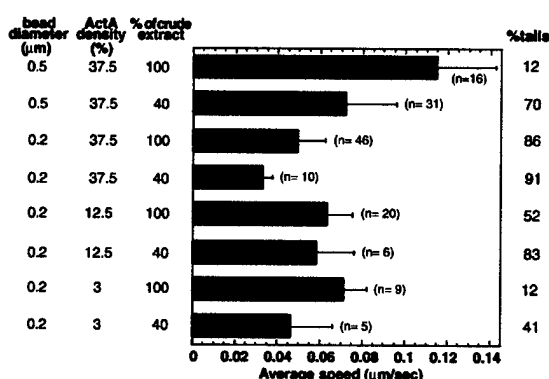
0960-9822/01/\$ – see front matter  
© 2001 Elsevier Science Ltd. All rights reserved.

## Results and discussion

The high density of actin filaments in comet tails formed by pathogenic bacteria such as *Listeria monocytogenes* or *Shigella flexneri* has hindered their structural analysis. Consequently, we examined tails formed by latex beads coated with the *L. monocytogenes* surface protein, ActA [11], where we could control density of the tails by varying bead size and ActA concentration. Like *L. monocytogenes* in infected host cells, ActA-coated beads in *Xenopus* egg cytoplasmic extracts initially form a symmetric cloud of actin filaments, which subsequently breaks symmetry to form the comet tail [11, 12]. The frequency of symmetry breaking for beads 0.5  $\mu\text{m}$  in diameter increased dramatically when the crude extract was diluted to 40% of its initial concentration, while the average speed decreased only moderately (Figure 1).

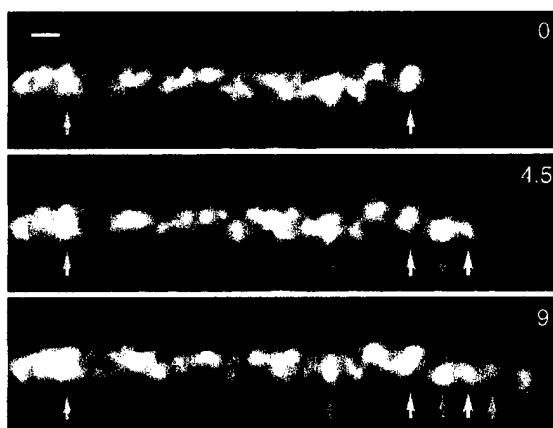
Photoactivation experiments have shown that fiducial marks placed on the actin polymer of comet tails inside infected cells remain stationary with respect to the host cell while the bacterium advances, and these results suggest that actin polymerization occurs exclusively at the bacterial surface [13]. To obtain direct evidence for the site of actin polymerization in tails associated with ActA-coated beads in cytoplasmic extracts, we used the recently

Figure 1



Speed and propensity for comet tail formation under different conditions. The bead size, ActA surface density, and extract concentration are listed for each of eight conditions in which bead average speed ( $\mu\text{m}/\text{sec}$ ) and percent tail formation were measured. Speed of 0.2  $\mu\text{m}$  beads did not vary significantly among the conditions tested. The number of beads tracked for average speed is listed. Between 100 and 1000 beads were scored at each condition for percent tail formation.



**Figure 2**

Fluorescence speckle microscopy of comet tails. We incubated 0.5  $\mu\text{m}$  beads with 37% of their surface area coated with ActA in full-strength *Xenopus* egg extract in the presence of trace amounts of rhodamine-actin to obtain a speckled pattern of tail labeling. The time sequence shows movement of a bead in the rhodamine channel. The formation of new speckles only at the front of the tail indicates that actin filament assembly is restricted to the bead-tail interface. Speckles remain stationary while the bead is moving. Colored arrows point to individual actin speckles, with the same color referring to the same speckle at different time points. Time is indicated in the upper right corner in seconds. The scale bar represents 1  $\mu\text{m}$ .

introduced speckle microscopy technique [14, 15]. When comet tails were assembled on 0.5  $\mu\text{m}$  ActA-coated beads in the presence of trace amounts of rhodamine-actin, new actin speckles appeared only at the tail-bead interface as the bead advanced and, once formed, the speckles remained stationary with respect to the substratum (Figure 2). The speckle pattern within the tail did not change significantly with time except for stochastic disappearance of individual speckles during depolymerization. Although the intensity of spots showed fluctuations, no new speckles appeared away from the bead. Thus, actin filaments assemble primarily, if not exclusively, at the bead-tail interface.

Electron microscopy (EM) of comet tails under these conditions (Figure 3a), as well as EM of bacterial tails (see Supplementary material), revealed dense arrays of actin filaments. Dilution of the extract to 40% did not significantly change the overall structure of tails. The superposition of filaments precluded clear visualization of their organization in the tail core. However, Y-junctions between actin filaments were consistently observed in sparser regions, including on the surface of the bead away from where the tail emerged (Figure 3b) and at the sides (Figure 3c) and rear (Figure 3d) of the tails.

To gain insight into the structure of the tail core, we used smaller beads, lower ActA densities, and more-diluted

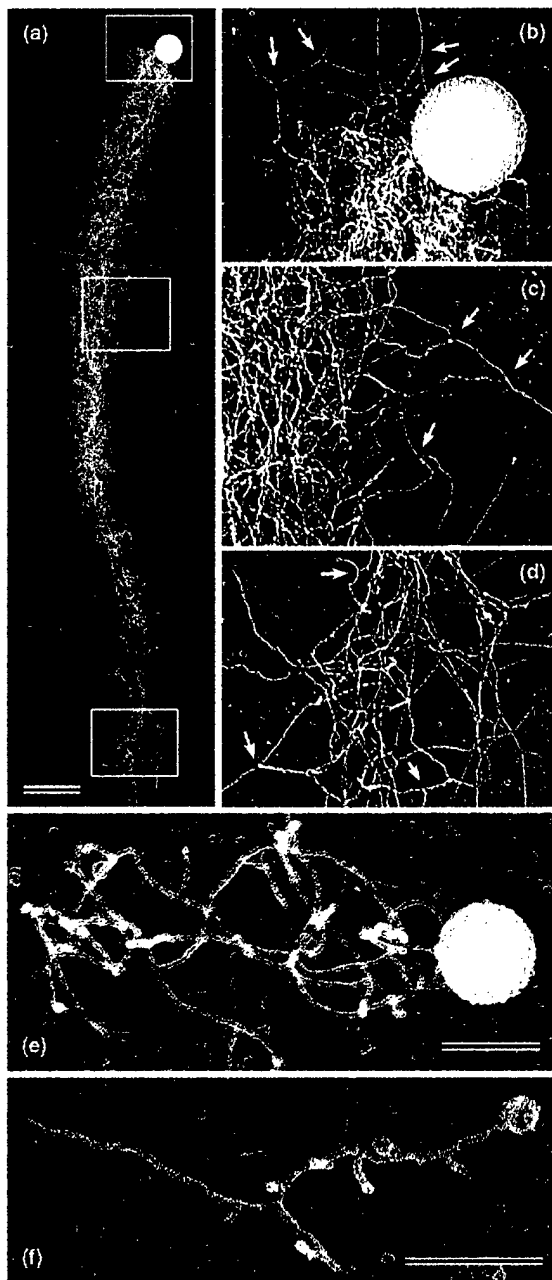
extracts. Beads with a 0.2  $\mu\text{m}$  diameter formed tails and moved over a broad range of conditions, though more slowly than did 0.5  $\mu\text{m}$  beads (Figure 1). Decreasing the density of ActA surface coating from the optimal 37.5% [11] down to 3% had little effect on average speed (Figure 1). However, structurally these tails and clouds were sparser and allowed for better visualization of actin filament organization (Figure 3e). The number of filaments contacting the bead surface as well as the filament density along the tail varied widely, and this finding is consistent with the theoretical predictions of fluctuation behavior previously reported for bead-tail association [12]. At sub-optimal ActA concentrations, often fewer than 10 filaments from the tail contacted the surface of 0.2  $\mu\text{m}$  beads (Figure 3e), but this seemed sufficient for motility.

For the smallest beads tested, which were 0.05  $\mu\text{m}$  in diameter, we could not observe persistent motility and therefore could not measure average speed. In EM preparations, these beads were never seen with more than one filament attached (Figure 3f). Many beads were devoid of filaments, and many branched filament assemblies lacked beads (not shown), both of which suggest that filaments were nucleated at the bead surface but were subsequently detached. This is consistent with the hypothesis that the filament-bead interaction is not permanent but undergoes cycles of association and dissociation. A bead with only one filament could easily lose it and therefore not move regularly, whereas the many crosslinked filaments of larger beads ensure a more stable association and persistent movement.

Y-junctions between actin filaments in sparse tails were clearly seen near the bead surface and throughout the tail, and long, axial, nonbranching filaments were not observed in such tails. Y-junctions had the same characteristic angle of approximately 70° (Figures 3 and 4a,b) as in lamellipodia [4, 10] or in Arp2/3-actin assemblies in vitro [5, 6]. Filament branches near the bead were frequently of similar length (Figure 4a), and this finding suggests that branch formation occurred near the barbed end as in the observations of Pantaloni et al. [16]. In our system, however, branching at the barbed end may be explained simply by restriction of activation of the Arp2/3 complex by ActA, which is localized at the bead surface. This is consistent with biochemical evidence showing that ActA stimulates Arp2/3 nucleation of actin polymerization [17, 18]. However, Y-junctions were also often highly asymmetric, with branches differing in length (Figure 4e), and this observation suggests that capping activity terminated the elongation of barbed ends. Some filaments appeared kinked at approximately 110° (supplementary angle to 70°) (Figure 4e,i), which suggests that capping of a parental filament could occur shortly after nucleation of a daughter filament. Actin clouds, which were always present in



Figure 3



Comet tails assembled by ActA-coated beads under different conditions. (a–d) 0.5  $\mu\text{m}$  bead with 37.5% of its surface area coated with ActA in 40% *Xenopus* egg extract. (a) An overview shows the very dense array of twisted actin filaments in the tail. (b–d) Enlargements of the boxed regions show Y-junctions (arrows) in different parts of the tail. (e) A 0.2  $\mu\text{m}$  bead with 12.5% of its surface area coated with ActA in 30% extract forms a sparse tail; Y-junctions are seen everywhere in the tail. (f) A 0.05  $\mu\text{m}$  bead with

preparations, had the same basic structure as tails except for the distribution of the actin array around the bead.

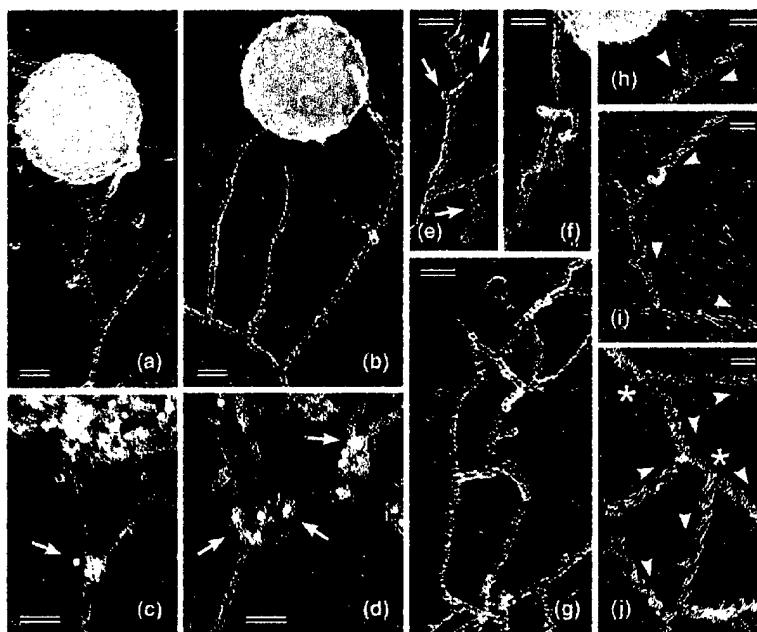
Localization of the Arp2/3 complex was performed by immunogold EM with a polyclonal antibody raised against the p21-Arc component of the Arp2/3 complex [19]. In agreement with light microscopic data [19], the Arp2/3 complex was found throughout the tails (not shown). Using sparse actin filament arrays, we detected the Arp2/3 complex at individual Y-junctions (Figure 4c,d), as it was previously found for Y-junctions in lamellipodia [10]. These results are consistent with the concept that Y-junctions in comet tails are formed in the course of dendritic nucleation mediated by the Arp2/3 complex.

To distinguish such Y-junctions from other kinds of junctions formed by crosslinks after nucleation, we analyzed filament polarity by decorating actin filaments with myosin subfragment 1 (S1) and showed that Y-junctions had pointed ends at the junction and barbed ends facing away from the junction (Figure 4h–j). This finding is consistent with the prediction of the dendritic nucleation model. Although these pointed-end-to-side Y-junctions were the most abundant crosslinks between actin filaments in tails and clouds, barbed-end-to-side (Figure 4j) and side-to-side junctions (not shown) were also observed. Even in the absence of a polarity marker, the existence of these crosslinks could be deduced from the formation of closed loops of actin filaments (Figure 4f,g). Such junctions indicate the presence in the comet tail of crosslinking molecules other than the Arp2/3 complex, such as  $\alpha$ -actinin [20].

A striking feature of clouds and tails associated with ActA-coated beads was the twisted appearance of the actin filaments. The persistence length for a filament of pure actin is approximately 10  $\mu\text{m}$  [21], and they break at a radius of curvature of less than 180 nm [22]. However, many filaments in tails appeared curved or twisted over distances less than 1  $\mu\text{m}$ , with some showing curvature of less than 50 nm (e.g., Figure 4f,g). Although we cannot exclude that some twisting may have resulted from sample preparation, we note that free filaments or filaments having just one point of interaction with another filament were usually straight, whereas twisted filaments were usually restrained by at least two crosslinks (Figure 4f,g). These observations suggest that twisting is a consequence of a force applied to crosslinked filaments. One possible origin of the force that causes twisting may be the binding energy of ADF/cofilin, which is known to change the intrinsic twist of actin filaments [23] and may also change

37.5% of its surface area coated with ActA in 40% extract is associated with a single branching filament. The scale bars represent (a) 1  $\mu\text{m}$  and (e,f) 0.2  $\mu\text{m}$ .

Figure 4



Filament-filament interactions in comet tails. (a,b) Y-junctions at the bead surface. (c,d) Immunogold staining (10 nm colloidal gold) with an antibody to p21-Arc detects Arp2/3 complex at Y-junctions (arrows). (e) Asymmetric Y-junctions where one of two sister branches is very short (arrows) result in a kinked filament appearance. (f) A twisted filament that has two points of interaction with another filament; there is one interaction at the Y-junction, and there is a linkage near the free end. (g) Numerous closed loops within the tail suggest other types of filament crosslinking in addition to Y-junctions. (h-j) S1 decoration reveals filament polarity in different types of junctions (arrowheads point to the direction of the pointed ends). (h) In a Y-junction at the bead, the barbed end of the shorter branch is associated with the bead, and the pointed end interacts with the side of another filament. (i) Y-junctions lacking one of the two branches give an impression of kinked filaments. (j) Barbed-end-to-side interactions between actin filaments (asterisks) in a tail. Conditions: 0.2  $\mu$ m beads with (a-d, f-h) 12.5%, (i,j) 6%, or (e) 3% of their surface area coated with ActA were incubated in (f) 20%, (c,d) 25%, (a,b) 30%, (e) 40%, or (g-j) 50% extract. The scale bars represent (a-g) 50 nm and (h-j) 100 nm.

its mechanical properties. Torsional stress operating on a filament constrained at both ends would be expected to cause writhing of the filament and result in deformations such as we observe.

The twisted nature of the filaments may explain the disparity between our observations and previous reports using thin-section EM. In thin sections, a dendritic and twisted structure would produce images of short, randomly oriented filaments, as has been reported [7, 8]. The parallel axial filaments reported by Sechi et al. [9] are definitely distinct from our observations, but these may be characteristic only of comet tails that have protruded substantially beyond the cellular surface and are in contact with the plasma membrane all along their length. Such protrusions have different protein composition from that of intracellular tails [9], and the actin filament half life is more than 10-fold longer than the half life in intracellular tails [24].

Our observations of comet tails associated with ActA-coated beads demonstrate significant similarity at the supramolecular level with the structure of lamellipodia in three distinct ways: dendritic organization of comet tails, localization of the Arp2/3 complex to branch points, and pointed-end-to-side polarity of Y-junctions. These structural features are consistent with the hypothesis that comet tails, like lamellipodia, use a dendritic nucleation

mechanism for protrusive motility [10]. The simple kinetic properties of comet tails in combination with their defined structure permit a further evaluation of actin polymerization-driven motility. The fluorescence speckle microscopy assay demonstrates that moving comet tails assemble actin filaments only at the bead-tail interface, and this result is in agreement with conclusions drawn previously from photoactivation analysis [13]. A consequence of this property is that the spatial organization of the tail reflects the kinetics of actin assembly and therefore permits us to infer the age of a structural element from its position within the tail, the youngest structures being located next to the bead or bacterium and the older structures being located progressively farther away along the tail. Conservation of the dendritic structure throughout the length of the tail, therefore, implies continuous nucleation of new filaments at the bead surface. Since barbed filament ends arise only at the bead-tail interface, the abundance of apparently free barbed ends throughout the tail suggests both the continuous release of the barbed ends of filaments from the bead surface and their capping. Both characteristics are predicted by the array treadmill model [3] but have not been previously demonstrated experimentally.

The observation that a small number of actin filaments interacts with the bead surface at any one time suggests that only a few working filaments are needed to generate

the force required for motility. Consistent with this observation, significant reduction of ActA density on the bead surface and the concomitant reduction of actin filament density in the tail did not substantially affect the rate of head movement. This finding suggests that the number of pushing filaments was not a limiting factor under our experimental conditions. The elastic Brownian ratchet model for force generation by actin polymerization [25] requires some freedom of association for an individual filament to grow and push. Implicit in this concept is that only an ensemble of filaments can provide a statistically stable association of the machinery with the interface and support persistent bead motility. Filaments in the ensemble may not all be behaving identically at any given time; while some may be adding subunits and pushing, others may be in transient tight association. The working comet tail seems to have a high degree of crosslinking in addition to branching, which allows accumulation of torsional stresses to twist the actin filaments, the significance of which remains to be determined. Our results suggest that a dendritic nucleation mechanism is responsible for creating a coherent filament ensemble and that an array treadmill process is responsible for maintaining it in a steady state that can generate the pushing force necessary to propel bacteria or ActA-coated beads.

### Materials and methods

Purification of ActA, coating of polystyrene beads (Polysciences), and light microscopic motility assays were performed as described [11]. For motility assays with fluorescent speckle microscopy, rhodamine-actin was added to extracts at 150-fold lower concentrations compared to regular conditions, and this resulted in a proportion of labeled actin of approximately 0.1%. To allow for easy localization of tails, we also added fluorescein- $\alpha$ -actinin to the extracts at concentrations sufficient for continuous tail labeling and visualized it in a different channel. For EM, thicker motility chambers than those for light microscopic assays allowed us to decrease the shearing force upon the separation of coverslips. A 2  $\mu$ l sample of motility mix (ActA-coated beads in *Xenopus* egg extract supplemented with tetramethylrhodamine iodoacetamide-labeled G-actin and an ATP-generating mix) was sandwiched between two coverslips (22  $\times$  22 mm and 22  $\times$  18 mm) separated by two strips (2 mm wide) of teflon tape attached near the edges of the larger coverslip. After incubation at room temperature in a humid environment, chambers were opened in a dish containing 0.2% Triton X-100 in *Xenopus* buffer (XB) [11] with or without 2  $\mu$ M phalloidin. The structure of the tails was similar in the presence or absence of phalloidin. The fluorescence intensity of comet tails in the living population did not significantly change after detergent treatment and fixation, and this finding indicates that our procedure was adequate to preserve filaments in tails. Although some tails were washed out during this procedure, many tails remained attached to the coverslip. Coverslips were washed with XB, fixed with 2% glutaraldehyde, and processed for EM as described [26]. Immunostaining for the Arp2/3 complex [10] and S1 decoration [26] were done as described.

### Supplementary material

A supplementary figure showing comet tails assembled by *L. monocytogenes* in full-strength *Xenopus* egg extract can be found with the electronic version of this article at <http://current-biology.com/supmatin.htm>.

### Acknowledgements

We gratefully acknowledge Peter Jackson for providing *X. laevis* to make egg extract and Steve Limbach for excellent maintenance of electron microscopic equipment. This work was supported by National Institutes of Health grants R01 AI36929 (J. A. T.) and GM 25062 (G. G. B.), by a fellowship from the

David and Lucile Packard Foundation (J. A. T.), and by American Cancer Society grant CB-95 (G. G. B.).

### References

1. Dramsi S, Cossart P: **Intracellular pathogens and the actin cytoskeleton.** *Annu Rev Cell Dev Biol* 1998, 14:137-166.
2. Loisel TP, Boujemaa R, Pantaloni D, Carlier MF: **Reconstitution of actin-based motility of *Listeria* and *Shigella* using pure proteins.** *Nature* 1999, 401:613-616.
3. Borisy GG, Svitkina TM: **Actin machinery: pushing the envelope.** *Curr Opin Cell Biol* 2000, 12:104-112.
4. Svitkina TM, Verkhovsky AB, McQuade KM, Borisy GG: **Analysis of the actin-myosin II system in fish epidermal keratocytes: mechanism of cell body translocation.** *J Cell Biol* 1997, 139:397-415.
5. Mullins RD, Heuser JA, Pollard TD: **The interaction of Arp2/3 complex with actin: nucleation, high affinity pointed end capping, and formation of branching networks of filaments.** *Proc Natl Acad Sci USA* 1998, 95:6181-6186.
6. Blanchoin L, Amann KJ, Higgs HN, Marchand JB, Kaiser DA, Pollard TD: **Direct observation of dendritic actin filament networks nucleated by Arp2/3 complex and WASP/Scar proteins.** *Nature* 2000, 404:1007-1011.
7. Tilney LG, Portnoy DA: **Actin filaments and the growth, movement, and spread of the intracellular bacterial parasite, *Listeria monocytogenes*.** *J Cell Biol* 1989, 109:1597-1608.
8. Zhukarev V, Ashton F, Sanger JM, Sanger JW, Shuman H: **Organization and structure of actin filament bundles in *Listeria*-infected cells.** *Cell Motil Cytoskeleton* 1995, 30:229-246.
9. Sechi AS, Wehland J, Small JV: **The isolated comet tail pseudopodium of *Listeria monocytogenes*: a tail of two actin filament populations, long and axial and short and random.** *J Cell Biol* 1997, 137:155-167.
10. Svitkina TM, Borisy GG: **Arp2/3 complex and actin depolymerizing factor/cofilin in dendritic organization and treadmill of actin filament array in lamellipodia.** *J Cell Biol* 1999, 145:1009-1026.
11. Cameron LA, Footer MJ, van Oudenaarden A, Theriot JA: **Motility of ActA protein-coated microspheres driven by actin polymerization.** *Proc Natl Acad Sci USA* 1999, 96:4908-4913.
12. van Oudenaarden A, Theriot JA: **Cooperative symmetry-breaking by actin polymerization in a model for cell motility.** *Nat Cell Biol* 1999, 1:493-499.
13. Theriot JA, Mitchison TJ, Tilney LG, Portnoy DA: **The rate of actin-based motility of intracellular *Listeria monocytogenes* equals the rate of actin polymerization.** *Nature* 1992, 357:257-260.
14. Waterman-Storer CM, Salmon ED: **Actomyosin-based retrograde flow of microtubules in the lamella of migrating epithelial cells influences microtubule dynamic instability and turnover and is associated with microtubule breakage and treadmill.** *J Cell Biol* 1997, 139:417-434.
15. Keating TJ, Borisy GG: **Speckle microscopy: when less is more.** *Curr Biol* 2000, 10:R22-R24.
16. Pantaloni D, Boujemaa R, Didry D, Gounon P, Carlier MF: **The Arp2/3 complex branches filament barbed ends: functional antagonism with capping proteins.** *Nat Cell Biol* 2000, 2:385-391.
17. Welch MD, Iwamatsu A, Mitchison TJ: **Actin polymerization is induced by Arp2/3 protein complex at the surface of *Listeria monocytogenes*.** *Nature* 1997, 385:265-269.
18. Zalevsky J, Grigorova I, Mullins RD: **Activation of the Arp2/3 complex by the *Listeria* ActA protein: ActA binds two actin monomers and three subunits of the Arp2/3 complex.** *J Biol Chem* 2000, in press.
19. Welch MD, DePace AH, Verma S, Iwamatsu A, Mitchison TJ: **The human Arp2/3 complex is composed of evolutionarily conserved subunits and is localized to cellular regions of dynamic actin filament assembly.** *J Cell Biol* 1997, 138:375-384.
20. Dabiri GA, Sanger JM, Portnoy DA, Southwick FS: ***Listeria monocytogenes* moves rapidly through the host-cell cytoplasm by inducing directional actin assembly.** *Proc Natl Acad Sci USA* 1990, 87:6068-6072.
21. Ott A, Magnasco M, Simon A, Libchaber A: **Measurement of the persistence length of polymerized actin using fluorescence microscopy.** *Phys Rev E* 1993, 48:R1642-R1645.

22. Arai Y, Yasuda R, Akashi K, Harada Y, Miyata H, Kinoshita K Jr, Itoh H: **Tying a molecular knot with optical tweezers.** *Nature* 1999, **399**:446-448.
23. McGough A, Pope B, Chiu W, Weeds A: **Cofilin changes the twist of F-actin: Implications for actin filament dynamics and cellular function.** *J Cell Biol* 1997, **138**:771-781.
24. Robbins JR, Barth AI, Marquis H, de Hostos EL, Nelson WJ, Theriot JA: ***Listeria monocytogenes* exploits normal host cell processes to spread from cell to cell.** *J Cell Biol* 1999, **146**:1333-1350.
25. Mogilner A, Oster G: **Cell motility driven by actin polymerization.** *Biophys J* 1996, **71**:3030-3045.
26. Svitkina TM, Borisy GG: **Correlative light and electron microscopy of the cytoskeleton of cultured cells.** *Methods Enzymol* 1998, **298**:570-592.